THE UNIVERSITY OF CHICAGO

SMELLING FROM THE MOUTH: PERCEPTUAL EXPERIENCE, LEARNING & NEURODYNAMICS OF RETRONASAL OLFACTION

A DISSERTATION SUBMITTED TO

THE FACULTY OF THE DIVISION OF THE SOCIAL SCIENCES

IN CANDIDACY FOR THE DEGREE OF

DOCTOR OF PHILOSOPHY

DEPARTMENT OF PSYCHOLOGY

BY

RUI HE

CHICAGO, ILLINOIS

DECEMBER 2022

Table of Contents

List of Figures

List of tables

Acknowledgments

The thesis would have never become a reality if it weren't for the inspiration, support, and kindness of many wonderful individuals.

Foremost, I would like to express my deepest gratitude and thanks to Dr. Leslie Kay for providing guidance, patience, and encouragement. Her mentorship is invaluable, and she taught me how to be an independent scientist as well as a compassionate person. I would like to thank my committee members Dr. Wim van Drongelen for inspiring my interest in signal processing and offering great insights into the project, and Dr. Jai Yu for demonstrating how good science is done.

I am also thankful to my lab members; Dr. Boleslaw Osinski for introducing me to coding and animal surgeries, Dr. Shane Peace for great scientific discussions, Dr. Andrew Sheriff for sharing codes and brilliant ideas, Vivian Nguyen, Abigail Stuart, Jamie Zeng for always being reliable on animal care and experiments, Daisy Li and Yu Ji for being a strong advocate for my research.

I want to thank the Department of Psychology and the Institute of Mind and Biology for giving me space and support to flourish and finish this project.

Finally, I would like to thank my family for loving me unconditionally. My cat, Chimeow He, who welcomes me home every day. My fiancée, Lifeng Chen, who have shared the exciting as well as the difficult moments with me for the last three years and have willingly committed to being part of my life. My parents, Guoxin He and Xiaodan Lu, who always believe in my decisions and think this is the best dissertation without even speaking English.

Abstract

Odorants can activate the nasal epithelium from two directions, either orthonasally from the nares via nasal breathing or sniffing or retronasally through the mouth during eating and drinking. Retronasal olfaction is associated with a higher threshold for detection than orthonasal olfaction, and a different pleasantness rating. Rozin (1982) proposed that there exists a duality of olfactory perception via the two olfactory routes. Recent electrophysiological and imaging studies showed odorants entering the retronasal olfactory route elicit different peripheral neural responses in the glomerulus and mitral cell firing in the olfactory bulbs (OB). Functional networks engaged in retronasal olfaction also show differential activities in higher cortical regions, which may underlie the perceptual differences between the two routes. Here, I use olfactory learning behavioral and electrophysiological studies to study the perceptual qualities of the two olfactory routes and circuit interactions. In Chapter 3, rats were pre-conditioned to odorized solutions delivered only retronasally and then tested in an orthonasal Go/No-Go odor discrimination task. I found significant learning rate improvement for the retronasally pre-exposed odorants in a volatility-dependent manner, and the result suggests that retro- and orthonasal routes can generate similar perceptual qualities if the odors are strong enough. Chapters 4 and 5 describe a retronasal Go/No-Go behavioral experiment in conjunction with local field potential (LFP) recordings in the olfactory and gustatory systems - piriform cortex, gustatory cortex, and olfactory tubercle. I characterize the respiratory and licking behaviors and the oscillation patterns in the gamma (45-100Hz) and beta (15-30 Hz) frequency bands during the retronasal odor discrimination task. Gamma band power is significantly suppressed while beta band power demonstrates an odor-cue effect between the positively and negatively reinforced retronasal odorants. LFPs recorded OB, OT, PC, and GC show coupling with the

sensorimotor inputs and are coherent in the beta band during the retronasal odor sampling period. I explore the LFPs during sleep and the effect of olfactory training in Chapter 6. With a sleep scoring algorithm of OB gamma and hippocampal LFP, I compare the sleep pattern pre- and post-olfactory training, showing behavioral difference in sleep time. Together, I wish to shed some light on the neural dynamics in retronasal olfaction.

CHAPTER 1: Introduction

The field of olfactory studies is mostly dominated by orthonasal olfaction, which refers to the process of odorants entering the nasal cavity through the nostrils. Retronasal olfaction is a second olfactory route by which odorants enter the nasal cavity through the nasopharynx. While orthonasal olfaction carries information about the external environment, retronasal olfaction commonly reflects the internal state and food consumption.

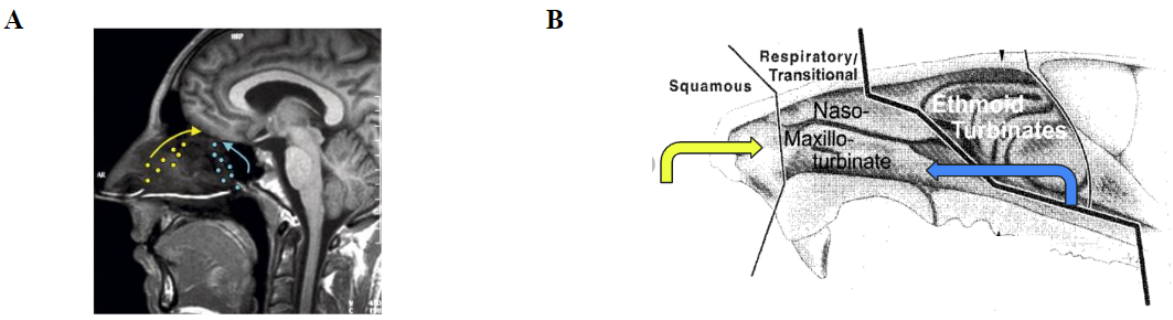

Figure 1.1. Schematic Diagrams of retronasal vs. orthonasal olfaction. (A) Orthonasal (yellow) and retronasal (blue) routes in humans (Small et al., 2015); (B) Orthonasal (yellow) and retronasal (blue) routes in rats (adapted from Wetmore et al., 1999)

Retronasal olfaction is relatively understudied in the fields of neuroscience and psychology for several potential reasons. First of all, pure retronasal experiences rarely occur in a natural setting and cannot be easily isolated without also exposing subjects to odorants orthonasally. Secondly, it is intuitive to assume that olfactory perceptual experience is mainly driven by the chemical profile of odorants. Based on this assumption, research on olfactory

quality is therefore concentrated on the psychophysical properties of odorants because the two routes would be assumed to produce the same perceptual experience, except for perhaps differences in the concentration of odorants as they reach the sensory epithelium in the nose. Because of the technical difficulty in isolating retronasal experience and the assumption of odorant-determined olfactory percepts, retronasal olfaction is often overlooked.

Retronasal and orthonasal olfaction are not identical

Retronasal and orthonasal olfaction are different in many ways. Retronasal and orthonasal olfaction involve distinctive behavior patterns (sniffing vs. chewing, licking, and swallowing). These behavior patterns, together with the physical characteristics of the olfactory routes, affect the temperature, concentration, time course, and airflow of an olfactory input, resulting in qualitative differences in olfactory experiences. The two olfactory routes are both multisensory but in different ways. Orthonasal olfaction involves somatosensory and trigeminal activation around the nose, whereas retronasal olfaction also involves oral sensation within the mouth and often combines with taste. In humans, retronasal olfaction is linked to higher detection thresholds and increased difficulty in identifying and localizing odorants (Pierce & Halpern, 1996; Hummel & Livermore, 2002; Hummel et al., 2006). Rozin (1982) proposed the idea of the duality of olfaction, which described that olfactory experience is qualitatively different between the two routes, based on the discrepancy he observed between the two olfactory routes in terms of pleasantness and intensity rating of items such as cheese and fish. Hannum et al. (2018) show that participants are worse at matching an unfamiliar or a similar odor reference to test odorants when the reference and test odorants are presented via different

routes, suggesting that the same chemical profile may generate two percepts that are different not only quantitatively but also qualitatively.

Olfactory Anatomy

The perceptual differences between retro- and orthonasal olfaction inspire inquiries about peripheral neural responses and functional network engagement between the routes. There have been a number of comprehensive and well-written reviews that provide in-depth information on olfactory cell types, circuits, and pathways (Giessel & Datta, 2014; Harberly, 1985; Imamura et al., 2020; Shepherd, 2004). Here, I summarize the key characteristics of mammalian olfactory anatomy in the framework of retronasal and orthonasal olfaction comparison.

An odorant activates an ensemble of olfactory sensory neurons (OSN) in the nasal epithelium, depending on its chemical components. The OSNs expressing the same odor receptors send their axons through the olfactory nerve and converge onto the same pair of glomeruli on either side of each olfactory bulb (OB) (Fig. 1.2). In the glomerular layer (GL), the axons of the OSNs make contact with the dendrites of both glutamatergic mitral and tufted cells and GABAergic and dopaminergic periglomerular interneurons. The mitral and tufted cells (M/T cells) are the two main types of projection neurons in OB and are morphologically similar. Mature M/T cells have a primary (apical) dendrite extending into the GL, synapsing onto one glomeruli and the small axon cells; their secondary dendrites extend horizontally in the external plexiform layer (EPL), where M/T cells form dendrodendritic synapses with granule cells, the GABAergic interneurons. The somata of tufted cells are mostly located in the EPL, whereas the

somata of mitral cells are concentrated in the mitral cell layer (MCL). Granule cells are the small interneurons in the inner layer of the OB called the granule cell layers (GCL).

The projection neurons, M/T cells, in the main OB project to multiple brain regions, including the anterior olfactory nucleus (AON), the nucleus of the lateral olfactory tract, the piriform cortex (PC), the entorhinal cortex (EC), the olfactory tubercle (OT), and the cortical nucleus of the amygdala (Brunjes et al., 2005; Haberly & Price, 1977; Wesson & Wilson, 2011; Figure 6.2). The physiological characteristics and innervation patterns are slightly different between the mitral and tufted cells; tufted cells only innervate the anterior part of the olfactory system including part of AON and OT. Mitral cells in the main OB have further projections that innervate the anterior and posterior PC, AON and EC (Igarashi et al., 2012; Imamura et al., 2020; Nagayama et al., 2010).

In the scope of this dissertation, the electrophysiological study focuses on the three higher brain regions: PC, OT, and GC, in addition to the OB. Their roles in odor hedonics, olfactory learning, memory, and multisensory integration make them crucial to retronasal olfaction.

Often referred to as the olfactory cortex, PC receives the majority of input from OB. It demonstrates odor-evoked activity carrying information about the identity, intensity, and timing of odorants (Bolding & Franks 2017). It is also connected to the hippocampus (HPC) and has been shown to participate in olfactory-related tasks such as discrimination, fear conditioning, and odor object recognition (Shaffer et al., 2018; Wilson & Sullivan, 2011). The pyramidal cells in PC also project back to granule cells in OB, providing centrifugal feedback to modulate the neuron excitability in OB. PC is functionally divided into the anterior and posterior PC, with the posterior PC receiving more associate inputs (Haberly & Price, 1978). It has been proposed that

OT should be called tubular striatum by Daniel Wesson (2020), who has extensively studied OT and its role in odor hedonics. As the new name proposal suggests, OT is involved in motivation, reward and addiction (Fitzgerald et al., 2014, Gadziola et al., 2015) not just odor sensing[1]. GC neurons are not only taste-responsive and encode taste hedonic information (Katz et al., 2001; Samuelsen et al., 2012). GC neurons also respond to olfactory stimuli (Maier et al., 2015, Maier, 2017). The densely reciprocal connections between GC and PC may support flavor integration associated with retronasal odors.

[1] Research in Dr. Daniel Wesson's lab are excellent and provided me with great inspiration for this dissertation. I am using the name Olfactory Tubercle (OT) for this dissertation to be consistent with documents I generated previously for the dissertation.

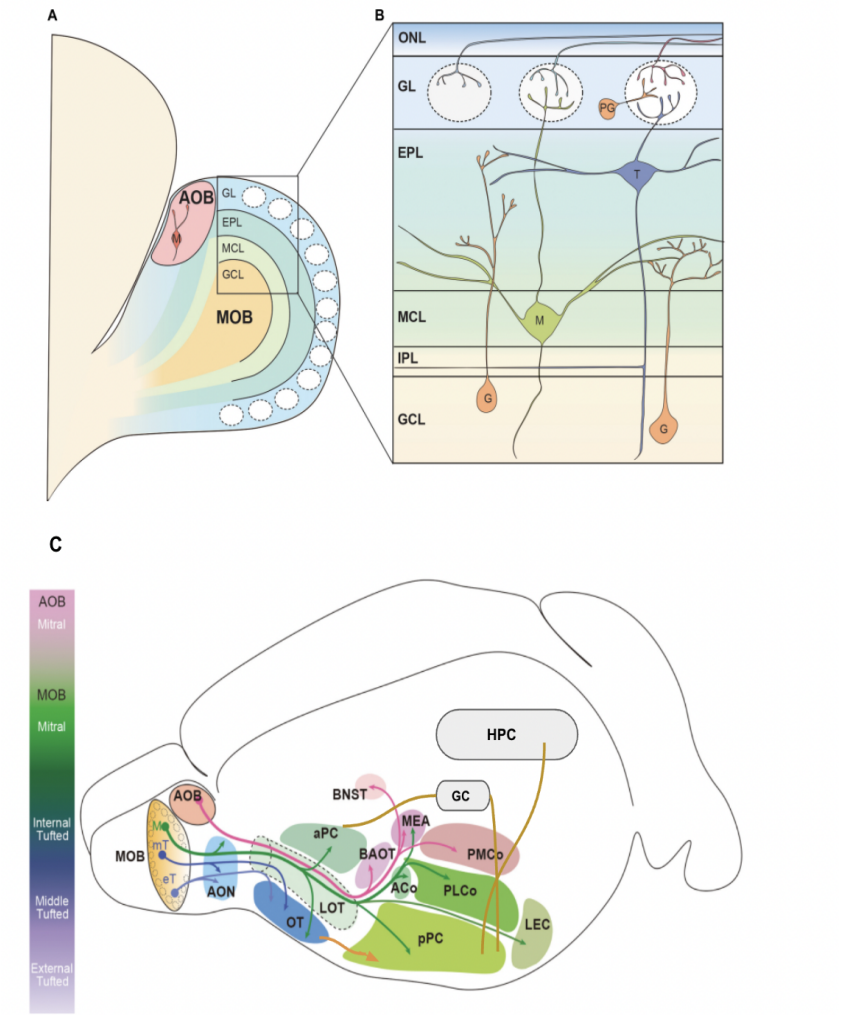

Figure 1.2. The neural circuit in the rat olfactory bulb cell layers (A) and the anatomy of the rat olfactory system (B). **(A)** The main olfactory bulb (MOB) located in the anterior end of the brain consists of multiple cell layers. Olfactory sensory neurons (OSN) send axons through the outer layer of the olfactory bulb, the olfactory nerve layer (ONL). Their axons form neuropil called glomeruli with the dendrites of mitral (M) and tufted (T) cells and small neurons surrounding them in the glomerular layer (GL). The somata of tufted cells are found closer to the pial surface in the external plexiform layer (EPL), and the somata of mitral cells in the mitral cell layer (MCL). Granule cell interneurons (GC) extend their axons from the innermost granule cell layer (GCL) and form dendrodendritic synapses with M/T cells in the EPL. **(B)** Tufted cells in the main OB innervate more anterior brain structures including part of the anterior olfactory nucleus (AON) and the olfactory tubercle, while mitral cells project more extensively through the lateral olfactory tract (LOT) to OT, the anterior and the posterior piriform cortex (aPC, pPC), the medial amygdaloid nucleus (MEA), the anterior and posterolateral cortical amygdaloid nucleus (MEA; PLCo), and lateral entorhinal cortex (LEC). The accessory olfactory bulb projects to the bed

nucleus of the accessory olfactory tract (BAOT), the striatum (BNST) and the amygdala (MEA, PMCo). PC reciprocally connects to both OB and GC and projects to the hippocampus (HPC). (Figure adapted from Imamura et al. 2020)

Implications for retronasal olfaction

The chemical profile of a monomolecular odorant remains the same regardless of the route and activates a similar set of OSNs and glomeruli (Gautam & Verhagen, 2012; Rebello et al., 2015). Calcium imaging in rats and mice indicates that retronasal olfaction, when compared to orthonasal olfaction with the same airflow rate, evokes a weaker response with a longer delay (Furudono et al., 2013; Gautam & Verhagen, 2012). An EEG study in humans also showed that context (*e.g.,* whether the odorant is food-related) and familiarity of an odorant interact with the source of the odorant (orthonasal or retronasal) to affect both perceptual intensity and the odor-event-related potential (Hummel & Heilmann, 2008). A study by Craft and colleagues (2021) showed both retronasal and orthonasal olfactory stimuli activate mitral cells, and the average firing rate peaks in a similar frequency range from 5Hz to above 20-30Hz. The elevated firing of mitral cells lasts longer and goes back to baseline level after 2 seconds for retronasal stimuli, whereas firing rate changes induced by orthonasal stimulation quickly recover in 0.5 seconds. The decreased intensity and different timing in the periphery may explain the higher threshold and lower sensitivity for retronasal olfaction.

It is still unclear how the quantitatively different neural responses might translate into qualitatively different perceptual experiences. The olfactory system has to be able to maintain a consistent odor percept independent from odor intensity driven by chemical concentration for tasks like odor localization and flavor acquisition. On the one hand, there are several neural

mechanisms for concentration-invariant neural responses, but the proposed mechanisms are all within the scope of orthonasal smelling. Imaging studies that include the sensory epithelium show the variance in input from OSNs is normalized and sequentially gives rise to a more consistent output amplitude and spatial distribution in the mitral and tufted cells (Storace & Cohen, 2017). Cortical and higher-order neural responses in mammals and insects, which arguably represent odor identity, have a more reliable odor-specific firing pattern regardless of various concentration levels of an odorant (Bolding & Franks 2017; Cleland et al., 2012; Stopfer et al., 2003; Wilson & Sullivan 2011). This suggests that within a certain range of concentration fluctuation, the quality of an odorant would not be affected.

The quality of an odorant may change when the concentration changes drastically. Gross-Isseroff and Lancet (1988) showed in humans that pairs of the same odorants at the identical concentration are perceived to be similar when presented together; the similarity rating goes down to less than 10% when one of the odorants is diluted 100-fold relative to the other. In mice and rats, odorants of biochemical significance, such as pheromone or pheromone-derivative, can also produce concentration-dependent effects. For example, trimethylthiazoline (TMT), a molecule found in fox urine and widely used to study fear and anxiety in rodents, is aversive and may elicit avoidance behavior in high concentrations in a novel open field but not when the concentration is low (Fendt & Endres, 2008). Banana-like isoamyl acetate is often used as a neutral odorant for olfactory research and can become aversive once presented in high concentration in a mice study (Fortes-Marco et al., 2015). Whether retronasal and orthonasal routes generate, the same quality may depend on differences in the effective concentration of the

same odorant. Is the difference in concentration between the two olfactory routes mitigable, or is it significant enough to elicit substantially different neural states?

In addition to distinctive peripheral neural activation, retronasal olfaction occurs during eating or drinking, which recruits other sensory modalities including gustation and somatosensation. These activated neural systems may add to the synthetic perceptual difference between ortho- and retronasal perception of the same odor. Small et al. (2005) used fMRI and demonstrated strong blood-oxygen-level-dependent (BOLD) responses in the amygdala, hippocampus, and insula when odors were delivered orthonasally. Retronasally delivered odors, on the other hand, activated the central sulcus, a brain region often associated with orosensory inputs. Moreover, the gustatory cortex is shown to be necessary for retronasal but not orthonasal olfaction in rats (Blankenship et al., 2019).

Neural oscillations in olfaction

Neural oscillations in the olfactory system reflect coordination within and between brain regions associated with olfactory learning (Frederick et al., 2016; Kay et al., 2008) and can provide a gateway for understanding the neural networks involved in retronasal olfaction. Several types of oscillations have been characterized in the olfactory bulb local field potential (LFP), which can be categorized by frequency bands including theta (2-12 Hz), beta (15-30 Hz), and gamma (40-100 Hz) oscillations. In rats, theta band oscillations overlap with the respiratory input (2-12 Hz) that activates OSNs in a rhythmic nature. Respiration can be tracked by the OB LFP theta oscillation during sniffing for odor sampling and breathing at rest (Kay 2005; Rojas-

Líbano et al., 2014). OB theta rhythm may also be coupled with hippocampal theta when rats engage in olfactory-cue-guided navigation tasks (Sheriff et al., 2021).

Gamma oscillations were first described by Adrian (1942) in response to odor stimulation. Since then, numerous studies have been focusing on the mechanism and the functional roles of olfactory oscillations. Gamma and beta oscillations in the OBs are generated from the dendrodendritic microcircuits between the excitatory glutamatergic mitral/tufted cells and inhibitory GABAergic granule cells (Fourcaud-Trocmé et al., 2014; Lagier et al., 2007; Osinski et al., 2018; Schoppa, 2006). Both gamma and beta oscillations may be present in odor processing as different neurocognitive modes arise, with gamma associated with early odor sampling and beta associated with later sampling or responding (Frederick et al., 2016).

The power of gamma oscillations increases with task demand when rats discriminate extremely similar odorants and correlates with performance for fine odor discrimination (Beshel et al., 2007; Frederick et al., 2016). Genetically modified mice with disruption of GABA-A receptors on OB granule cells show increased gamma oscillatory power in the OB network and improved fine odor discrimination when compared to the wild-type littermate (Nusser et al., 2001). The antennal lobe for insects is the brain structure analogous to the vertebrate olfactory bulb and also displays odor-evoked oscillations (20-30 Hz in insects). Stopfer et al. (1997) show that silencing the inhibitory network in the honeybee antennal lobe abolishes odor-evoked oscillations and suppresses the bees' ability to discriminate similar odorants. Taken together, the research points to the functional importance of gamma oscillations in fine odor discrimination.

Odor-evoked beta oscillations in the OB and PC can be elicited by repeated presentations of highly volatile odorants (Lowry & Kay, 2007). Beta power also increases when rats acquire

operant odor discrimination tasks (Kay & Beshel, 2010; Martin et al., 2004) and transfer learned rules on a novel odor set (Frederick et al., 2017). GABAergic granule cells receive centrifugal inputs from the piriform cortex and other parts of the olfactory and limbic systems, and their excitability gates the power of beta oscillations and mediates the transition to beta or gamma oscillation in the OBs (Osinski & Kay, 2016; Osinski et al., 2018). Although the functional role of beta oscillations remains ambiguous because it can occur with or without learning, the importance of top-down input that modulates granule cell excitability suggests that beta oscillation involves a more global network.

Cross-frequency coupling plays a significant part in understanding how information is processed through the coordination of brain structures. Functional connectivity in the brain identifies structures with correlated activity in the frequency band and phase when an animal or human is engaged in certain behavioral, perceptual, and cognitive states (Bowyer, 2016; Fries, 2015). Analytical tools used in understanding functional connectivity may include coherence and phase-amplitude coupling analysis in the frequency or correlation and granger analysis in the time domain.

Coherence denotes a constant phase relationship between two signals, and the strength of coherence may suggest coordination within the network. Coherence in the olfactory system has been extensively studied. The olfactory bulb receives input from OSNs during the inhalation cycle in a rhythmic manner. OB LFP is highly entrained by respiration-related rhythm and shows high coherence between OB theta frequency and respiration across different behavioral states (Jessberger et al., 2016; Kay & Laurent, 1999; Rojas-Líbano et al., 2014). The OB signal is also coherent with LFP recorded in the cortical areas, including anterior and posterior PC, entorhinal

cortex, and hippocampus (Chabaud et al., 1999; Kay & Freeman, 1998; Martin et al., 2007). Strong OB-PC coherence in the beta band can be observed with repeated odor exposure (Osinski et al., 2018). Beta coherence relies on the top-down inputs to OB (Martin et al., 2004) and has been hypothesized to play a functional role in rule transfer olfactory learning (Frederick et al., 2016). The characteristic of OB beta coherence with multiple brain structures and required centrifugal input to sustain the oscillation again reinforces the argument that beta oscillation is a global event in olfactory processing whereas gamma is more restricted locally in the OB.

Context and learning effects on olfactory electrophysiology

Environmental context, past experience, and learning can affect how an odor stimulus is processed in the olfactory system including OB (Cleland et al., 2002, 2012; Freeman & Schneider, 1982; Kay & Laurent, 1999; Mandairon et al., 2006), and PC (Mouly et al., 2001; Pashkovski et al., 2020; Wilson & Sullivan, 2011). Even at the very first stage of neural processing, Kay and Laurent (1999) showed that OB mitral cells change firing patterns to the same odorant once the context associated with the odorant changes. It is possible that the olfactory route contains or serves as contextual information for olfactory processing.

Due to the high experience- and context-dependent nature of olfaction, the study of olfactory routes needs to address the roles that the different routes play in the learning process, where the information gained from one route should be effectively shared with the other in flavor acquisition. Chapuis et al. (2007) showed that although odor presented near water alone (i.e., orthonasally) was sufficient to induce conditioned food aversion with LiCl injection in rats, adding the odorant into the water (both retronasally and orthonasally) elicited a stronger aversive

response that was also more resistant to extinction. This additive effect was consistent with a technique used to accelerate odor-taste association acquisition (Darling & Slotnick, 1994; Kay & Laurent, 1999). Blankenship et al. (2019) showed that rats learn faster and in fewer days to preferentially respond to positively reinforced retronasal odorants compared with orthonasal odorants. With their learning paradigm, the animals showed no transfer of preference between orally infused odorants to airborne odorants. Together, these results suggest that although olfactory learning may arise from both routes, learning strength, efficiency, and perceptual quality may differ significantly across olfactory routes.

Olfactory memory consolidation and sleep

Olfactory memory shows some differences relative to memories in other sensory modalities like vision and hearing. Odor-cued memory is more emotionally involved (Herz & Cupchik, 1995; Herz et al., 2004) and evokes autobiographical memory in human studies (Chu & Downes, 2000, 2002; Hacklander et al., 2019) known as the "Proust Effect"[2]. Olfactory memory is hard to extinguish after being acquired in both humans and rodents (Bodyak & Slotnick, 1999; Stevenson et al., 2000), and exposure to certain odorants during critical periods can have long-lasting effects on one's adult life (Moriceau & Sullivan, 2004; Wilson & Sullivan, 2011). Unlike the input from visual, auditory, and somatosensory stimuli first relayed through the thalamus, the OB directly projects to the amygdala and entorhinal cortex, one synapse away from the

[2] In the novel "In search of lost time, Vol 1. Swann's way" by French novelist Marcel Proust, when the protagonist eats a Madeleine and drinks floral tea, the scents of the pastry and tea immediately bring back the old childhood memory. I also want to mention this book because the Kay Lab read it together during the COVID-19 pandemic period, and that is a good memory inspired by the study of olfaction.

hippocampus. The amygdala is essential for fear and emotion (See review: Ledoux 2007). The activation of NMDA receptors in the basolateral amygdala can protect newly formed associative learning from extinction (Portero-Tresserra et al., 2013). The importance of the hippocampus in declarative memory and spatial learning cannot be emphasized enough (See review: Bird & Burgess, 2008; Voss et al., 2017). These unique configurations may be fundamental for the emotional and memorable characteristics of olfactory memory. This dissertation project includes an olfactory learning experiment over days using rats with electrodes implanted in the olfactory system. Therefore, I want to take the opportunity to explore how olfactory memory is consolidated in sleep after training.

Memory in the brain is hypothesized to be in the form of distributed ensembles of neurons that are concurrently or sequentially activated in a Hebbian fashion (Buzsáki, 2005; Hebb, 1949). The role of sleeping learning and memory consolidation has gained increasing attention in the past couple of decades. The study of sleep patterns and neural reactivation of memory during sleep focuses heavily on the hippocampus (Buzsáki, 2015; Ramadan et al., 2009; Siapas & Wilson, 1998) and some regions of the neocortex such as the prefrontal cortex (Liu et al., 2016; Muzur et al., 2002; Sirota et al., 2003).

Sleep in mammals is broadly divided into two stages, Rapid Eye Movement (REM) and non-REM (NREM), characterized by stereotypical neural activity patterns. REM sleep in rats and mice is associated with high theta (4-12Hz) power in the hippocampal LFP, high-frequency low-amplitude neocortical LFP, and absence of neck muscle movement except for intermittent muscle twitches (John et al., 2017; Manabe et al., 2011; Tsuno et al., 2008). Disruption of REM sleep is associated with learning impairment, fear conditioning interruption, and prevention of

the formation of some spatial and emotional memory (Abel et al., 2013; Boyce et al., 2017; Walker & Stickgold, 2006). However, sleep interruption can be inherently stressful and may have downstream effects on memory formation, (just imagine you are awakened by another species 10-times larger than you in the middle of the night). The causal relationship between REM sleep and memory consolidation was not established until Boyce et al. (2016) abolished hippocampal theta by optically inhibiting GABA neurons in the medial septum, which projects to the hippocampus and drives theta rhythm. Silencing the medial septum GABAergic neurons disrupted theta activity, erased novel object place recognition, and impaired fear-conditioned memory, and the impairment effect is exclusive to REM sleep but no other sleep stages.

Non-REM (NREM) sleep refers to all the other sleep stages besides REM. NREM is typically characterized by slow waves and ripples (see review: Carskadon & Dement, 2005) and therefore is often referred to as slow-wave sleep (SWS). During slow-wave sleep after training, sharp-wave ripple (SPW-R) events (150-250Hz) increase in the hippocampus (Buzsáki, 1989; Eschenko et al., 2008; Fernandez-Ruiz et al., 2019), and disruption of SPW-R can disrupt memory consolidation (Girardeau et al., 2009). SPW-R can happen during sleep or in an awake state and are important for synaptic plasticity and memory (Buzsáki, 1989, 2015; Colgin, 2016). In the hippocampus, bursts of place cell activity lasting 100-200 ms co-occur with SPW-R, and the firing of the place cell ensembles follow the same sequential order activated during waking but in a time-compressed cascade during SPW-R (Buzsáki, 1986; Carr et al., 2011, 2012). Replay activity is argued to consolidate a memory event into the broader network of existing memory during sleep and serves to mediate memory retrieval when awake (Roumis & Frank, 2015).

The topic of sleep has become increasingly intriguing as more research has emerged on olfactory network characteristics and memory reactivation during sleep or sleep-like stages such as under urethane anesthesia (Barnes et al., 2014; Bagur et al., 2018; Manabe et al., 2011; Narikiyo et al., 2014; Wilson & Yan, 2010). The piriform cortex is structurally similar to the hippocampal archicortex with a three-layer structure and both structures receive associative inputs. CA3 pyramidal cells in the hippocampus are characterized by abundant recurrent fibers, similar to the anatomy of the pyramidal cells in the PC, which also emit recurrent collaterals. Similar models using cholinergic modulation of the pyramidal cells can effectively encapsulate gamma and theta oscillations in the piriform cortex and hippocampus CA3 (Liljenstrom & Hasselmo, 1995). SPW-Rs are found in the olfactory system including anterior PC (Mori et al., 2011) and OT (Narikiyo et al., 2014). This similarity between CA3 in the hippocampus and the piriform cortex raises the question of whether the piriform cortex is engaged in sleep and memory consolidation in a similar way as the hippocampus, especially for cognitive tasks involving olfaction and gustation. Furthermore, flavor formation or odor-taste associations require crosstalk between the piriform cortex and the gustatory cortex (Maier et al., 2012).

Olfactory oscillations are modulated by sleep/wake states including changes in respiration, coordination between brain regions and fast frequency power (Eeckman & Freeman, 1991; Jessberger et al., 2016). Bagur et al. (2018) were able to exploit the LFP characteristics associated with sleep, such as weaker gamma frequency power in the OB and a high ratio between theta (6-9Hz) and delta (1.5-4Hz) power, to discriminate sleep states (Waking/REM/NREM). They also observe a reduction of beta oscillations in the OB during REM, suggesting that the olfactory networks may act differently in REM and NREM.

Summary

It is an intriguing question in neuroscience and psychology how the same sensory input involves the receiver's physical agency (nose vs. mouth) as a modulator to generate distinctive perceptual experiences and engage the olfactory network differently. While orthonasal olfaction is well-studied in previous research, more research is needed to characterize the neural responses evoked by retronasal olfaction and to identify the overlap and divergence in the olfactory system by the same odorant via different routes.

This dissertation project is driven by the ultimate question of whether an odor is perceived the same or differently retronasally vs. orthonasally. I set out to further understand the behaviors, learning processes, and neural mechanisms related to retronasal olfaction. The neural circuits in the olfactory system and its electrophysiological characteristics in combination with the high-context-dependent nature of olfaction allow me to build hypotheses around retronasal olfaction. Chapter 2 outlines the behavioral paradigms for retronasal and orthonasal odor experiences, the electrophysiological study focusing on the olfactory oscillations in LFP, and the statistical analytical tools used in the project. Chapter 3 is adapted from my publication in Chemical Senses (2021), where I examined whether two routes share common olfactory percepts using a learning transfer behavioral paradigm. The behaviors rats engage in when discriminating two retronasal odorants and how the sensorimotor inputs from licking and breathing contribute to the LFPs in the olfactory system are summarized in Chapter 4. The related olfactory gamma and beta oscillations are characterized in Chapter 5, allowing us to draw a comparison between the neural states for retro- and orthonasal olfaction. Chapter 6 is an exploration of the olfactory

system in a putative memory consolidation process after retronasal discrimination training, probing learning effects on the neural networks.

CHAPTER 2: Methods

To understand retronasal olfaction, I used both behavioral and electrophysiological analyses. Behavioral studies allowed me to interrogate perceptual similarities and differences across the two routes and examine the validity of the dual-olfaction theory (Rozin, 1982). Electrophysiological studies provide a description of the electrophysiological pattern representing the retronasal route. They answer the questions of how retronasal olfaction engages the central olfactory system and whether the features extensively studied in orthonasal olfaction are universal to olfaction or specific to the orthonasal route. The sleep studies allow me to go a step further to address the consolidation processes that may be involved in olfactory learning.

For the behavioral analyses, three types of instrumental training were used, as shown in Figure 2.1: (A) retronasal conditioning trials where rats passively receive odor exposure, (B) orthonasal discrimination trials where rats learn to discriminate two air-borne odorants, and (C) retronasal discrimination trials where rats learn to discriminate two odorized solutions.

Behavioral study overview

Chapter 3 contains two behavioral experiments; Experiment 1 (n=16) examines whether the retronasal exposure in Figure 2.1A affects subsequent orthonasal learning Figure 2.1B. Experiment 2 (n=4) is a proof-of-concept study aiming to show that the results from Experiment 1 are based on rats' capability to detect and discriminate odorants when presented retronasally using retronasal discrimination trials (Figure 2.1C). Chapters 4 and 5 are based on the behavioral and electrophysiological results collected in Experiment 3 done in naive rats (n=8) with electrode implants. The same type of training as Experiment 2 was used for Experiment 3 but on three different odor sets, and sleep was monitored before and after training. Passive odor presentation

using a saturated cotton swab presented to the rat was done to validate the quality of the electrophysiological recording.

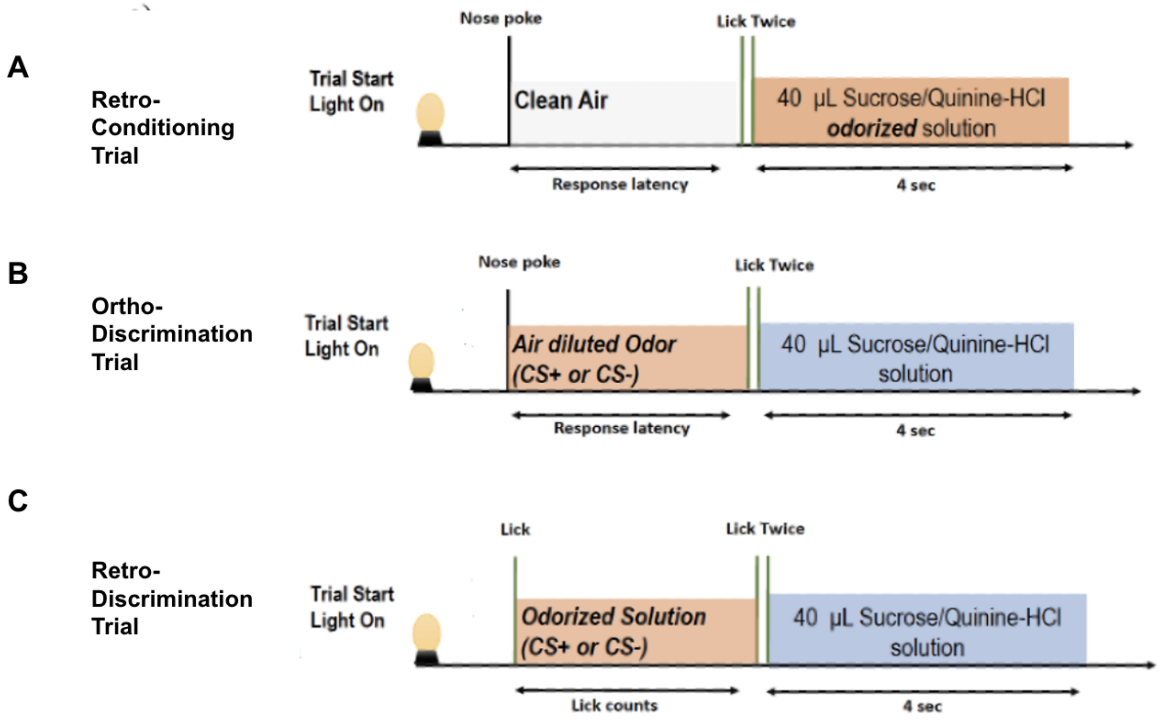

Figure 2.1. Schematics of experiment procedures. (**A**) During a retronasal conditioning trial, a rat receives clean air during a nose poke in the odor port and licks the spout twice to receive an odor+taste solution. Orthonasal odorants are removed via a concentric vacuum. (**B**) A rat is tested on the orthonasal discrimination task where odorized air is delivered, and the rat chooses to either lick or not lick for the reinforcer solution associated with the odorant. (**C**) To test rats' discrimination ability for retronasal odorants, dispensing of the odorized solution is initiated by one lick, and if the rat continues licking (more than 2 licks), the sweet or bitter reinforcer is delivered (Figure adapted from He et al., 2021).

Animal Care and Water Deprivation

All rats used in the projects were gradually water-restricted over 5 days until a 23-h water deprivation was reached before the instrumental training. During training, they were provided with ad libitum water for one hour at the same time every day. All procedures were performed under veterinary supervision and approved by the University of Chicago Institutional Animal Care and Use Committee in accordance with the Association for Assessment and Accreditation of Laboratory Animal Care.

The instrumental training sessions were conducted in an operant conditioning modular test chamber (ENV-008, Med Associates, Georgia, VT) and programmed with Med-PC-IV software. An odor port equipped with an infrared beam sensor records the start time and duration of each entry. A house light located at the back of the box was illuminated at the beginning of each trial to signify the opening of the door, which is adapted from a CD ROM drive and programmed by an Arduino driver and grants access to the odor port. A lick spout with a concentric vacuum was located inside the odor port and connected to a vacuum line adjacent to the liquid dispenser. The vacuum was turned on during the retronasal conditioning phase to remove orthonasal odorants, rendering the experience purely retronasal (Rebello et al., 2015). Solenoid isolation valves with separate tubing mounted on a wall outside the operant chamber dispense ~40 μL of liquid each time they are activated in a trial. Licking is measured by an infrared photobeam located in front of the lick spout or by extraction from the PC LFP (Chapter 4). The odor (*i.e.*, retronasal) and taste solutions are delivered through separate odor delivery tubing and separate internal tubing in the lick spout to avoid cross-contamination. Odorants in

the orthonasal condition were diluted to approximately 15% of saturated vapor with air and delivered using our standard protocol (Kay & Beshel, 2010; Frederick et al., 2011).

Experiment 1

Training Schedule: Water-restricted rats were conditioned to an odorized sweet solution and an odorized bitter solution in the retronasal phase and tested on the orthonasal odor discrimination tasks to discriminate either the pre-exposed odor pair or a novel odor pair matched for volatility (Figure 2.1A). Rats learned the instrumental orthonasal discrimination task with some degree of variability across subjects, and there was further variability in learning the first transfer of the instrumental task from the training odor set to a second odor set (Frederick et al., 2017). Thus, to remove the confound of the instrumental learning from the evaluation of perceptual transfer from retronasal to orthonasal tasks, all rats were pretrained to 2 orthonasal training odor sets that were different from the odorants used in the testing conditions (Table 1) and learned to perform them to at least 80% correct. Once rats learned the orthonasal odor discrimination task, they were then moved to the first round of 2-day retronasal conditioning.

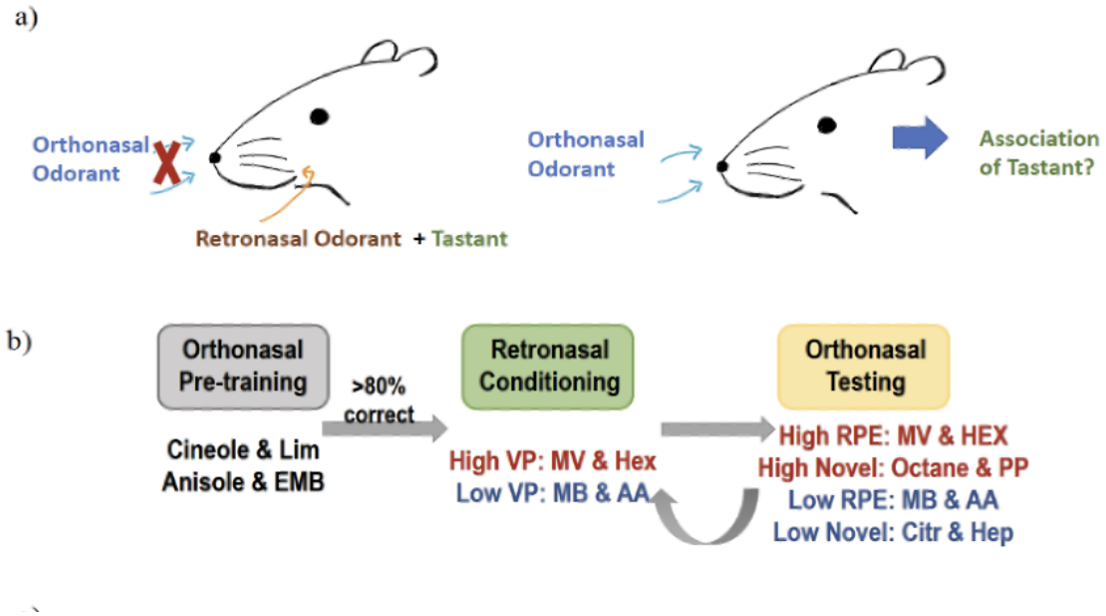

Figure 2.2. Training Schedule for Experiment 1. (A) the study aims at looking at whether rats can recall having experienced the association between pure retronasal odorant and tastant when exposed to the odorant orthonasally. (B) Experiment 1 includes 3 phases: Orthonasal pretraining,retronasal conditioning, and orthonasal testing phase.

Table 1. Odor Sets in Experiment 1

Odor Set	**A**			**B**		
	Odor	CAS #	Theoretical Vapor Pressure (kPa, 25C)	Odor	CAS #	Theoretical Vapor Pressure (kPa, 25C)
Pre-training	1,8-Cineole	470-82-6	0.220	Limonene	138-86-3	0.206
Pre-training	Anisole	100-66-3	0.566	Ethyl 2-methylbutyrate	7452-79-1	1.048
High Volatility RPE	2-Hexanone	591-78-6	1.778	Methyl valerate	624-24-8	1.47
High Volatility Novel	Octane	111-65-9	1.874	Propyl Proprionate	106-36-5	1.902
Low Volatility RPE	Methyl Benzoate	93-58-3	0.051	Amyl Acetate	628-63-7	0.524
Low Volatility Novel	Citronellal	106-63-0	0.033	3-Heptanol	589-82-2	0.043

Six odor sets were used in Experiment 1. Odorants are matched by vapor pressure and are counterbalanced when assigned to CS+ or CS- during the experiments. Values retrieved from http://pubchem.ncbi.nlm.nih.gov/ or manufacturer websites.

Go/No-Go Orthonasal discrimination

Rats were trained to discriminate a pair of odorants delivered orthonasally (Figure 2.1A): the CS+ odorant in an airstream predicted delivery of a sweet sucrose solution upon continued licking, and the CS- odorant predicted a bitter-tasting quinine-hydrochloride solution with continued licking. A light at the back of the operant box was illuminated to signify the start of a trial, and the door to the odor port at the front of the box opened after 1 s. An entry attempt to the odor port activated odorized air delivery, and the odor stayed on until the rat retracted from the

port. After the onset of odor delivery, the rat can wait for a trial to end in 5 s or reach forward to lick the spout twice to initiate delivery of 40 μL 0.005M quinine-HCl solution or 40 μL 0.1 M sucrose solution depending on the orthonasal odorant. The light is extinguished 2 s after the reinforcement occurs, and the odor port door closes slowly to allow the animal to withdraw from the port to await the next trial. If no nose poke in the odor port is detected, the door closes 10 s after opening. The lick spout is rinsed by a stream of water, followed by a vacuum epoch to remove any liquid residue between trials. Each session consists of 75 CS+ and 75 CS- trials randomly interleaved.

Retronasal Conditioning and Orthonasal testing

Retronasal exposure trials (Figure 2.1B) have a similar structure to trials in the orthonasal discrimination task, but clean air is delivered upon nose poke entry to the odor port. One of the 2 odorized aqueous reinforcers, 0.1 M sucrose mixed with a 0.01% v/v CS+ odorant or 0.005 M quinine-HCl mixed with 0.01% CS- odorant, is presented with 50% probability once the rat licks twice on the lick spout after the door opened. Odorant volatilized in the air is removed continuously by a concentric vacuum to avoid orthonasal detection (Rebello et al., 2015). All rats are given the opportunity to perform up to 150 trials once per day for two days. In the experiment,all were conditioned for more than 100 trials per session. After retronasal conditioning, they are tested in the orthonasal paradigm for 2 days. Half of the rats are tested in the orthonasal condition on the RPE odorants, which have been presented in the previous retronasal conditioning session, and the other half are tested on a novel odor set (control) matched for volatility to the odors used in the retronasal conditioning. Following orthonasal

testing, retronasal conditioning on the same RPE odors is repeated for one day, and then the rats are tested on the other orthonasal condition (novel or RPE). The whole process is repeated for odor sets of different vapor pressures. The testing conditions are within subjects. The testing order and contingency are counterbalanced across subjects.

Go-/No Go Retronasal odor discrimination session

In the retronasal odor discrimination task (Figure 2.1C), rats perform a nose poke in the port and lick the spout twice to receive an odorized solution (CS+ or CS-). Any residual odor solution is sucked away by vacuum 3 seconds after delivery, and rats can respond by either continuing licking or withdrawing from the port. A correct response was to keep licking the spout for sucrose in response to CS+ or to withdraw from the port in response to CS- to avoid the bitter taste. The lick spout is then automatically rinsed, and the water is removed with the vacuum between trials.

In Experiment 2, each session consists of 100 trials that rats can attempt. A trial automatically concludes if rats do not initiate licking 10 seconds after the door opens. Experiment 3 implements an adjustment of Experiment 2 for the number of trials in each session and how a trial is initiated. A trial no longer automatically ends 10 s after its onset. A lick is required to initiate a trial, and rats are given 6 s to sample an odorized reinforcer and another 6 s to decide either to keep licking or to withdraw from the odor port and then the trial is concluded. With the change, a rat is required to be actively engaging in the tasks until the program finishes a session with100 trials or after 1.5hr of training. Data collected when rats are not motivated in the session (attempted <70%) can be excluded from the analysis.

Experiment 2: Go/No-Go Retronasal Odor Discrimination Validation

Experiment 2 is a proof-of-concept study aiming to show that the results from Experiment 1 are based on rats' capability to detect and discriminate odorants when presented retronasally (i.e., the RPE odorants in Table 1). In these retronasal odor discrimination tasks, rats perform a nose poke in the port and lick the spout twice to receive an odorized solution (CS+ or CS-). Any residual odor solution is sucked away by vacuum 3 seconds after delivery, and rats can respond by either continuing licking or withdrawing from the port. A correct response is to keep licking the spout for sucrose in response to CS+ or to withhold licking and withdraw from the port in response to CS-. The lick spout is automatically rinsed, and the water is removed with the vacuum between trials. The order of test odor sets was counterbalanced for the 4 rats used in Experiment 2.

Experiment 3: Go/No-Go Retronasal Odor Discrimination and Rule Transfer

Experiment 3 is an elaboration of Experiment 2 and is performed with the same operant conditioning box and setup as Experiment 2. The only change implemented is an adjustment for the number of trials in each session, how a trial is initiated and the number of odor sets used. A trial no longer automatically ends 10 s after its onset. A lick is required to initiate a trial, and rats are given 6 s to sample an odorized reinforcer and another 6 s to decide either to keep licking or to withdraw from the odor port, and then the trial is concluded. With the change, a rat is required to be actively engaging in the task until the program finishes a session with100 trials. Data collected when rats are not motivated in the session can be excluded from the analysis.

Experiment 3 has a total of 4 phases (Schematic in Figure 2.3). In the lick training phase, rats receive ~40 μL odorized solution (CS+) followed by 0.1M sucrose solution for 3 days to habituate to the experimental setting. In the second phase, Training (T), a second odorized solution (CS-) is added and predicts the delivery of a 0.05M quinine-HCl solution. Rats learn to discriminate CS+ from CS- and respond accordingly. After reaching 80% correct for the retronasal GNG session for 2 days, rats are then transferred to a novel odor pair for 4 days (R1) and the second novel odor pair for 4 days (R2). A total of three odor pairs (Table 2) are used, and the presentation order is counterbalanced for the 8 rats.

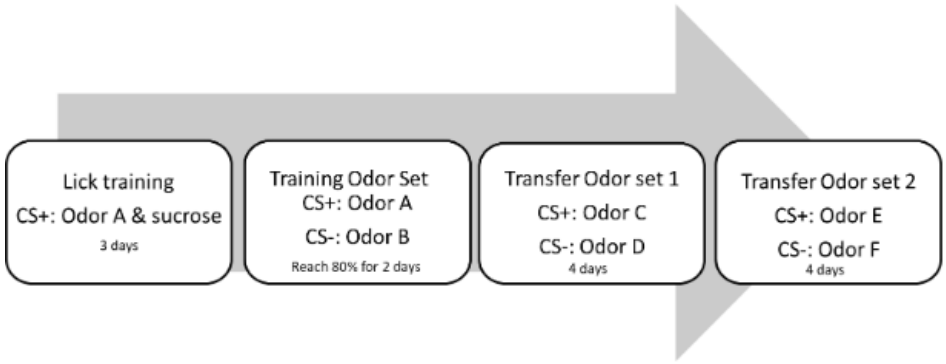

Figure 2.3. Schematic diagram for Experiment 3 on retronasal discrimination training and rule transfer.

Table 2. Odor sets used in Experiment 3

Odor Set	**CS+**			**CS-**		
	Odor	CAS #	Theoretical Vapor Pressure (kPa, 25C)	Odor	CAS #	Theoretical Vapor Pressure (kPa, 25C)
1	1,8-Cineole	470-82-6	0.220	Limonene	138-86-3	0.206
2	Anisole	100-66-3	0.566	Ethyl 2-methylbutyrate	7452-79-1	1.048
3	2-Hexanone	591-78-6	1.778	Methyl valerate	624-24-8	1.47

Three odor sets were used in Experiment 3. Odorants are matched by vapor pressure and are counterbalanced when assigned to CS+ or CS- during the experiments. Values retrieved from http://pubchem.ncbi.nlm.nih.gov/ or manufacturer websites.

Electrophysiological Methods

Electrode Implant

Rats were implanted with electrodes for electrophysiological recording in Experiment 3 to understand the neural network engaged in retronasal odor discrimination. Before each surgery, rats are given a subcutaneous injection of a ketamine cocktail (50 mg/kg ketamine, 0.75 mg/kg acepromazine, 5 mg/kg xylazine) for anesthesia and 0.1 ml buprenorphine for analgesia. Pedal reflex and respiratory frequency are monitored to maintain anesthesia, and an additional dose of ketamine is administered if rats are responsive during the surgery. Bipolar electrodes (100 μm diameter wire; ~1 mm vertical tip separation) are implanted in the left olfactory bulb (OB; +8.3 mm AP, 1.5 mm ML, ~4 mm DV), anterior piriform cortex (aPC, +0.5 mm AP, 3 mm ML, 7.5 mm DV, 15 degree from vertical), olfactory tubercle (OT, +1.6 mm AP, 2 mm ML, 8.5 mm DV), gustatory cortex(GC, +1.4 mm AP, 5 mm ML, 4 mm DV) and hippocampus (HPC, -4 mm AP, 3 mm ML,2 mm DV). Signals from electrodes are monitored during implants until the LFPs

are reversed across the two leads of the bipolar electrodes, indicating the two electrodes are positioned across the cell layer. A thermocouple electrode is implanted ~6mm anterior to the nasal suture. Reference and ground wires are attached to screws secured to the skull over the left and right cerebellum. Connector pins for electrodes and reference and ground wires are inserted into a round threaded headstage (Ginder Scientific) and cemented with dental acrylic. The experimental protocol starts two weeks after surgery for the rats' recovery.

LFP recording

All LFP data are sampled at 2 kHz with a Multichannel System 32-channel basic wireless recording in MCRack software (http://www.multichannelsystems.com/downloads/software).

Passive Odor Presentation

After the two-week recovery period from surgery to implant electrodes (see below), rats are plugged into a Multichannel System wireless transmitter head stage and placed in a transparent polycarbonate housing cage with clean cage bedding. Before the first presentation of the odorant, rats are allowed to move freely for 5 min for a baseline recording. The standard deviation of a 50s clean LFP signal without movement artifact during the baseline recording is used to normalize the odor-evoked oscillations for that session. Afterward, a selection of odorants across a range of volatilities is used because beta oscillation power changes as a function of chemical volatility (theoretical vapor pressure), which can also be a proxy for odor intensity (Lowry & Kay 2007). An experimenter places a cotton swab saturated with pure odorant and presses a button to track odor exposure for about 5 s. Each odorant is freshly

prepared before the experiment and presented in a block of 12 trials with >5 s between trials and 180 s between blocks. In orthonasal passive presentation trials, approximate odor onset times are recorded with a 5-volt TTL pulse triggered by the experimenter pressing a button when they place the cotton swab in front of the rat's nose.

Retronasal Odor Discrimination session: Rats are left in the operant behavior chamber before the start of a training session for 300 seconds. A 50-second recording within 300 seconds (manually scanned without artifacts) establishes the baseline power and coherence for the session. During a retronasal olfactory licking trial, an infrared beam sensor is activated at the time when rats start licking at the lick spout, and an output card connected to the Med-PC system sends 5-volt TTL pulses that signal the start of a trial.

Sleep: Rats (n=5) are placed in their home cage for 90 minutes before and after training and LFPs are recorded from OB, OT, PC, GC, and HPC. The HPC electrode was used to monitor sleep stages. Video recordings are implemented for motion tracking, and the recording and videos are synchronized by a TTL sent to activate a light captured in the video and MCRack simultaneously.

Spectral Analysis

Data recorded with the MCRack system are loaded into MATLAB into a .mat data file with raw LFP signals and TTL data that marks experimental time points. All analysis was performed in MATLAB (R2018, R2021). All trials are aligned to the onset of a button press for passive orthonasal trials or the onset of the first lick for retronasal trials, and all trials are manually scanned for movement artifacts and are removed from data analysis if contaminated by

significant movement artifacts. Power spectral density, power spectrograms, and coherence are processed with the multi-taper method using the Chronux toolbox (Bokil et al., 2010). The procedure takes the convolution of fast Fourier transform of the time series and selected taper and then averages over the tapers. The multi-taper method can reduce noise and can be used to process short time periods (Thompson, 1982; Bokil et al., 2010). Power spectral density describes the distribution of power of the time series in the frequency domain. Coherence describes the correlation of the phase relationship between time series, with 0 denoting completely unrelated phase relationship and 1 denoting identical phase relationship. Coherence and the coherence spectrogram are calculated between all possible combinations of pairs of electrodes in OB, PC, GC. and OT. The value of calculated coherence is then arctanh transformed from the range of 0 to 1 to a normal distribution of 0 to infinity, referred to as z-coherence (Kay & Freeman, 1998). The parameters used in the multitaper analysis include time-bandwidth product, number of tapers, and size of moving window are adjusted based on the length of time series and type of analysis. Parameters are selected to optimize the peaks in coherence and power spectrum without over-smoothing on the frequency domain and the exact parameters used for each data set are articulated in the specific method section within each chapter.

CHAPTER 3: Transfer of retronasal olfaction exposure to orthonasal learning

To investigate whether retronasal and orthonasal routes generate qualitatively similar percepts[3], we pre-exposed rats to both appetitive and aversive odor–taste associations in a pure retronasal experience (Experiment 1, see Method Figure 2.2). We hypothesized that if the two olfactory routes generate similar percepts, retronasal learning should transfer to orthonasal Perdiscriminate retronasally pre-exposed (RPE) odor sets compared with novel odor sets. Because olfactory learning can be affected by the strength of the stimulus, we use both high- and low-volatility odorants. We show that learning transfer from pure retronasal experience to orthonasal odor discrimination is possible for the high-volatility odorants, suggesting that the two olfactory routes can share similar percepts if the odors are strong enough.

Methods

Statistical analysis for Experiment 1 looked at the learning rate and performance for the post-exposure orthonasal learning tasks. Latency to initiate licking after entry to the odor port and licks made in a trial are extracted from all trials for analysis. The average latency of CS+ and CS- trials for each session for all rats is calculated and paired-sample t-test were used to compare the mean latency of CS+ and CS- to examine whether rats are capable of discriminating 2 odorants. Performance is measured by the reward CS+ trials and unreinforced CS- trials divided by the total attempted trials normalized by the number of each trial type [P = Pcs+ correct/(2*Pcs+ attempt) + Pcs- correct/(2*Pcs- attempt)]. Within a moving block of 5 trials with

[3] This chapter is mainly adapted from my publication on Chemical Senses. Reference: He, R., Dukes, T. C., & Kay, L. M. (2021). Transfer of odor perception from the retronasal to the orthonasal pathway. *Chemical Senses*, *46*.

one trial step increments, a t-test was used to compare the latency for CS+ and CS- trials until a significant difference between CS+ latency and CS- latency ($\alpha < 0.05$) was reached for each session. Three-way repeated-measures ANOVAs are used to analyze the effects of retronasal pre-exposure, odor volatility, and test day on session performance and learning rate. Statistical analyses are performed in MATLAB, using functions *anovan* and *multicomp* for post hoc multiple comparisons.

Results

Response latency and licking behaviors

Rats show different response latencies and licking behaviors to CS+ and CS- in the orthonasal discrimination, which the rats learned (i.e., reached at least 80% correct) before starting the main experiment. They discriminate between CS+ and CS- odorants and prefer the sucrose solution over the quinine solution. Figure 3.1 demonstrates typical behavior during retronasal conditioning and orthonasal discrimination. Latency to lick the spout diverged as a rat learned to discriminate odorants in the orthonasal task (Figure 3.1A, average latency to lick was CS+: 0.62 ± 0.33s; CS-: 4.2 ± 1.6 s). A 5-s latency means that the rat refrained from licking the spout when the CS- was presented and waited until the end of the trial. To confirm that rats prefer sucrose to quinine solution, the average number of licks for sucrose is significantly higher compared with that for quinine once the reinforcer is delivered (Figure 3.1B, sucrose: 21.1± 4.3 lick; quinine: 6.5 ± 4.5 lick). Corresponding to trials with the 5 s latency, the lick count was zero in Figure 3b when a rat did not respond to the CS-.

The latency to lick in the retronasal conditioning session was not significantly different between CS+ and CS- trials (Figure 3.1C, average latency to lick was CS+: 0.61 ± 0.58s; CS-: 0.59 ± 0.35 s), which is consistent with an absence of external cues by which the rats could predict the reinforcer. The lack of differential response for CS+ and CS- at odor sampling was observed for each retronasal session individually when comparing the mean latency to lick for CS+ and CS- in each session (unpaired t-tests, all $P > 0.05$). In the retronasal task, once the rats started licking the odor-taste solution, they did show a preference for the CS+ odorized sucrose solution compared with the CS- odorized quinine (Figure 3.1D: sucrose: 20.9 ± 5.4 lick; quinine: 5.9 ± 2.1 lick). Rats prefer sucrose to quinine solution regardless of the presence of odorants.

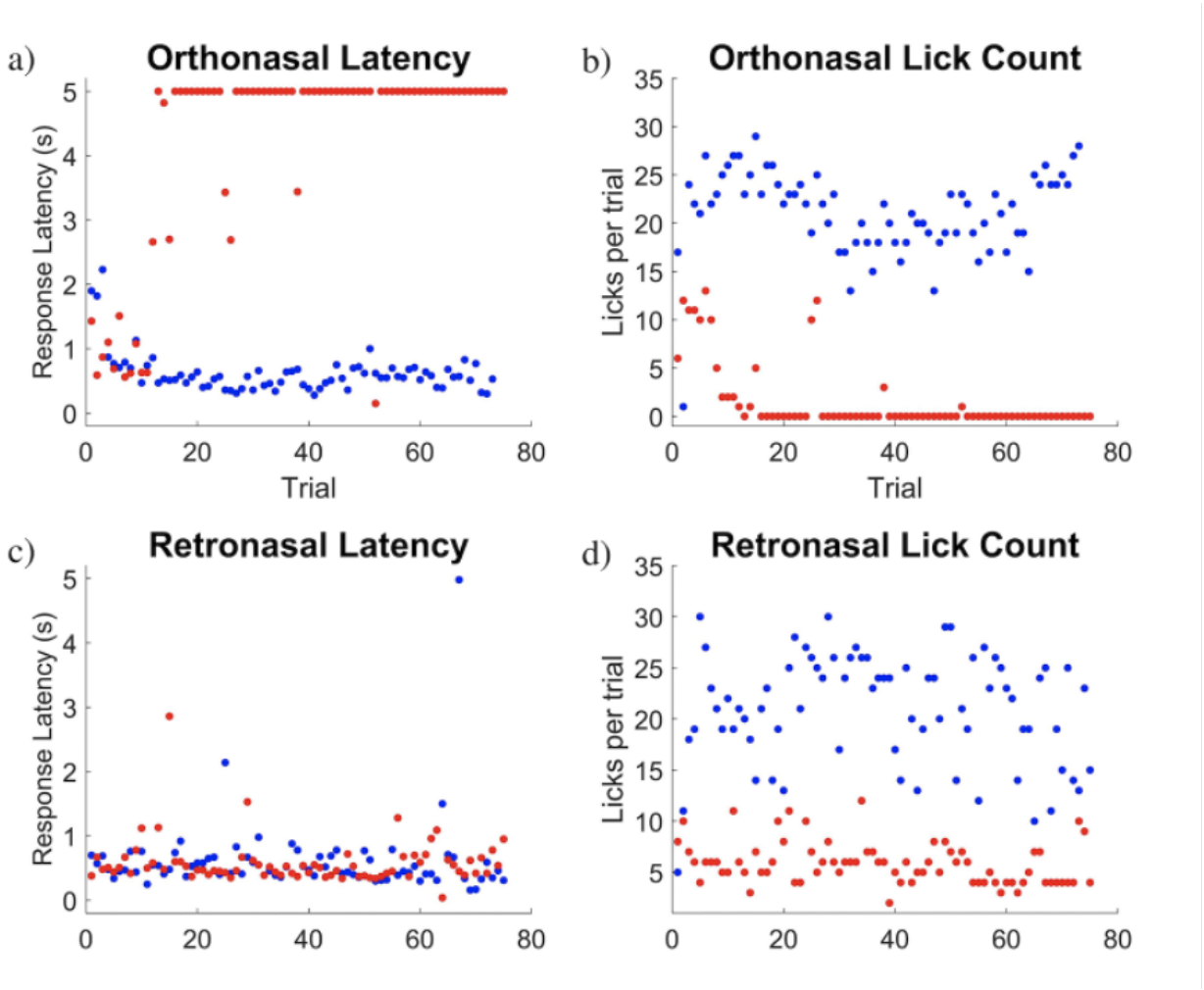

Figure 3.1. Latency and lick count of retronasal and orthonasal sample sessions. For an orthonasal session, the rat detected the airborne odorant with (a) different response latencies for CS+ (blue) and CS− (red), (b) licked for the reinforcer sucrose with CS+ or withheld from licking for CS−. Once he received the solution, the number of licks was higher for CS+. For a retronasal pre-exposure session, the rat showed (c) no response difference in approaching the lick spout for CS+ versus CS−, but (d) the number of licks was higher for sucrose once he received the odor–taste solution.

Volatility-dependent transfer from retronasal experience to orthonasal discrimination

For overall performance, the second-day performance was significantly better than the first day performance as rats progressed in the learning process (Day 1 performance: 85.6 ± 1.4%; Day 2 performance: 92.0 ± 1.1%; $F(1,123) = 18.9$, $P < 0.001$, $\eta^2 = 0.16$). A main effect of

the odor volatility on performance (high-volatility performance: 91.2 ± 1.0%; low-volatility performance: 85.6 ± 1.4%; $F(1,123) = 6.31$, $P = 0.013$, $\eta^2 = 0.05$), confirming that stronger odorants are easier to discriminate. We did not observe a significant main effect of the pre-exposure odorants or interaction between the independent variables in performance attained (Figure 3.2A).

When examining the learning rate (Figure 3.2B), we estimated the number of trials needed to reach significant response latency differences between odorants in the orthonasal session and found significant main effects of volatility ($F(1,123) = 6.68$, $p = 0.011$, $\eta^2=0.06$) and testing day ($F(1,123) =11.95$, $p < 0.001$, $\eta^2=0.10$), indicating that more volatile odorants are learned faster and significant discrimination occurs earlier on day 2. Retronasal pre-exposure was not significant as a main effect when comparing the learning rate between the RPE odorants and novel odorants, but we observed a significant interaction between RPE and vapor pressure ($F(1,123) = 4.21$, $P=0.043$, $\eta^2=0.036$). We deconstructed the interaction with a post hoc multiple pairwise comparison test with Bonferroni correction of the significance level. The results showed that the animals, on average, learned to discriminate the high volatility RPE CS+ and CS- odorants faster than the low volatility RPE odorants (high volatility discrimination learned in 7.8± 3.8 trials; low volatility 15.4± 12.1 trials, $p=0.008$). The other pairwise comparisons showed no significant differences; the learning rate for the novel high-volatility odorants and low-volatility odorants was 11.7 ± 10.6 trials and 12.6 ± 9.9 trials ($P = 1$ with Bonferroni correction).

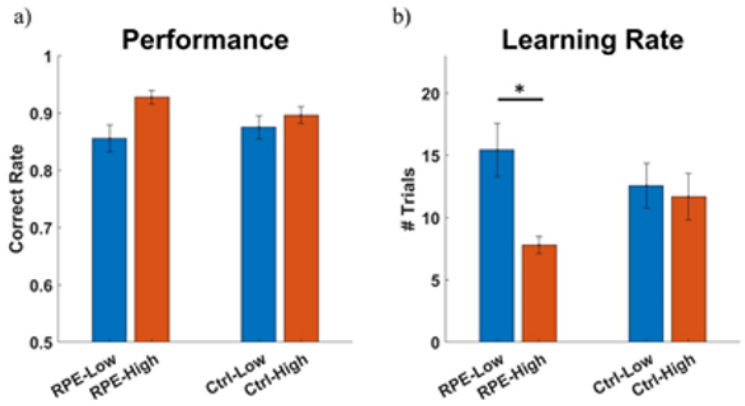

Figure 3.2. Overall performance (**a**) and learning rate (**b**) across conditions for Experiment 1. (a) There was a main effect on the odorant volatility (high orange, low blue; $P = 0.01$), but not on the retronasal pre-exposure on the overall performance ($P = 0.9$). (b) The trials needed to learn the odorants in the orthonasal task are significantly fewer for retronasal pre-exposed high-volatility odorants. Asterisk indicates significant learning rate differences between the retro-low and retro-high odorants.

Rats can detect and discriminate retronasal odors

The design of E1 was based on 2 assumptions that the odorants were detectable in the solutions and that rats retained the memory of the RPE odor for 2 days while we tested them on the orthonasal task. We performed a follow-up experiment E2 with four animals to test these assumptions. Rats first sampled an odorized solution in plain water and could continue licking for the following associated taste reinforcer. For the first set of odorants, the rats took an average of 5.25 ± 1.89 days to perform the task over 75% (Figure 6a). Once they mastered the first task (correct >85%), they were transferred to the second retronasal odor set. The rats were able to perform the task at above 68% the task at above 68% the first day on the new sets and maintained a correct rate above 65% for the 3 days of testing. Therefore, rats were able to detect and discriminate the retronasal odorants at the concentration used in E1. Additional rats tested

for another day showed that they too learned the odor-taste association quite reliably within the first 2 sessions (data not shown). The instrumental behavior to continue to lick the lick spout to receive more water and the reinforcer, which was not required for the odor-taste mixtures in E1 retronasal exposure, may be hard to master and required more than 2 days of practice for the first odor set. However, because all rats learned the discrimination on the first day of the second odor set, it is reasonable to conclude that associations are formed quickly even if the instrumental learning used in E2 takes a few days initially. To exclude possible contextual cues other than retronasal odorants, the odorized solutions were replaced by plain water and performance decreased to 46.1 ± 5.6%, which is not different from chance.

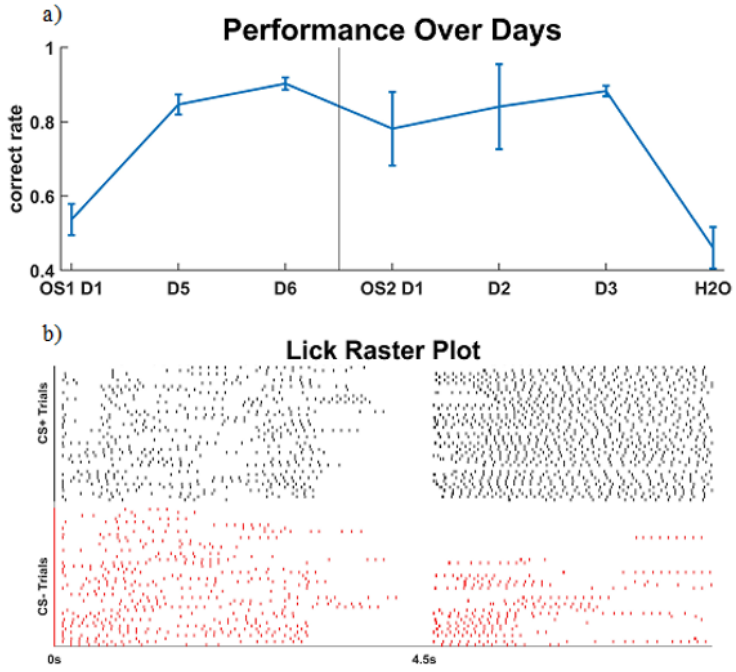

Figure 3.3. (**a**) Performance over days for E2 in which rats (n = 4) were trained in a retronasal task to discriminate the odorants in solution at the concentration used in E1. Performance started at approximately 50% chance level, reached 90% on Day 6, and maintained at 80% when the rats were transferred to the other odor set. When odorized solutions were replaced with water, the performance dropped back to chance level. (**b**) Example of a lick raster plot sorted by trial types

over time (blue: CS+; red: CS−; earlier trials on the bottom). Note that the rat ceases producing the second lick bout after smelling the CS− odorant retronasally after around 20 trials of CS−.

Discussion

In summary, consistent with our prediction, high-volatility odor pairs are faster to learn and easier to discriminate. In terms of the retronasal pre-exposure effect, the results have mixed outcomes; compared with the novel odorants, the RPE odorants did not show the main effects of significantly better performance or learning rate, which supports the theory that there exists a duality of olfactory perception via the two olfactory routes (Rozin, 1982). Nevertheless, we observed an interaction between retronasal pre-exposure and odorant volatility, that more volatile RPE odorants are learned faster compared with the less volatile RPE odorants, suggesting that retronasal pre-exposure affects subsequent orthonasal learning in a volatility-dependent manner. The results suggest that transference from retronasal to orthonasal experience is possible depending on odorant volatility, which implies that the two routes may share perceptual quality to some extent. The dual percept theory predicts that pre-exposure to retronasal experience with odors would not affect orthonasal learning, and these results cast doubt on the theory.

A recent study by Blankenship et al. (2019) argued that there is no apparent transfer of odor percept from the retronasal to the orthonasal route. In that study, rats were conditioned with 2 odorized solutions delivered passively via an intraoral cannula (i.e., retronasal stimulation), with one odorant followed by oral infusion of a sucrose solution and the other reinforced by plain water. After the conditioning, rats preferentially nose-poked to an odor port that was associated with retronasal odorants paired with sucrose. The conditioned retronasal odor preference,

measured by increased nose poking to the odor port associated with the CS+ odorant delivered orthonasally, failed to transfer the preference to airborne odorants, suggesting that retronasal and orthonasal odorants are perceptually different. In Experiment 1, performance estimated for the whole session of 150 trials was not significantly different between retronasally pre-exposed and novel odorants, and this negative result is consistent with the hypothesis that the 2 pathways produce different percepts. However, the lack of a performance difference may be attributed to a ceiling effect. The rats in our study were pre-trained in the orthonasal discrimination task on different odors, and after learning to transfer, the learned rule to new odor sets performance is high and robust to the subsequent odor sets (Frederick et al., 2017). Therefore, the rats performed at high performance levels overall (88 ± 11%), and learning rate instead of performance may be a better indication of perceptual transfer for the task. Moreover, we used a different training paradigm from that in the study by Blankenship et al. (2019); in our study, licking to sample the retronasal odorants is an instrumental response rather than passive oral infusion. The sampling procedure is more similar to naturalistic flavor learning, perhaps engaging the animals to better process the odor identity, and the licking may deliver the retronasal stimulus more efficiently to the retronasal pathway. In Experiment 1, we also positively reinforced one odorant with sucrose and negatively reinforced the other with quinine, which may have promoted avoidance behaviors and led to a more salient effect.

One parsimonious explanation of our results may be that the different learning rates we observed for the RPE odors sets are odor-specific for each tested orthonasal pair. Although we have not observed significant odorant differences in learning rate in olfactory discrimination tasks used in the lab unless the odorants are very similar to each other (Frederick et al., 2017),

we cannot rule out this explanation due to the limit in choices of tasteless odorants used in the study. In this study, the odor-taste association within an odorant pair, as well as the order of testing conditions, were counterbalanced for all animals, such that the presentation order of odorants and the synergic effect of odor-taste association should have minimal odor-specific learning effects on the results. Our study showed that specific odorants or the physicochemical properties (e.g., volatility) of odorants and the behavioral training and testing paradigm may play significant roles in retronasal/orthonasal olfactory learning, and these effects should be accounted for in future studies.

Odor volatility affects the perceptual threshold

The same chemical may generate a similar percept via two routes as a combined result of the physical attributes of odorants and the two olfactory routes. We focused on the effect of theoretical vapor pressure as a measure of volatility and observed that the high-vapor-pressure odorants were easier to discriminate orthonasally and were learned faster when they had been retronasally pre-exposed with tastants. One factor in the interaction we observed between pre-exposure status and volatility is that the two olfactory routes show physical differences in humidity, temperature, and airflow, which may strongly interact with solubility. This poses a conundrum regarding the systematic characterization of a chemical environment when odorants enter the nasal epithelium. To address the limitation, Scott et al. (2014) simulated electro-olfactogram (EOG) activation at the nasal epithelium with thermodynamic modeling and showed that EOG amplitude follows a curvilinear shape as a function of solubility for both orthonasal and retronasal routes, but the retronasal route has a lower amplitude due to concentration differences and the limitation of flow rate. Monomolecular odorants within the range of medium

to high mucosal solubility (estimated by air/mucus partition coefficient) elicited relatively high intensity among ~300 odorants simulated, and the more volatile odorants we chose fall within this range of solubility. It is possible that there exists a threshold of some physical attribute such as solubility, volatility, and/or concentration of odorants for perceptual similarity across the 2 routes because learning is transferred in our paradigm only for the high-volatility odorants. This perceptual threshold may be different from the detection threshold and is supported by the weaker but similar glomerular activation patterns for retronasal versus orthonasal stimuli (Gautam & Verhagen, 2012). In the second experiment, we demonstrated rats' ability to detect and discriminate the odorants at the concentration used in E1 for both high- and low-volatility odorants, and the disparity in learning speed between the high and low pre-exposed odorant is not caused by the rats failing to detect low-volatility odorants.

Due to the limited choice of known tasteless odorants at the time that we planned this experiment, hexanone and methyl valerate were the only pair of high-volatility odorants that rats experienced retronasally, and therefore the faster learning rate could be because these 2 odorants are more easily distinguished orthonasally. We also considered the possibility of a retronasal odorant leak if the vacuum is not sufficient or if odorized liquid remains on the rats' whiskers so that they smelled the odorants orthonasally. These both would predict increased learning or performance for both low- and high-volatility odorants instead of the interaction observed in our study.

Neural explanations for shared percepts between routes

Our study showed that an odor percept may transfer from the retronasal route to the orthonasal route if the odor stimulus is strong enough (highly volatile or highly soluble). This may mean that the transfer depends on concentration, and there is ample evidence that neural circuitry in the olfactory bulb can produce concentration invariance in the physiological response. Olfactory information, by its nature, depends on concentrations of odorants that may fluctuate within a sniff cycle, over a breathing period, or between 2 olfactory routes, but the odor quality is maintained. Imaging studies on the periphery show the variance in input from olfactory sensory neurons in the nasal epithelium is normalized and sequentially gives rise to a more consistent output amplitude and spatial distribution in the mitral and tufted cells (Storace & Cohen 2017). Cortical or higher-order neural responses in mammals and insects, which arguably represent odor identity, have a more reliable odor-specific firing pattern regardless of various concentration levels of an odorant (Bolding & Franks, 2017; Cleland et al., 2012; Stopfer et al., 2003; Wilson & Sullivan, 2011). Spatial encoding of odor perceptual quality may serve as another argument for similar percepts across routes. Prior studies have shown that glomerular activation patterns may represent a "map" for odor identity (Johnson & Leon, 2000; Meister & Bonhoeffer, 2001; Wachowiak & Cohen, 2001), and overlapping of glomerular activation can predict perceptual quality overlap (Linster et al., 2001). Odorants from the 2 routes do evoke a similar glomerular ensemble once the odor information activates glomeruli as imaged on the dorsal OB (Gautam & Verhagen, 2012). The source of a difference in perceptual quality between retronasal and orthonasal routes is thus likely to arise somewhere besides the glomerular activation pattern. The same study also showed that retronasal odorants arrive at the nasal

epithelium more slowly than orthonasal odorants to initiate a response cascade. However, the temporal encoding of odor identity is relatively understudied for the two routes once an odorant binds to the olfactory receptors.

It is crucial to understand how animals can generate consistent perception yet maintain distinctive information about the source of odors when odorants enter from 2 different routes in flavor acquisition and odor learning. It is equally important to understand how multimodal effects such as odor and oral or nasal sensation may fundamentally alter the perceptual experience. Odorant-evoked behaviors and engagement of the neural systems may help unravel perceptual convergence and divergence of 2 olfactory inputs identical in chemical profile. In this study, we showed that learning transfer from retronasal to orthonasal perception is possible and depends on the odorant properties, suggesting that there can be a shared percept across the routes, contradicting the duality of smell theory (Rozin, 1982).

CHAPTER 4: Behavioral Analysis of Retronasal discrimination Tasks

Experiment 2 provides insights into rats' ability to discriminate retronasal odorants in Chapter 3. Here I continue to examine in-depth how retronasal discrimination tasks are acquired and transferred to new odor sets (rule transfer) using rats naive to the odor discrimination tasks (n=8, 4 males, 4 females). The previous study showed evidence that the volatility of the odor is a factor in whether or not retronasal preexposure affects the learning of the orthonasal task. This suggests that more volatile odorants may be easier to detect and discriminate when delivered retronasally.

Working with implanted rats allows me to focus more precisely on the behaviors associated with retronasal odor discrimination tasks, including licking and breathing, since they gate the inputs to the olfactory system. Unlike orthonasal odorants that are inhaled in somewhat discrete samples and bind to OSNs within a 100-150 msec sniff cycle, retronasal odorants are dispersed into the nasopharynx more slowly, and the speed of airflow can be affected by oral movements like licking or chewing. Therefore, we may expect fluctuation in respiratory and licking rates as the rats discriminate the odorants. Moreover, LFPs in the olfactory system may also reflect the sensorimotor inputs through high coherence with licking and respiration.

Methods

Retronasal discrimination task performance

Performance for a session is measured by the number of rewarded CS+ trials plus unreinforced CS- trials (trials without lick responses to the reinforcer) divided by the total attempted trials normalized by the number of each trial type [P = Pcs+ correct/(2*Pcs+ attempt) + Pcs- correct/(2*Pcs- attempt)]. Sessions with fewer than 50 trials are excluded from the data

analysis. A one-sided t-test is used to determine whether rats performed beyond the chance level of 0.5. Three-way repeated-measures ANOVAs are used to analyze the effects of rats, training type (T, R1, R2), and odor sets (Table 2) on retronasal discrimination performance. The first qualified session and the last two sessions for T, the four sessions for R1 and R2 are used for the statistical analyses performed in MATLAB, using functions *anovan* and *multicomp* for post hoc multiple comparisons.

Breathing and Licking Extraction

In the retronasal odor discrimination tasks, water-restricted rats sample odorants and consume reinforcers by licking. Rats are obligatory nasal breathers, meaning that they are capable of breathing at the same time as eating or swallowing. In the study, we monitor the sensorimotor inputs from licking and breathing during the experiment. Respiration is monitored using thermocouple electrodes implanted in the nasal cavity (See Methods).

Licking is extracted from local field potential recorded from the ventral PC or ventral OT electrode. Due to the electrodes' positions, they also pick up very high frequency EMG signals from the jaw muscle and can be used as an approximation of licking behavior. Figure 4.1 demonstrates the process of lick extraction. The raw signal recorded in the ventral piriform cortex or olfactory tubercle is passed through a 200 Hz high-pass filter. Each burst in the high-pass filtered signal corresponds to a lick, as verified by video recording. A lick corresponds to a peak of the envelope of the processed signal.

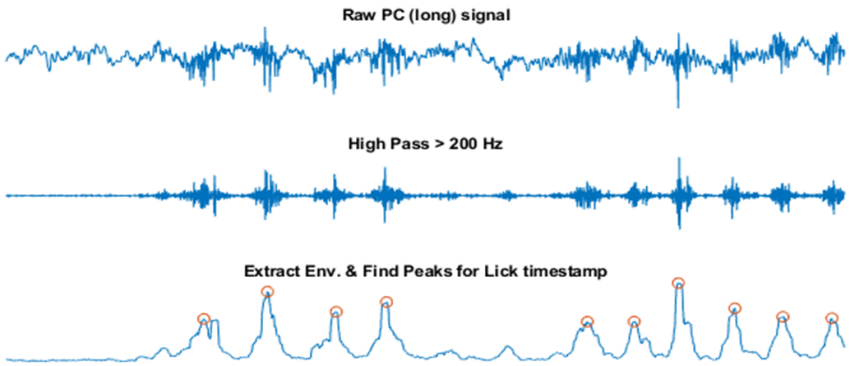

Figure 4.1. Extraction of lick signal from piriform cortex LFP. (A) An example of a 2-second LFP recording in the ventral piriform cortex. (B) The signal from (A) is passed through a 200 Hz high-pass filter. (C) Licks are extracted by locating the peaks of the envelope of the filtered signal. The amplitude of signals is adjusted for demonstration.

Results

Acquisition of retronasal odor discrimination task discrimination

Training is designed to ameliorate avoidance effects and novelty phobia. Rats show fear of novelty when first introduced to new environments and tasks. Furthermore, the use of aversive stimulus like quinine could result in lack of motivation. Therefore, we take these into consideration. The 3-day pre-training licking session accustomed the rats to lick from the concentric lick spout. By the end of the third session, the water-restricted rats were motivated to finish all 50 trials of CS+ with sucrose within 30 minutes. When the CS- (quinine) was introduced in T, 4 out of the 8 rats attempted less than 5 CS- trials, and 7 of them did not finish the 100 trials on the first day. Therefore, final performance evaluation is based on the first qualified session (i.e.,rats attempted more than 50 trials) and the last two sessions for T.

All rats acquired the T odor set and reached performance above 50%. Performance for each rat over three learning phases are plotted in Figure 4.2A. A one-sided t-test comparing

average performance to the chance level at 50% is used to estimate whether rats learned odor discrimination trials (Figure 4.1B). Rats quickly picked up the task once they overcame the aversion to quinine trials and performed above chance in the first session where they attempted more than 50% of the trials in a session. Rats needed 6-12 days to reach the performance criterion of 80% during the training phase.

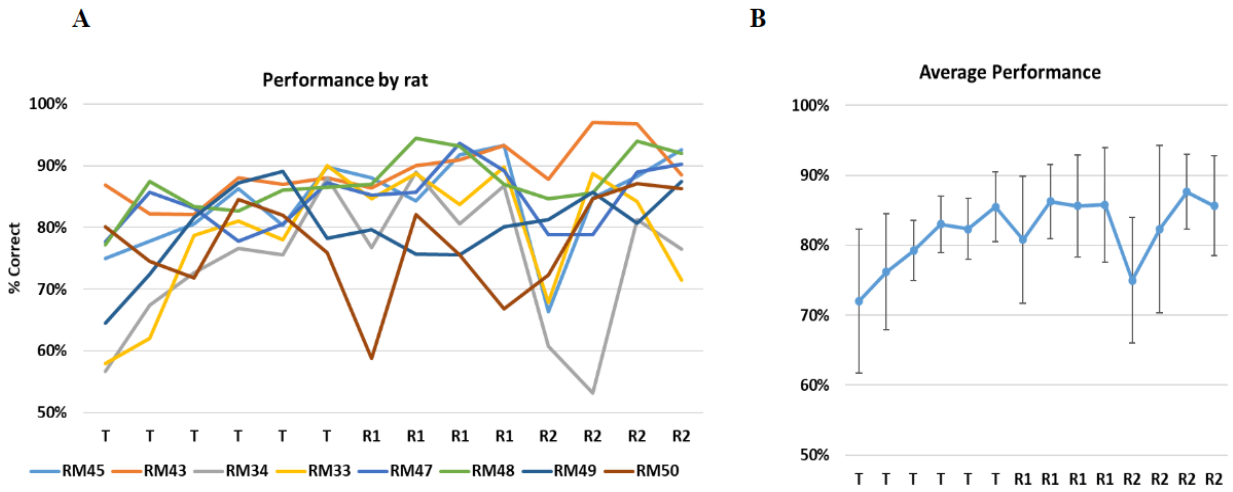

Figure 4.2. Retronasal discrimination task performance. (A) Performance is calculated by the percentage of correct trials over the total trials in each session. The percentage of correct trials is plotted for the first three sessions and the last three sessions for training odor pair (T) and four days for both rule transfer odor pair (R1, R2). (B) Average performance for all rats (n=8) on the same day of the training phase with standard deviation. The average performance is significantly above chance at 50% for all days (one-sided t-test, $\alpha > 0.01$).

The performance is significantly different between training phases ($F(2,95) = 10.04$, $p<0.001$, $\eta^2 = 0.31$, Figure 4.3A). The performance for R1 (84.6%, SE:1.6%) is significantly better compared to that of T (79.0%, SE:1.4%, $p<0.001$) and R2 (82.6%, SE:1.8%, $p=0.02$), but performance in T and R2 are not significantly different from each other ($p=0.68$). The

performance of T was hypothesized to be lower due to the novelty of operant learning. However, the performance of R2 is low may be due to the delay between R1 and R2 for two of the rats. Two rats (RM33 and RM34) were trained on R2 a month after they finished R1 training due to the COVID-19 lockdown, while the others were transferred to R2 immediately after R1. Both rats experienced a dip in performance, which may lead to lower average performance and larger variance for R2.

Odor volatility plays a role in retronasal odor learning as we see some evidence of retronasal learning transfer to orthonasal discrimination for high volatility odorants (He et al., 2021). Consistent with the hypothesis, the result shows a main effect of volatility ($F(2,95) = 4.42$, $p<0.016$, $\eta^2 =0.14$). The odor pair with the highest volatility, HEX and MV, has better average performance (84.6%, SE:0.9%), compared to the mid-volatility odor set, AA and EMB (81.3%, SE:2.0%, $p = 0.046$) and the low-volatility odor set, HEP and MB (average 80.4%, SE: 1.9% $p =0.037$). There was no difference between the low and medium volatility odor sets ($p=1$). This partially aligns with our original hypothesis that high-volatility odorants may be perceived as strong and easier to discriminate.

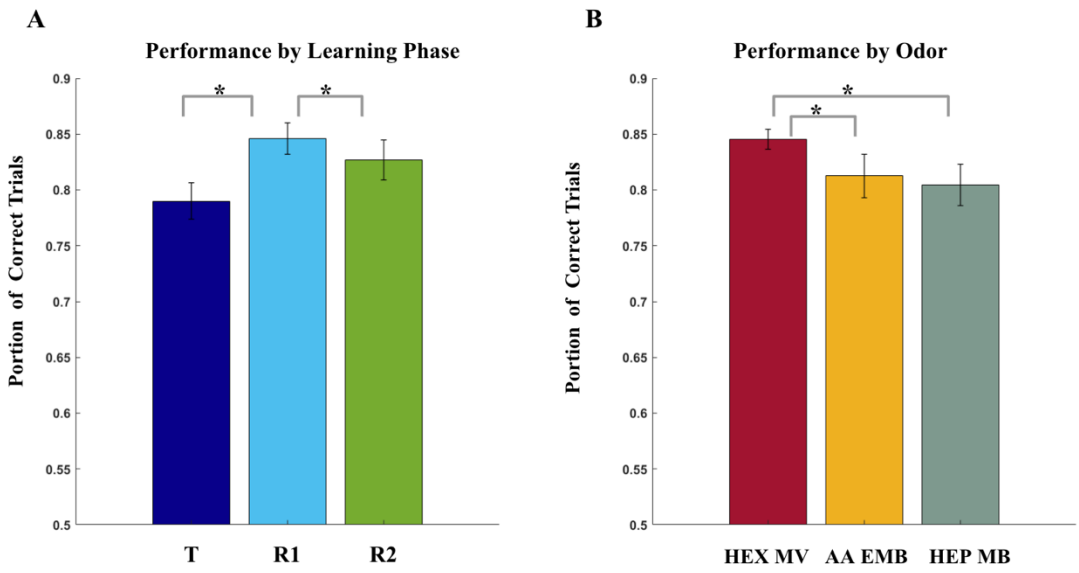

Figure 4.3. Performance of retronasal discrimination task grouped by (A) learning phases (T, R1, R2) and (B) odor pairs.

Respiration changes over time in a trial

I first examined the respiratory signal during the resting state to establish a baseline for the thermocouple electrode and OB theta recording. Figure 4.3A shows an example 5-second LFP recording from the OB and the nasal thermocouple (TC). Both signals are band-passed with a theta band 2-12Hz filter. The OB LFP closely follows the thermocouple signal in phase and amplitude, and a more detailed analysis is devoted to coherence relationships between OB LFP and respiration in Chapter 6.

The respiratory frequency for the resting state is calculated using a 50-second baseline recording collected prior to the experiment. The number of cycles is tallied for each second in each baseline recording, and ten baseline recordings are used for each animal (n=8). Figure 4.4 shows the distribution of respiratory cycle frequencies. The average respiratory frequency

extracted from the thermocouple electrode is 6.6 Hz, and the standard deviation is 1.34Hz. The average frequency of OB LFP is lower at 6.3 Hz (std: 1.3, p <0.01).

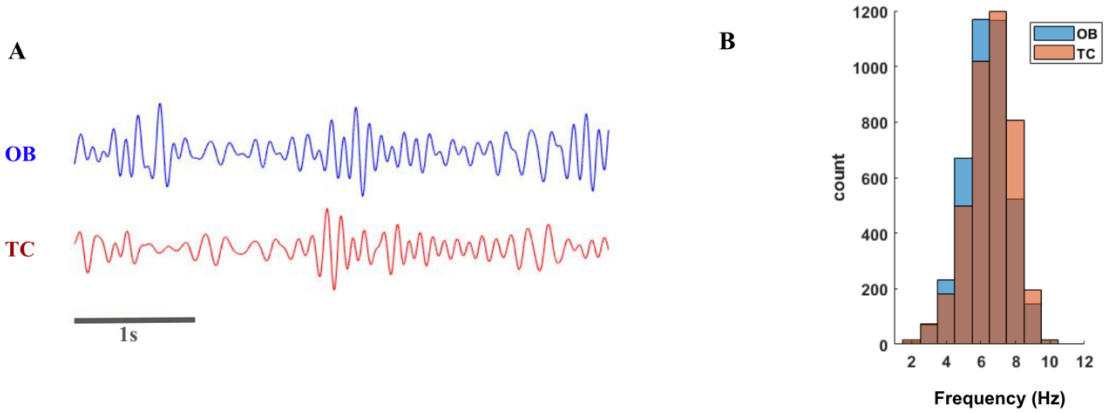

Figure 4.4. (A) Sample recording from OB LFP and thermocouple (TC) electrode. (B) Distribution of respiratory frequency recorded in the OB (blue) and TC (red).

Next, I examined the respiration rate change over a behavioral trial. An average respiratory frequency is calculated for each type of trial (CS+, CS-) and for sucrose reinforcement licking and post-CS- waiting time for each session (rat=8, a total of 110 sessions were used, and only sessions with a >50% attempt rate were used). Trials are aligned to the delivery of the odorized solution at time 0. The breathing rate extracted from the thermocouple electrode and OB theta show similar trends. The respiratory rate is higher before the odor onset at ~7 Hz and is maintained for the first second. Unpaired sample t-tests show that the breathing rates for CS+ and CS- start to diverge 1-second after onset and stay at ~6Hz for CS+ and ~6.5 Hz for CS-.

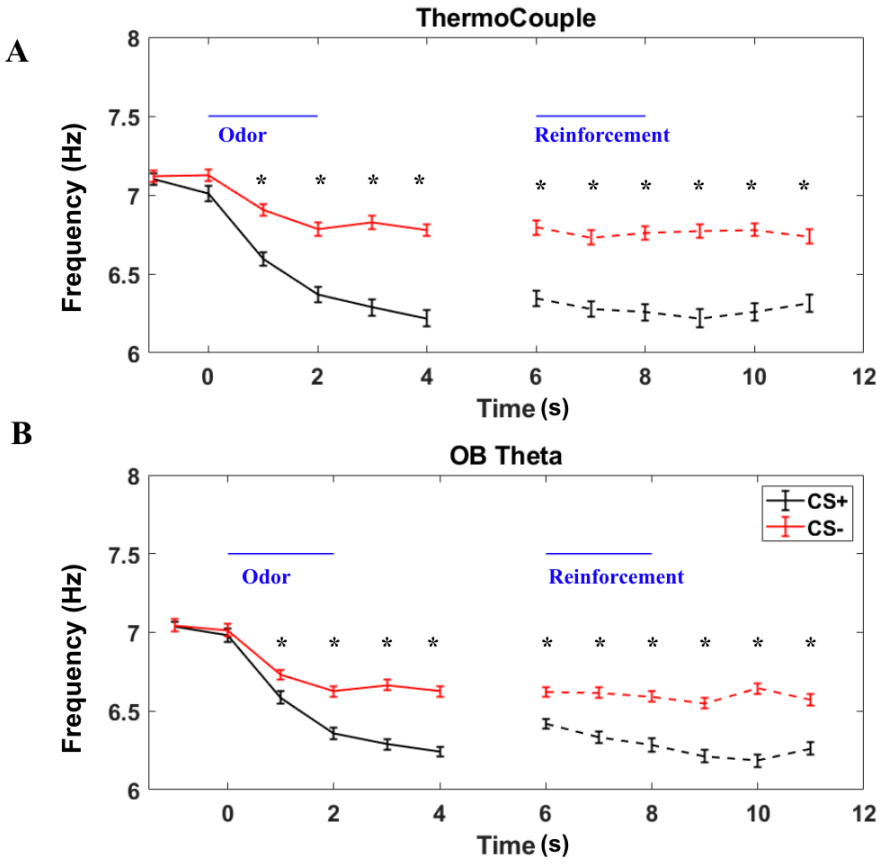

Figure 4.5 Respiration Frequency during retronasal odor discrimination experimental trials. Average respiratory frequency for each second (n=8, session = 110) with SEM recorded from (A) the thermocouple electrode or (B) extracted from the OB theta

Lick dynamics over time in a trial

Licking frequency is calculated by counting the number of licks in each second from one second prior to the onset of odor delivery (t=0) and 10 seconds after (Figure 4.6). Two licks are needed to activate the lick spout, and the lick rates are similar for CS+ and CS- at the beginning of a trial before t=1. CS+ licking frequency for the first second is significantly different from that of CS-, suggesting that rats only need a few licks within 1 second to discriminate two odorants. Rats continue licking at a high frequency ~5-6Hz for CS+ even after the solution is sucked away by the vacuum. The licking pattern extracted from ventral PC or OT LFP is consistent with the

licking pattern in Experiment 1, with a high licking rate for the reinforcement sucrose (7.3 ± 2.5Hz) and low for quinine (2.7 ± 1.7Hz).

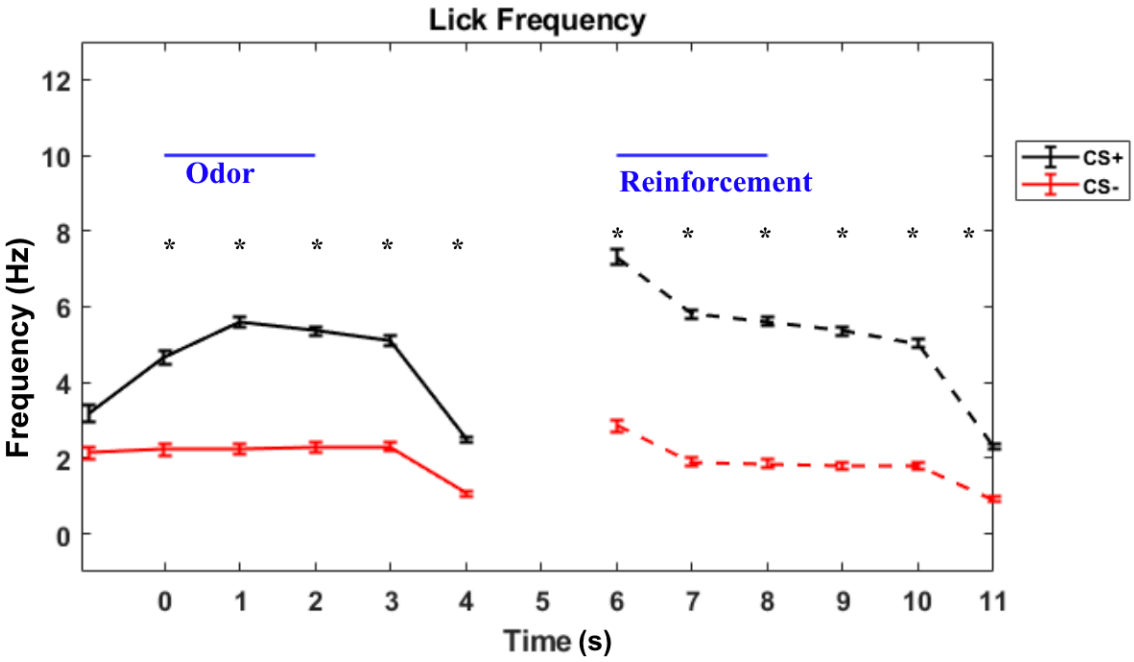

Figure 4.6. Licking behavior during retronasal GNG trials was analyzed with the LFP lick extraction method. Average licking frequency (rat = 6, session = 96) plotted over 10 seconds (Mean ±SEM). Time =0 denotes the onset of delivery of odorized solution (CS+ or CS-), and time = 6 denotes the onset of the reinforcer (sucrose or quinine).

Discussion

In this chapter, I provide a description of acquisition and rule transfer for retronasal learning and its related task-related experience. The average session performance showed significant main effects of the odor pairs that vary by volatility and the training phase. Similarly, orthonasal discrimination tasks (He et al., 2021; Rojas-Libano & Kay, 2012) show that chemical properties such as high sorption (tendency to be absorbed into water/mucus) and high volatility (tendency to leave a pure odor solution to the air) correlate with a stronger perceptual experience

and ease of discrimination. Consistent with the hypothesis, rats perform best at discriminating the two most volatile odorants, HEX and MV in the retronasal tasks. HEX and MV are also the high-volatility odorant pair that showed evidence of transfer to orthonasal learning in Chapter 3. The effect of volatility was elaborated in the discussion in Chapter 3.

The behavioral responses are stereotypic for the retronasal odor cues. CS+ is associated with continuous licking on the lick spout and a decrease in respiratory rate, whereas CS- is associated with a lower licking rate and higher respiratory rate. In this study, the rats are discriminated retronasal odorants in under 1 second, because the divergence of licking and respiratory rate both happen after 1 second of licking the odorized solutions. Although the retronasal route is considered to be slower, the results are consistent with the rapid identification of orthonasal odorants with a few sniffs and that of tastants within a lick (Weiss & Di Lorenzo, 2012).

Retronasal vs orthonasal odor sampling

Odor sampling behaviors in orthonasal olfactory discrimination tasks have been well characterized. Rats can discriminate monomolecular odorants in about 300 ms with a few (1-3) sniff cycles and often with an increase in sniff frequency (Uchida & Mainen, 2003; Kepec et al., 2007) The sampling duration required to discriminate two odorants may be affected by many factors such as sorption of chemicals (Rojas-Libano & Kay, 2012), type of tasks (Slotnick, 2007; Frederick et al., 2017) or even nose movement (Parker et al., 2020) just to name a few. The systematic sniffing behavior change is argued to be important for odor-guided behaviors and facilitates odor identification (Wesson et al., 2008).

In the retronasal trials, the respiration rate is on average higher beginning at the beginning of the trials and drops for both CS+ and CS- (Figure 4.5). The sniff rate may still be elevated because it is higher than the average baseline breathing recorded before the experiment, and the fast sniffing may be due to the expectation of a trial signaled by the house light 1 second before the rat can initiate a trial. This may suggest that fast sniffing for odor sampling is a universal characteristic not exclusive to orthonasal olfaction.

Licking may also modulate breathing frequency since the breathing rate is low when rats are actively consuming CS+ or CS-. Licking can also drive coherent neural activity by providing orosensory, taste and olfactory input in a rhythmic manner. Spiking of neurons in the insular cortex, amygdala, and orbitofrontal cortex are coherent with licking when rats lick a pleasant tasteful solution, and the coherence increase as the rats acquire a taste discrimination task (Gutierrez et al., 2010). Retronasal olfaction often involves oral movements like licking, chewing and swallowing during food consumption. A difference in the licking behavior may indicate a difference in stimulus input to the olfactory system.

CHAPTER 5: Oscillations in the Olfactory System: Frequency Analysis

Neural oscillations (See Chapter 1) in the olfactory system are a beautiful demonstration of dynamic processing in the brain. Instead of viewing the brain as a passive, stimulus-responsive organ, we should understand sensory processing in the brain as a dynamic process with both bottom-up and top-down modulations. To understand how the olfactory system is engaged in retronasal olfactory learning, I recorded LFP signals from the OB, OT, PC, and GC, intending to characterize how gamma and beta oscillations may change in response to odor delivery route, odor volatility, and learning. I begin by questioning whether the retronasal perceptual experience is characterized by the same set of physiological patterns as the orthonasal processes previously characterized in the lab (Kay & Beshel, 2010; Frederick et al., 2016).

Retronasal olfaction is associated with weaker nasal stimulus, prolonged and damped activation of glomeruli (Gautam & Verhagen, 2012; Furudono et al., 2013), and different contexts and behaviors (licking). Functional connectivity in the olfactory system is extensively researched in orthonasal paradigms but has not been characterized for retronasal olfaction. Gamma and beta coherence are hypothesized to facilitate inter-regional communication (Buzsáki & Schomburg, 2015; Engel & Fries, 2010), and the strength of beta OB-PC coherence is enhanced for orthonasal olfactory discrimination tasks when animals transfer learning to another task (Martin et al., 2004; Kay & Beshel, 2010; Frederick et al., 2016). The previous studies have laid the foundation and led me to speculate whether the oscillatory patterns of retronasal olfaction resemble those seen in orthonasal oscillation.

First, for the local network in the OB that generates gamma and beta oscillations, I hypothesize that gamma oscillations driven by respiration and odor stimuli may result in weaker

amplitude than in orthonasal smelling, especially in the later odor sampling trial as we see a decrease in respiratory rate. Beta oscillation power and coherence may increase due to the coordination within the network over learning. If beta coherence plays a functional role in task acquisition, I should expect the OB to become more coherent with other brain structures for the retronasal tasks.

Secondly, PC and OT receive direct and indirect inputs from the olfactory bulbs and show odor-specific responses (PC: Stettler & Axel, 2009; Bekker & Suzuki, 2013; OT: Xia et al., 2015). GC receives direct input from the PC (Maier, 2017). Gamma oscillations are also reported in the piriform cortex (Luna & Schoppa, 2008; Gonzalez et al., 2022) and the OT (Carlson et al., 2014), but whether population dynamics in these structures sustain a local excitatory-inhibitory network that generates gamma during retronasal olfaction remains unknown. Long-range coordination between brain regions in the beta frequency band has been widely reported in the brains when animals engage in learning and motor preparation (Bowyer, 2016). The coordination suggests that beta power in all structures may increase when animals engage in taste-driven, retronasal tasks.

Besides the differences in oscillatory patterns in brain structures, the setup of retronasal olfactory learning tasks allows me to examine the effect of the learning phase, odor hedonics, and volatility on both the temporal structure (duration) and the population dynamics of the neural network.

The strength of LFP coherence with the sensorimotor processes (respiration and licking) may indicate how sensorimotor inputs drive the network in different behavioral states. As discussed in Chapter 4, CS+ and CS- evoke different behavioral responses, I therefore

investigate these sensorimotor inputs to the olfactory system by examining the coherence between LFPs, respiration, and licking. These common sensorimotor inputs may entrain the LFPs in the olfactory or gustatory system as a shared input to the structures involved in retronasal odor processing.

Methods

This chapter focused on the frequency analysis of the LFP signals collected during Experiment 3. Chapter 2 provides details on the experiment paradigm and spectral analysis, and Chapter 4 summarizes the behavioral analysis from Experiment 3. Power and coherence for gamma and beta oscillations are calculated by the multitaper method, and the parameters are set as 5 time-bandwith products and 9 tapers for optimal frequency solutions.

Statistical Analysis of Power & Coherence in retronasal tasks

To understand the systematic effect of the odor cue valence (CS+ vs. CS-), the learning phase (training odor set T, rule transfer odor sets R1 and R2), and odor volatility (high-, medium-, low-volatility odor sets). I first process the data so that I can directly compare the difference between sessions and rats. I extracted raw LFP signals aligned to the odor onset: 1 second of pre-odor (Pre), 2 seconds of early odor sampling (Early), and 4 seconds of late (Late) odor sampling. I then calculated the power of the gamma and beta bands of the three segments for each trial. I perform normalization by dividing the early-odor and late-odor power by pre-odor power and subtracting from 1 to center the data for each trial at 0. For example, if an early-odor trial has a change in power of -0.1, it means that the power is dropped by 10% compared to

the amplitude of the pre-odor baseline. We then calculate the average changes in a session by averaging changes in power for all the correct and artifact-free trials in a session sorted by CS+ and CS-.

The chance coherence level between two brain structures is calculated by randomly shuffling 80 2-second LFP trials recorded during resting states before the experiment. The coherence between mismatching trials is around 0.3 for all possible combinations.

The effects of the independent variables are examined by a mixed model ANOVA by setting the effect of rats on the data as a random factor while other variables, including recording site, odor hedonics, odor sampling period, learning phase, and volatility, as fixed factors. Separate analyses were performed for gamma and beta power. Multiple comparison analyses with Bonferroni correction are then conducted for different levels within the same variable in order to understand the drivers of the main effects.

Signal Validation: Orthonasal odor-evoked oscillation

I first demonstrate the characteristics of LFP responses to odors for the orthonasal route. Figure 5.1A shows an example of the LFP signals in the recorded brain regions in response to repeated passive orthonasal exposure of amyl acetate, which is in the high volatility range (Lowry & Kay, 2007). The power is prominent in the beta frequency range in the OB (15-30Hz; Figure 5.1B; parameters: 5 time-bandwidth product, 9 tapers). Highly volatile odorants sensitize the olfactory network and induce strong beta oscillations over repeated presentations (Lowry & Kay, 2007). Coherence spectrograms (Figure 5.1C) for the sample recordings show high coherence in the beta band between OB-PC, OB-GC, and PC-GC.

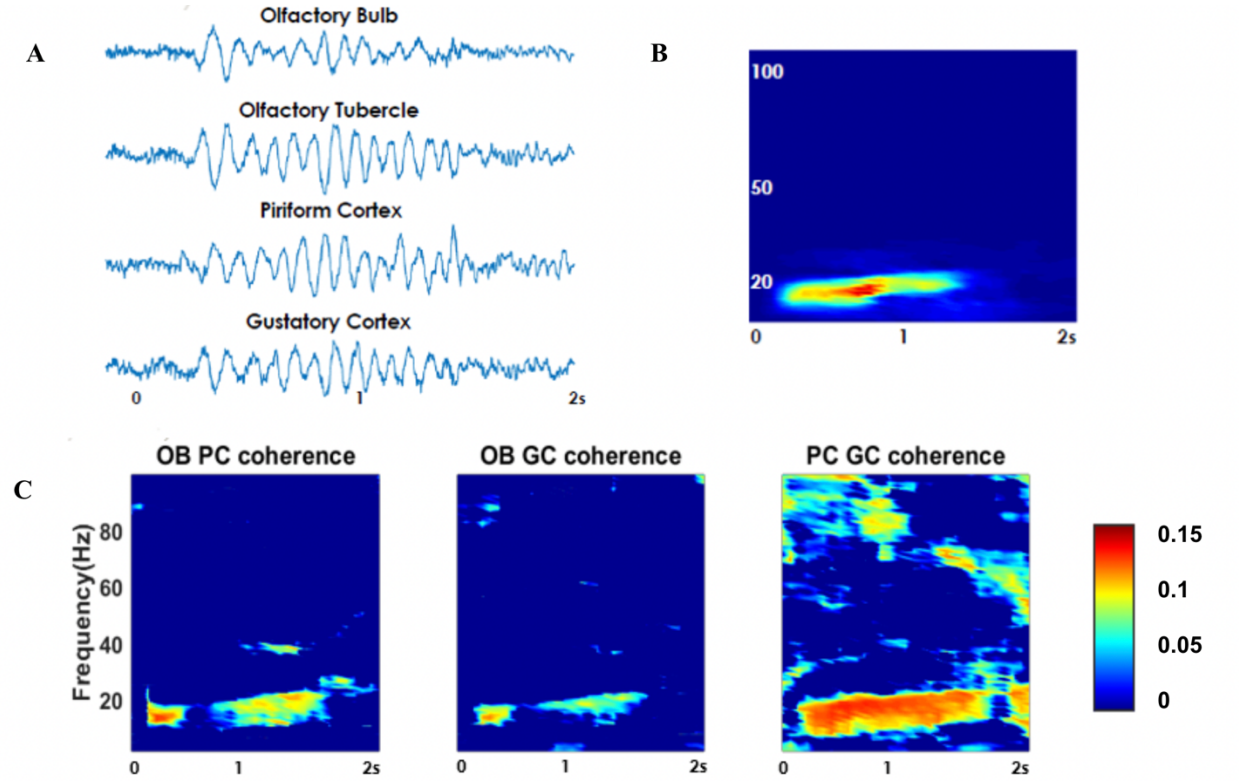

Figure 5.1. Single-trial orthonasal odor-evoked LFP. (A) Odor evoked beta in the brain structures recorded in response to amyl acetate. (B) Power spectrogram in the OB of the same signal displayed in A, showing high power magnitude in beta frequency (C) Coherence Spectrograms for OB and PC; OB and GC, and PC and GC calculated from LFPs in (A).

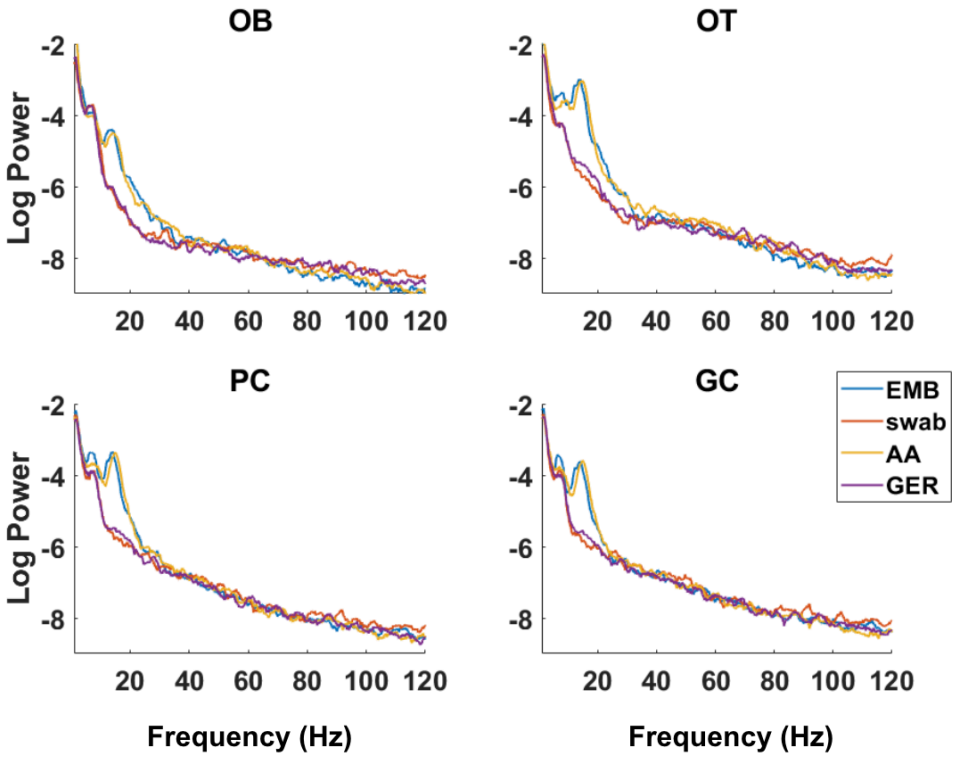

Figure 5.2. Power spectra during orthonasal odor presentation in the four brain areas. Three odorants, ethyl methylbutyrate (EMB), amyl acetate (AA), geraniol (GER) and a clean cotton swab. Power is averaged from 12 trials recorded in one session. Volatile odorants EMB and AA evoke elevated power in the beta frequency range in OB, OT, PC and GC. A low volatility odorant, geraniol, and an unodorized swab evoke little beta power.

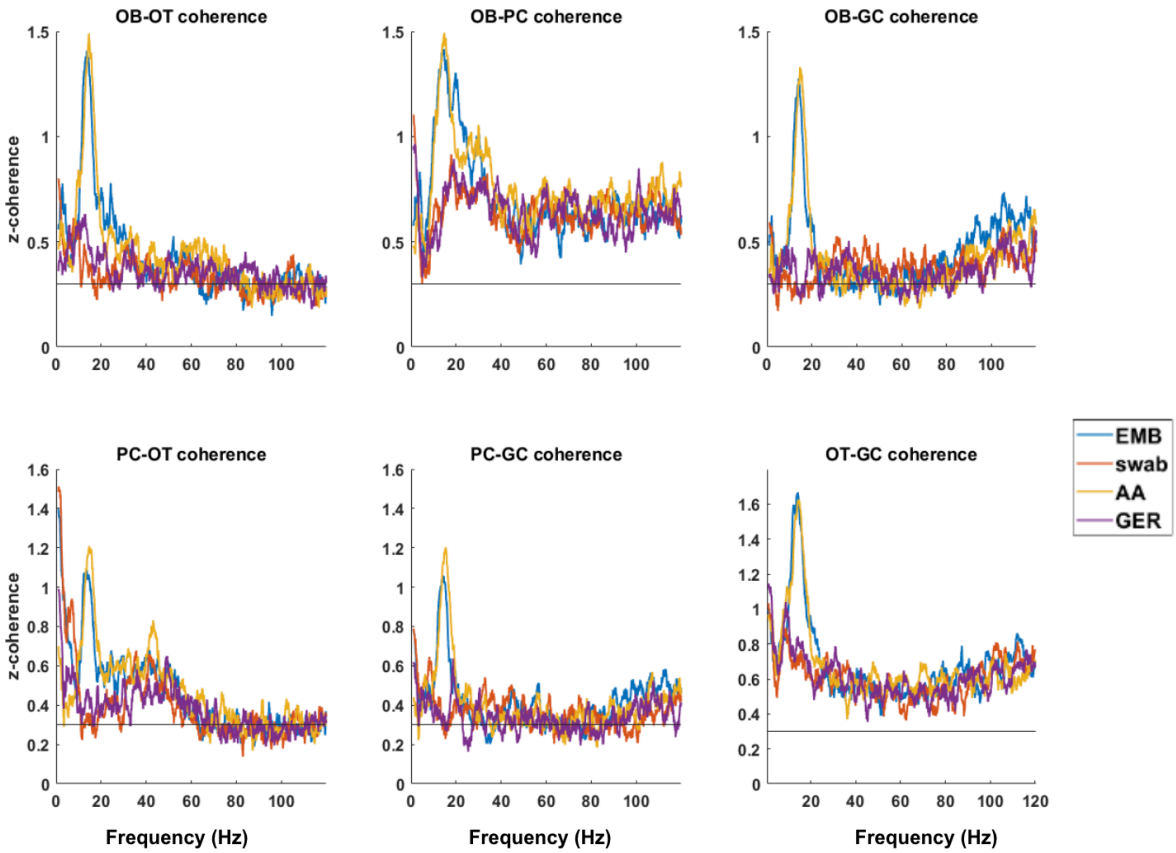

Figure 5.3. Coherence between brain structures during orthonasal odor presentations shows high coherence in the beta band. Black line (z-coherence=0.3) indicates coherence between mismatching signals.

Power spectra from (Figure 5.2) the OB signal are averaged across all clean trials out of the 12 trials for three odorants and clean swabs for one rat. High volatility odorants, such as ethyl methylbutyrate (EMB) and amyl acetate (AA), elicit strong beta power after sensitization, while low-volatility odorants, such as geraniol (Ger), show no significant difference from the unodorized swab in the beta range. The power spectra also verify the quality of signals that they are free from 60 Hz line noise. If signals were contaminated, one would expect a square-shaped

or single frequency increase in the power spectra around 60 Hz, which is not observed in the data.

Coherence between structures is plotted for the same orthonasal presentation sessions (Figure 5.3), and high coherence in the beta range is evident for the same odorants EMB and AA that elicited strong beta power. The odor-elicited and frequency specific coherence can also rule out the explanation that the high coherence is caused by volume conduction. If the signals were contaminated by volume conduction, one would expect high coherence across more frequencies.

Results

Figure 5.4 shows a sample of raw LFP signals recorded in a retronasal odor discrimination trial when the rat was actively sampling amyl acetate via the lick spout. In the sample data, it is apparent that the amplitude in the OB decreases once the rat starts licking the odorized solution and returns to normal amplitude about 1 second after the onset of licking. The respiration signal shown in red is extracted from the nasal thermocouple electrode, which matches the low frequency from the OB signals.

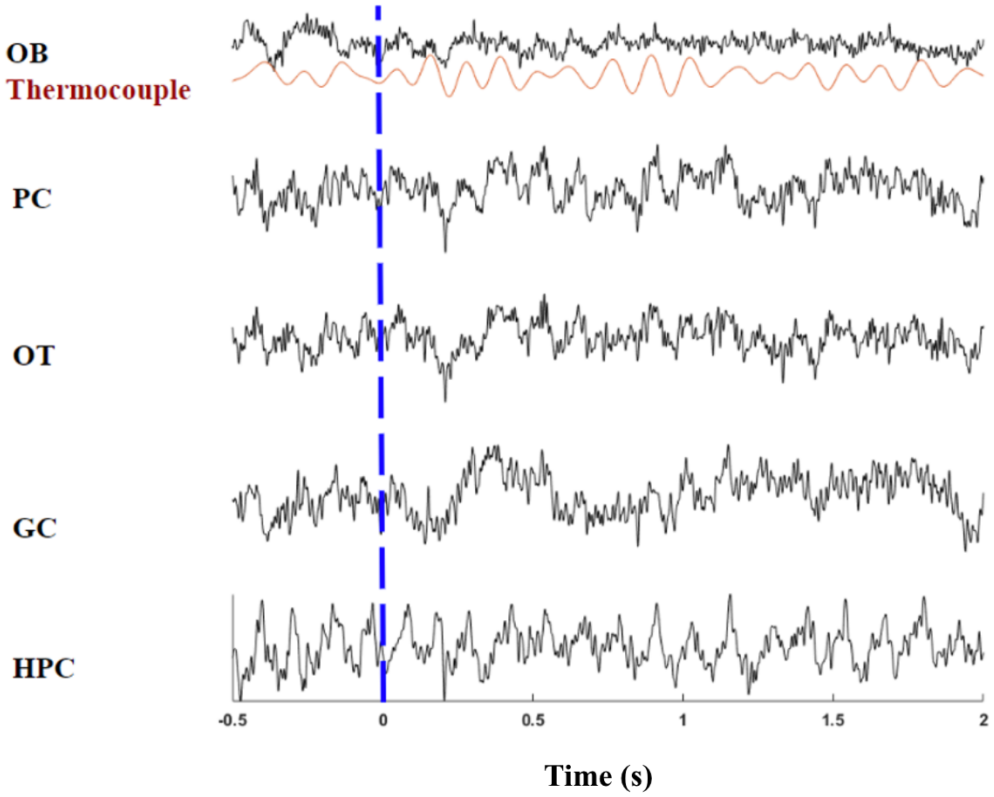

Figure 5.4. Raw LFP signal samples for 2.5 seconds were recorded in the OB, PC, OT, GC, and HPC during a retronasal odor discrimination trial. Signals are aligned to the onset of the odor at t=0. Amplitudes of the signals are all normalized by the standard deviation of a baseline recording with no motion artifacts and are on the same scale.

Spectrograms in Figure 5.5 show that the power of OB gamma and beta band oscillations changes over time. The spectrograms shown are averages of all trials in one sample session sorted by trial type (CS+, CS-) or the response periods (sucrose for trials on which they licked correctly after CS+ and waiting when the rat stopped licking after CS-). Gamma power drops when rats lick the odorized solution for both CS+ and CS-, and the power returns to pre-lick levels after 2 seconds. The 2-second gamma suppression is consistent across animals and sessions and aligns with the 2-second prolonged but lower mitral cell firing in response to

retronasal olfactory stimulus (Craft et al., 2021), suggesting that 2 seconds is a reasonable timeframe to examine the effect of retronasal odor exposure and discrimination.

Both gamma and beta power recover after 2 seconds from the decrease during odor sampling for CS-. For analysis, the waiting period for CS- trials is aligned to 6 seconds after the onset of the odor. Only the correct CS- trials were used for plotting the spectrogram so it is certain that the animals are not licking or sampling odor during the waiting period. The elevated power is not a result of odor input but could be caused by a sensitized olfactory network or centrifugal input from higher cortices required in learning discrimination.

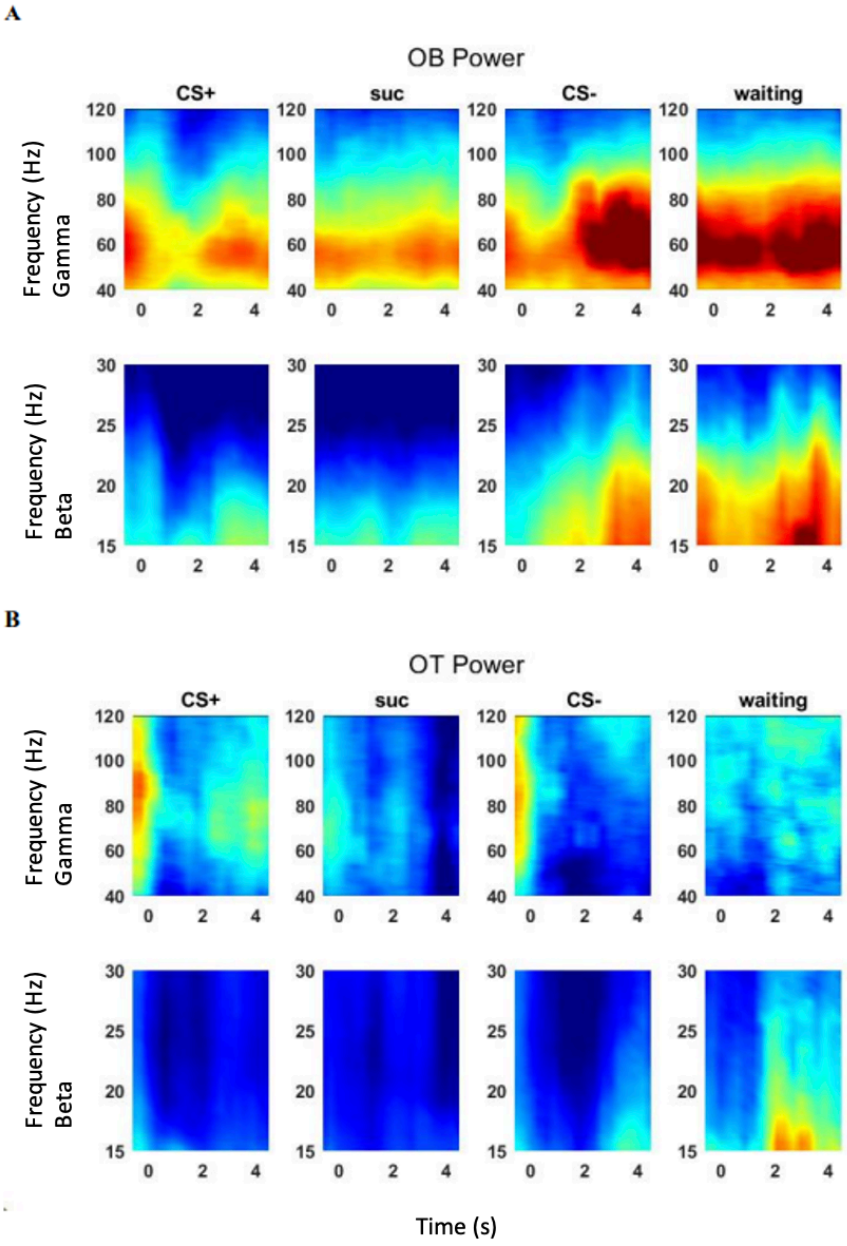

Figure 5.5. Spectrograms of gamma (upper row) and beta (lower row) power from one recording session. The colors in the spectrograms are plotted on the same log scale in gamma and beta bands for comparison and are categorized according to trial types, CS+ (n=42), CS- (n=43), and their responding period sucrose consumption after correctly responding to CS+ (n=49) and the waiting period after correctly withholding a response to CS- (n=25). Odorants used in the session are amyl acetate and hexanone. The y-axis of the spectrogram indicates frequency in Hz, and the x-axis indicates time in seconds.

Figure 5.5. Continued.

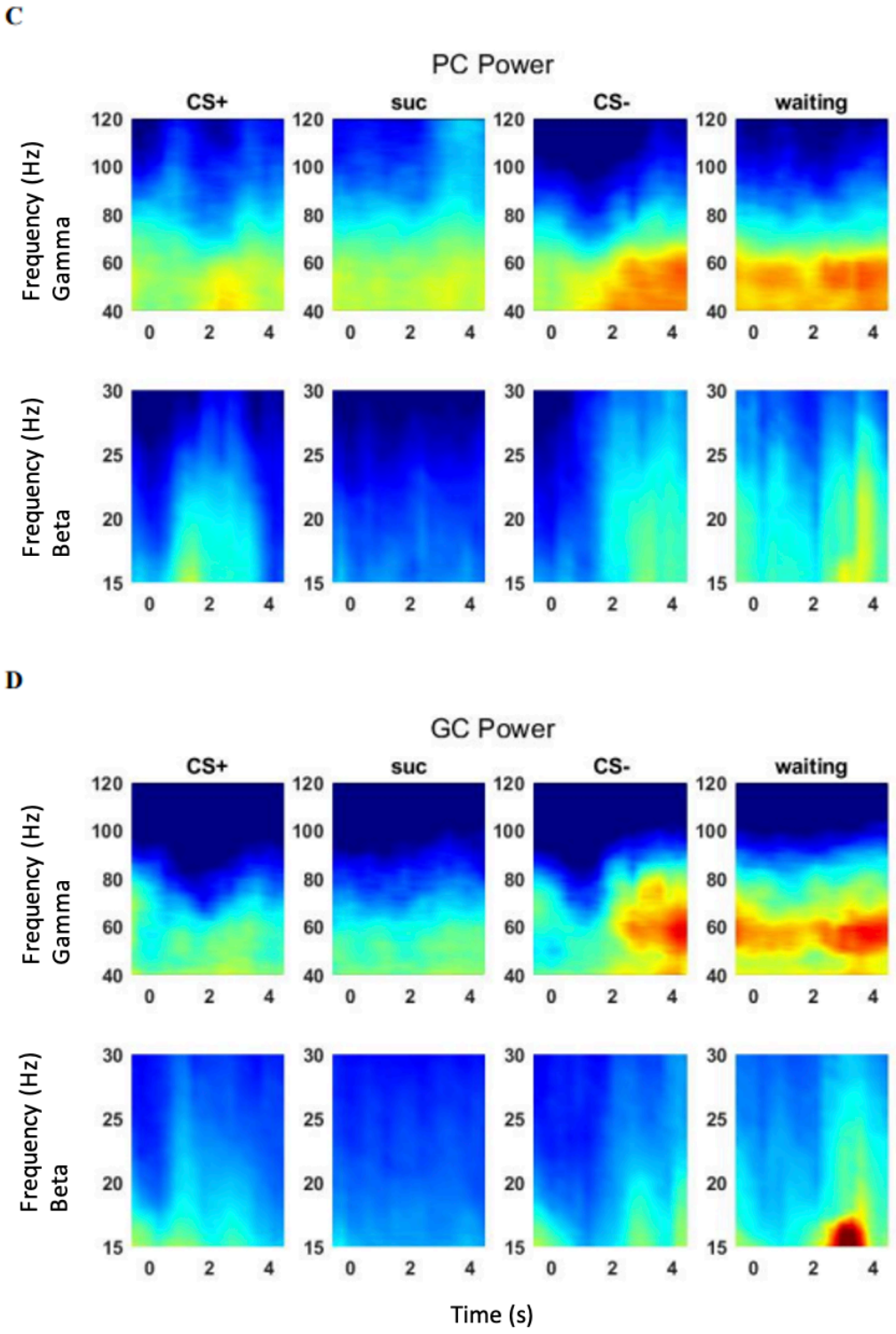

Gamma power during retronasal learning tasks

The previous section shows a qualitative picture of the LFP during retronasal odor discrimination and response. Here, I analyze these effects across all rats and odor sets. Figure 5.6A shows beta and gamma power changes across the odor sampling periods. The odor cue (CS+ vs CS-) has the largest effect on both gamma ($F(1,2013) = 90.23$, $p<0.001$, $\eta^2 = 0.035$) and beta power ($F(1,2013) = 137.34$, $p<0.001$, $\eta^2 = 0.037$). Multiple comparisons showed that during the early odor sampling period (first 2 seconds) gamma power in the OB is significantly weaker compared to the baseline. Gamma suppression during the first 2 seconds is more prominent for CS+ (power change =-.03, std = 0.0024) compared to CS- (power change =-0.015, std = 0.0016, p<.001). During late odor sampling of CS-, gamma power returns to the pre-odor baseline (power change = 0.004, p=1), while CS+ gamma remains suppressed (power change = 0.004) and is significantly different from the late odor sampling period for CS- ($p<0.01$).

Gamma power in the OT and anterior PC were similar to the OB. In the OT (Figure 5.6B), gamma power suppression is observed for both CS+ (power change =-0.01, std = 0.0021, $p<0.001$) and CS- (power change =-0.005, std = 0.0019, $p<0.001$) during the early odor sampling period. The suppression lasts into the later odor period for CS+ (power change =-0.01, std = 0.0021, $p<0.001$). Interestingly, the gamma power for CS- increases above the pre-odor period (power change =0.011, std = 0.0019, $p<0.001$) during the late odor period. Although the pattern of power dynamics is similar for PC (Figure 5.6C), gamma power for CS+ is only significantly different from the pre-odor period during the early odor period (power change= -0.0053, std = 0.0014, p =0.016) but not the late odor period (power change = -0.0048, std = 0.0016, p =0.063). CS- does not decrease gamma power in the PC at the early stage of odor sampling (power

change = -0.0034, std = 0.0007, p =1), but gamma power increases significantly above the pre-odor baseline during the later odor sampling period (power change = 0.011, std = 0.0016, p <0.001).

Gamma power in GC is relatively stable throughout the retronasal odor discrimination trials. The only significant effect is between the early (power change =0.003, std = 0.0015) and late-odor sampling period (power change =- 0.0012, std = 0.0018, p <0.001) for CS+.

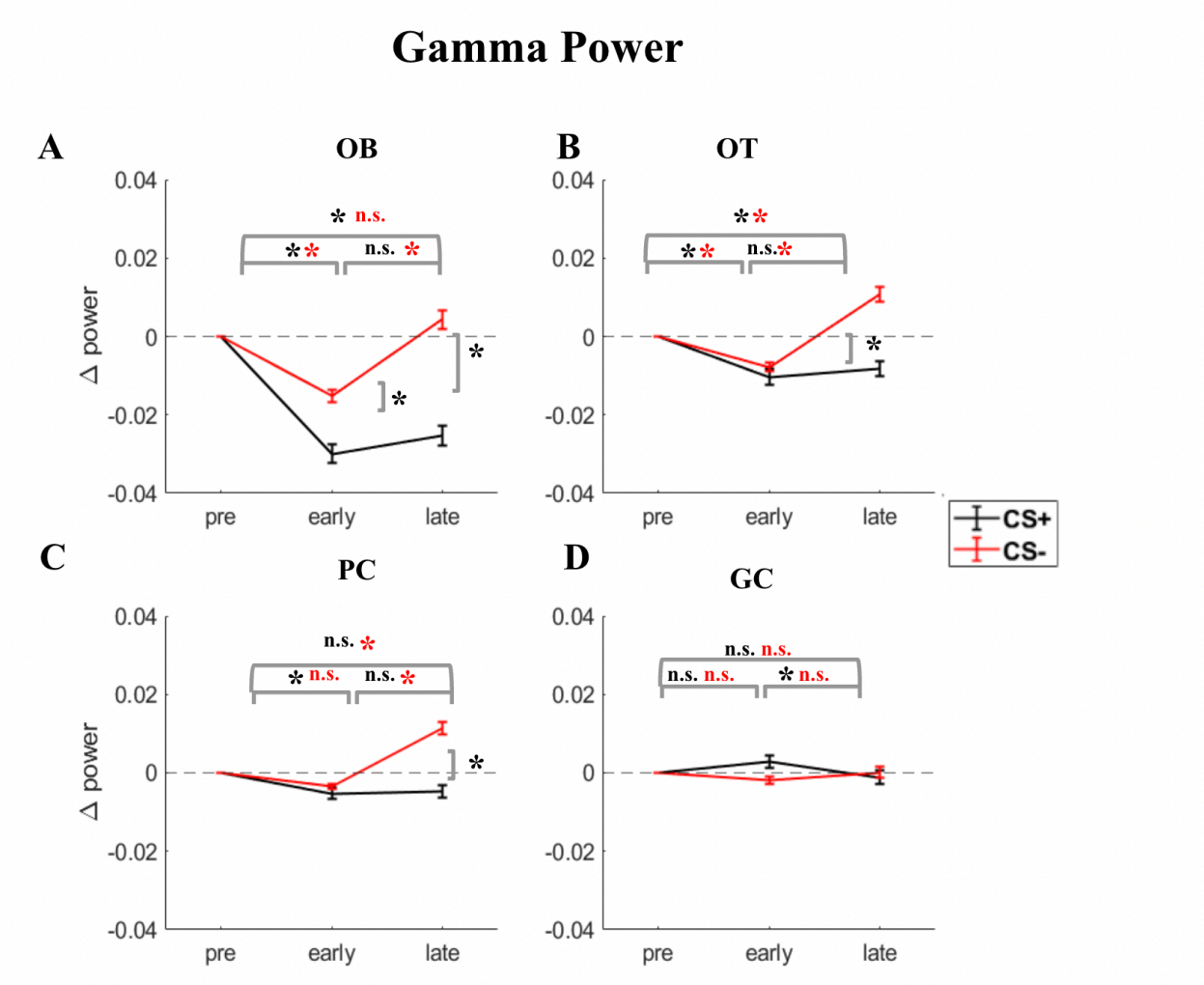

Figure 5.6 Average changes in power with SEM for gamma bands in (A) OB, (B) OT, (C) PC, and (D) GC. A horizontal line with black asterisks and letters denotes the significance level between two different time points aligned to odor onset for CS+; a horizontal line with red asterisks denotes that for CS-. An asterisk (*) indicates a significant level $p<0.05$, and any value above that is considered not significant (i.e., n.s.).

Beta power during retronasal learning tasks

The amplitude of beta power also decreased, similar to gamma, in the OB during the early odor sampling period (power change = -0.0156, std = 0.0022, p=0.008; Figure 5.7A). This suggests that the amplitude of raw LFP may be compressed when rats lick an odorized solution. CS- does not change the power in the beta band relative to the pre-odor period when rats sample the odor in the early odor period (power change =0.0025, std = 0.0017, p=1). Beta power is enhanced significantly during the later odor sampling period (power change =0.015, std = 0.0021, $p<0.001$).

Beta power tends to rise in both the OT and the PC during the retronasal odor discrimination trial. The power in OT increases significantly in the late odor sampling period for CS+ (power change = 0.001, std = 0.0013, p = 1), and in both the early (power change = 0.001, std = 0.0015, $p<0.001$) and late periods (power change = 0.025, std = 0.0025, $p<0.001$) for CS-. Piriform cortex also shows elevated beta power for both CS+ (early: power change =0.005, std = 0.0013, p=1; late: power change = 0.014, std = 0.0013, $p<0.001$) and CS- (early: power change =0.011, std = 0.00185, $p<0.001$; late: power change = 0.034, std = 0.0026, $p<0.001$).

Even though GC shows an apparent increase in beta power for both CS+ and CS-, the effect is not significant for CS+ (early: power change = 0.0087, std = 0.002, p = 1; late: power change = 0.013, std = 0.0025, p = 0.36). The lack of significance may be due to the large variance in the changes in power recorded in GC. Beta power is significantly increased for CS -,

(early: power change =0.002, std = 0.0015, p = 0.007; late: power change = 0.012, std = 0.0017, p<0.001).

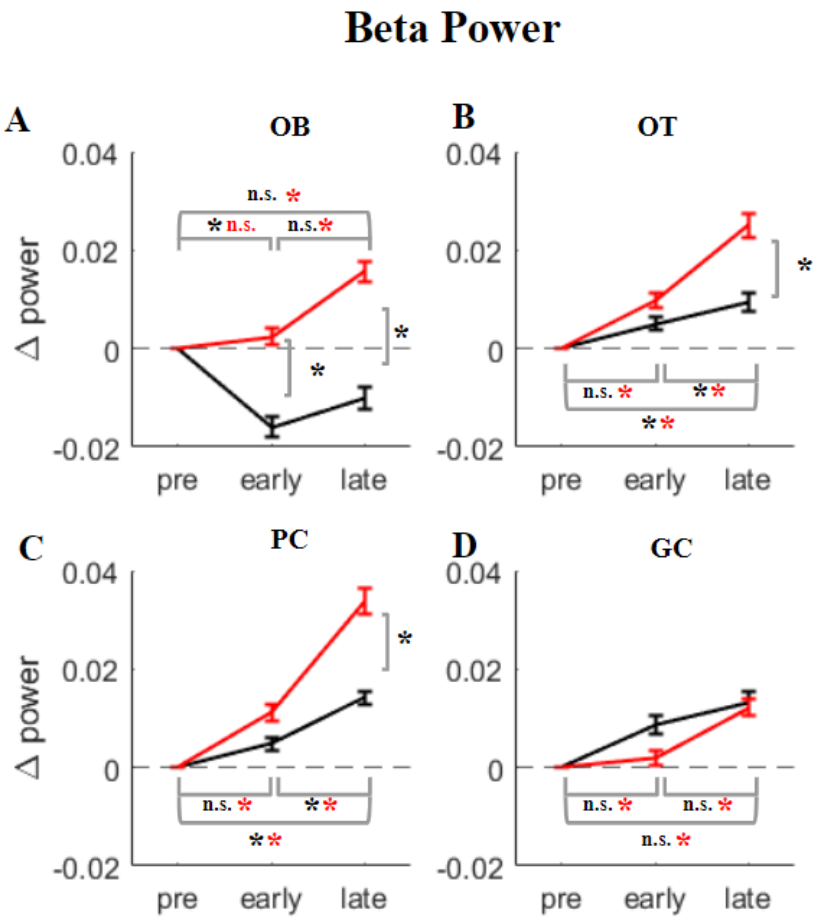

Figure 5.7. Average changes in power with SEM for gamma bands in (A) OB, (B) OT, (C) PC, and (D) GC. A horizontal line with black asterisks and letters denotes the significance level between two different time points aligned to odor onset for CS+; a horizontal line with red asterisks denotes that for CS-. An asterisk (*) indicates a significant difference (p<0.05), and any value above that is considered not significant (i.e., n.s.).

Coherence between brain structures

Coherence between structures ranges from 0.4 to 1.2, which is above the baseline coherence calculated by the mismatching trials, and the results are summarized in Figure 5.8. Both gamma and beta band coherence show an overall increasing pattern over time within a trial, despite the fact that gamma and beta power decreases in the olfactory bulb and other areas. This is consistent with our understanding of coherence. It does not have to correlate with the increase of power in the frequency band, because coherence is a measure of the consistency of phase relationships between signals within matched frequencies and not the size of those signals.

Odor cue (CS+ vs. CS-) affects beta coherence ($F(1,3033) = 25.2$, $p<0.001$, $\eta^2=0.002$) but not gamma coherence ($F(1,3033) = .27$, $p=0.6$). The effect size is small for the odor cues, and the presentation of odor stimulus can activate the coordination of the network regardless of the predictive value of the olfactory input. GC is more coherent with PC and OT in the beta frequency for CS- than CS+ (Figure 5.8. E and F). Interestingly, the olfactory cue's predictive value may evoke a more coherent pattern in the GC with OT and PC when a taste stimulus is absent, and when the predictive cue is aversive.

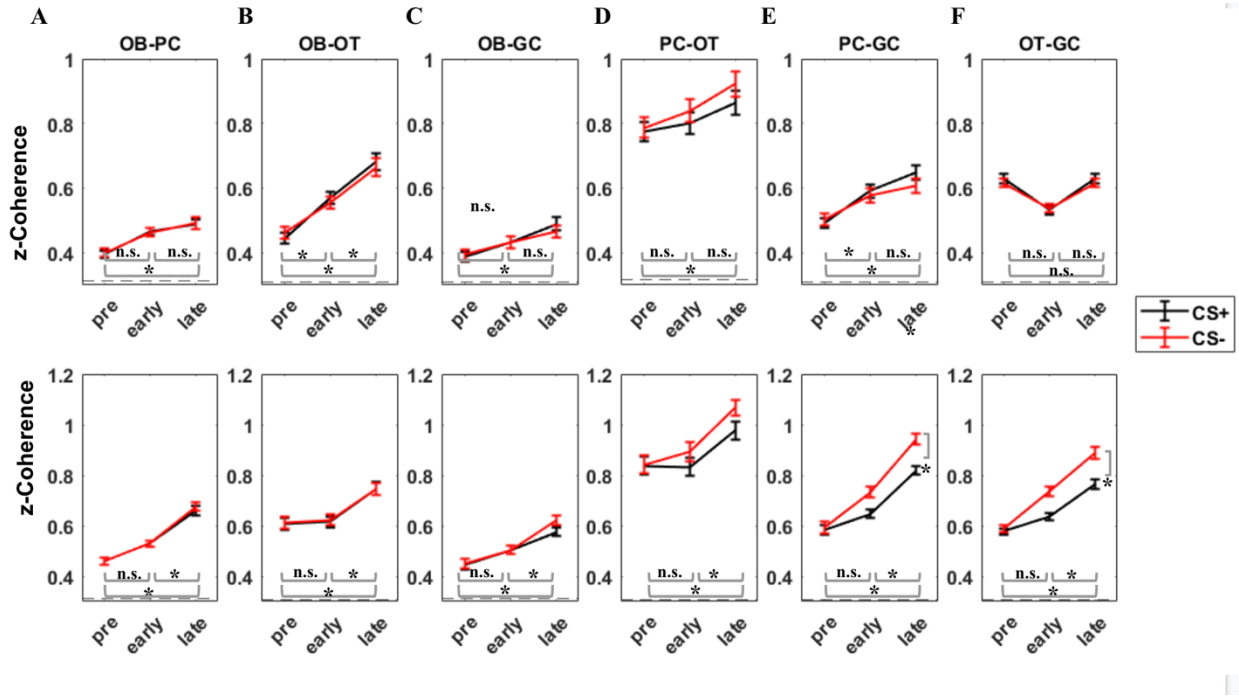

Figure 5.8. Coherence between brain structures in the gamma and beta range. An asterisk (*) indicates a significant difference ($p<0.05$), and any value above that is considered not significant (i.e., n.s.).

The effect of learning phases

The previous results summarize the power and coherence for all sessions regardless of whether the oscillation pattern changes during learning the three odor sets in sequence. The difference in performance across learning phases (see result in Chapter 4) also licenses me to investigate its effect on the oscillatory events. To understand whether olfactory oscillations change over the sequence of learning three odor sets, all data are grouped into three learning phases, training odor set (T1), rule transfer odor set 1 (R1), and rule transfer odor set 2 (R2) - the odor pairs used for each were counterbalanced across rats.

ANOVA analysis showed main effects of training phase for both gamma and beta power (gamma: $F(2,2013) = 15.94$, $p<0.001$, $\eta^2 =0.1$; beta: $F(2,2014)=15.32$, $p<0.001$, $\eta^2 =0.015$). The small effect size suggests that the training phase variable only accounts for a small portion of the variance in the model. After investigating further with multiple comparison analyses, we observed that gamma power changes (Figure 5. 9A) are not significantly different over the three learning phases when separated by odor cue and odor sampling period (i.e.,CS+ early, CS+ late, CS- early, and CS- late). OB, OT, and PC show similar temporal dynamics in that gamma power is suppressed throughout the early odor sampling of CS+ and elevated back or beyond the baseline pre-odor sampling period in the late odor sampling period. Fluctuation in gamma power in GC remains insignificant over the sequence of three learning phases.

Beta oscillatory power demonstrates a similar retronasal odor-evoked response for the three training phases. OB beta power decreases during CS+ and early CS- sampling periods, and PC and OT beta powers are elevated from the pre-odor sampling period. The pairwise comparison for beta power change showed no significant difference for learning phase in the OB, the OT, and the PC. In the GC, the beta power increase in CS- trials during early odor sampling for R2 is significantly higher than for T1 ($p<0.001$, Figure 5.9), and beta power increase at later odor onset for R2 is significantly higher than for R1 ($p<0.001$). Most comparisons that examine beta power change in T1, R1 and R2 do not show significant differences. With this data set, I fail to reject the hypothesis that beta power may increase over learning and may be enhanced at the rule transfer stage. However, we can observe from OT, PC and GC that beta power is higher for R2 compared to T1 consistently in all three higher cortical areas but not the OB. This pattern is also observed across sessions and different animals. It is

likely that learning modulates the olfactory network among higher order cortical areas in this retronasal task.

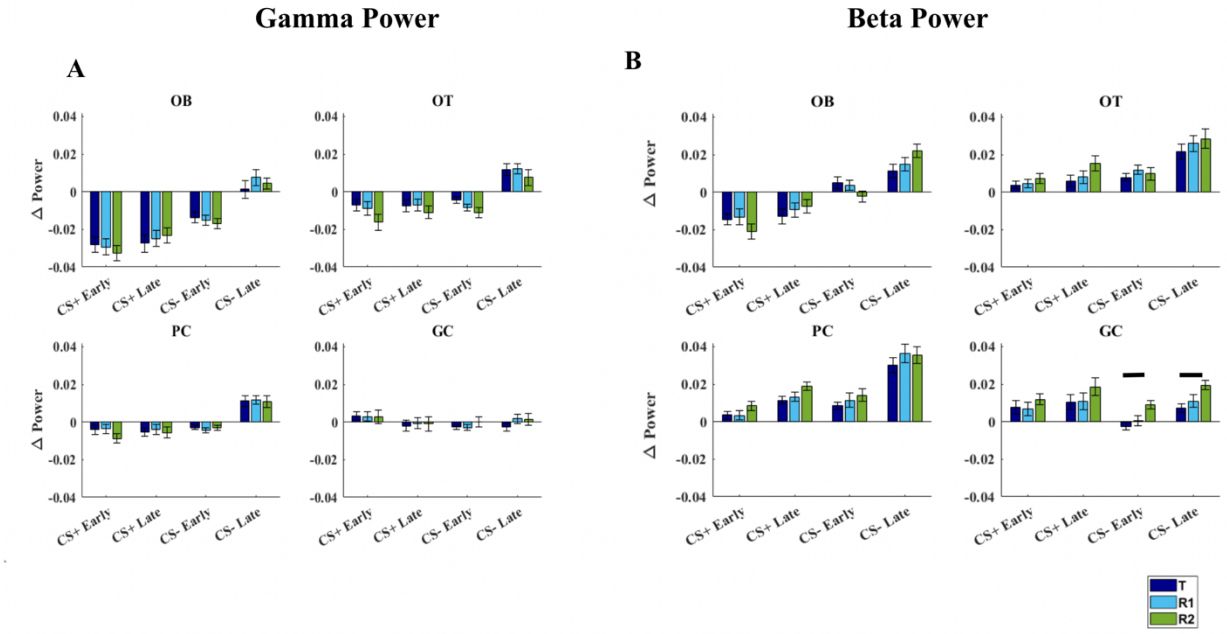

Figure 5.9. Power change grouped by learning phase. Changes in gamma power (A) are not significantly different among the three learning phases. (B) Beta power in GC shows a significant difference between T and R2. Black lines indicate significant differences ($p<0.05$).

Although the analysis of power did not indicate large effects of the learning phase, learning may still have an effect by changing the network coherence. The learning phase does have a significant effect on beta coherence ($F(2,3033)= 3.46$, $p = 0.031$, $\eta^2= 0.002$) and gamma coherence ($F(2,3033)=11.79$, $p <0.01$, $\eta^2 = 0.07$).

Multiple comparison tests are used to identify how the effect progresses over learning. In accordance with the small effect size, multiple comparison tests reveal no significant differences among the three learning phases. Gamma coherence between OB and GC is higher for R2 than for T (Figure 5.10). This is contrary to the original hypothesis that beta coherence would

increase, but the fact that GC shows significant network changes may suggest that retronasal olfaction is supported by a different olfactory network pattern and driving the different percept.

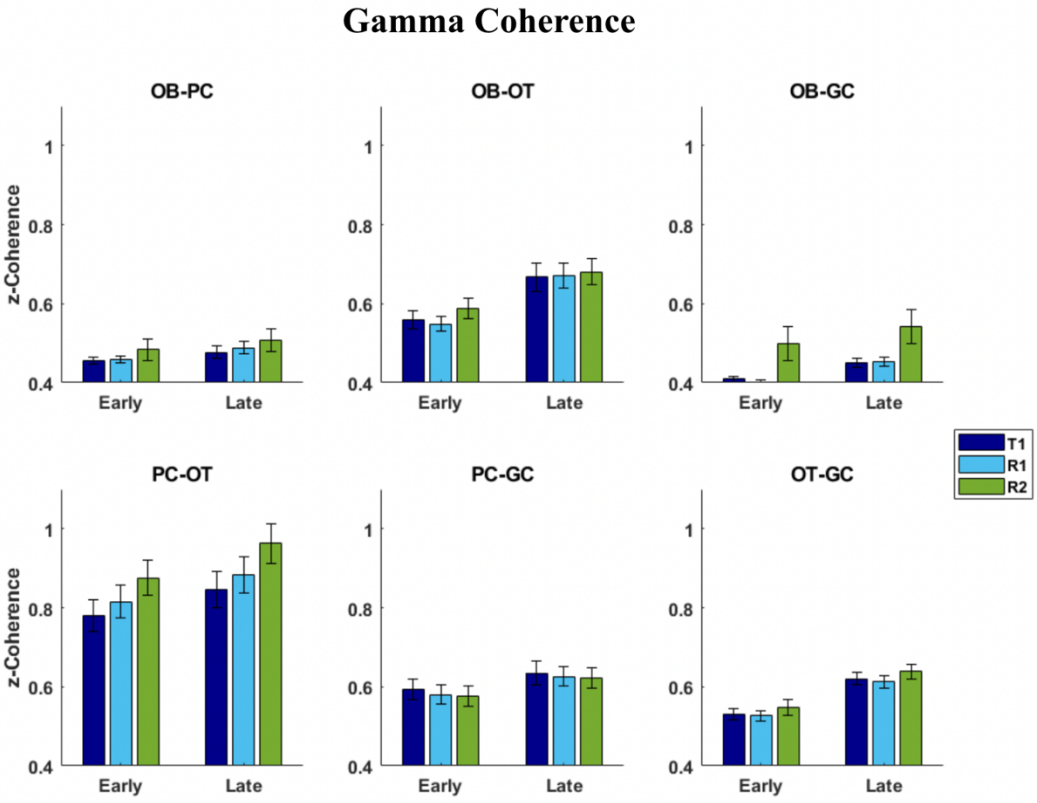

Figure 5.10. Gamma coherence grouped by learning phase. OB-GC coherence is significantly higher for R2 than T1, as indicated by the black line on the top right panel.

Alternatively, the learning effect can be examined by comparing data collected at different performance levels over learning from novice to expert in the task. Unfortunately, the data set we collected has limited our analysis of this learning effect for two reasons. First, rats are neophobic and may quit attempting after 2-3 quinine trials on the first day, making the novice data biased to CS+ recordings with few CS- trials. Secondly, rats can pick up the task quickly

and reach 60% accuracy within a few days (Figure 4.2), making the data set biased to recordings during high performance.

The effect of odor volatility

A similar analysis was performed to compare effects that may be due to the different volatilities of the three odor sets that were counterbalanced in order across the subjects (Figure 5.11). Pairwise comparison reveals no significant effect between the three odor sets in the early or late odor sampling phase, suggesting the odor-evoked dynamics are similar across odor sets. Previous research (Kay & Beshel, 2010) suggested that beta oscillations may increase as a function of volatility, and which led to our original prediction that high-volatility odorants like hexanone (HEX), methyl valerate (MV) may elicit stronger beta compared to low volatility odorants, heptanol (HEP) and methyl benzoate (MB). However, such a difference was not found in our results.

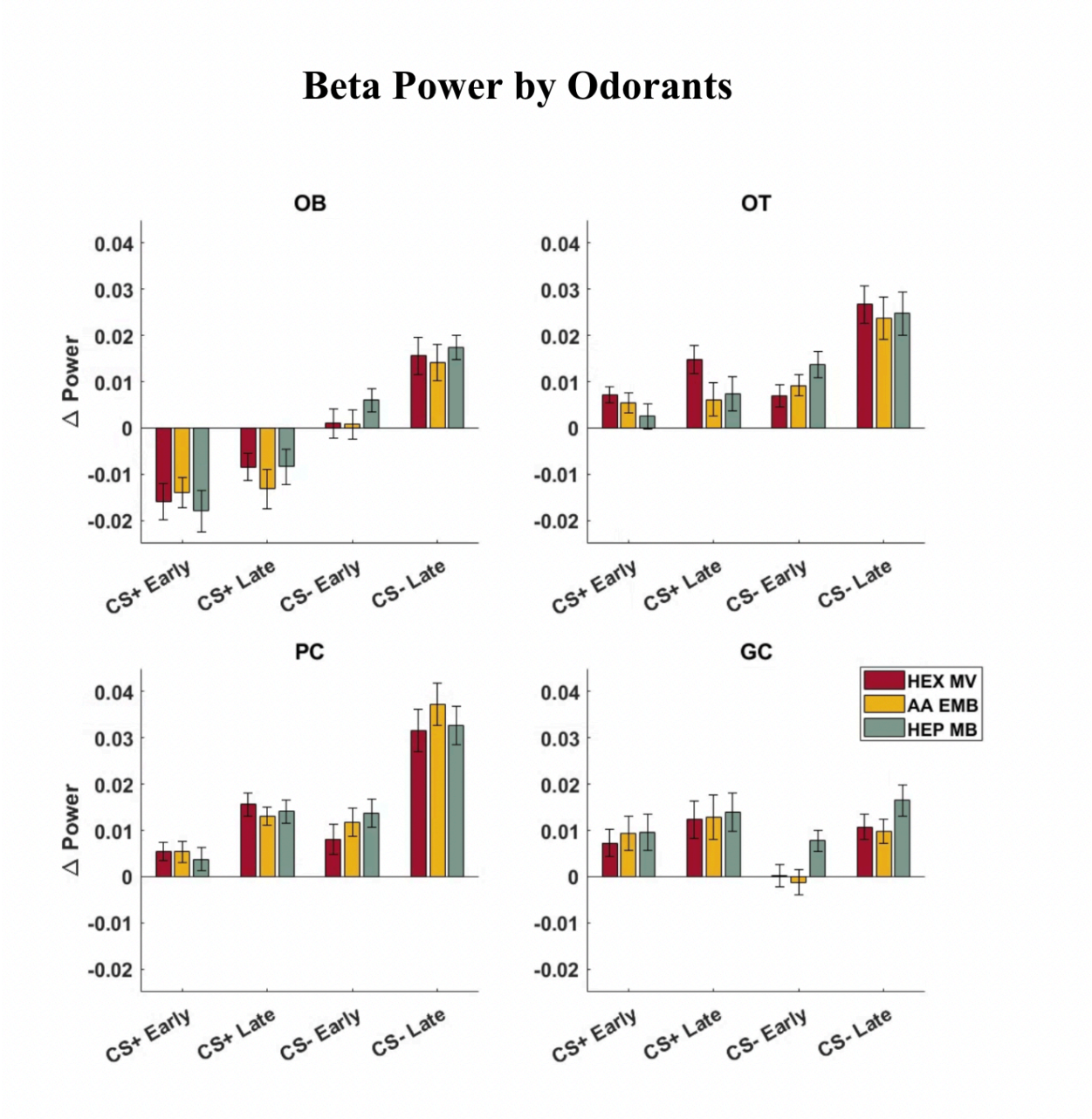

Figure 5.11. Beta power change shows effects between odor sets of different volatility levels.

Sensorimotor entrainment of LFP signals

CS+ and CS- in the retronasal discrimination task involve different behavioral patterns (Chapter 4), and I hypothesized that the two sensorimotor inputs, licking and respiration, may

modulate the neural network during retronasal discrimination tasks. The coherence between the LFP signals and the sensorimotor signals, respiration extracted from the thermocouple electrodes and licking extracted with PC LFP, should be high, and licking coherence should only occur when rats are licking. Figure 5.12A shows LFPs recorded in OB, OT, PC and GC are strongly coherent with respiration and peak at the respiratory frequency of around 6-8Hz. Licking is only coherent with LFP signals recorded in the CS+ and sucrose trials when rats are actively licking (Figure 5.12B).

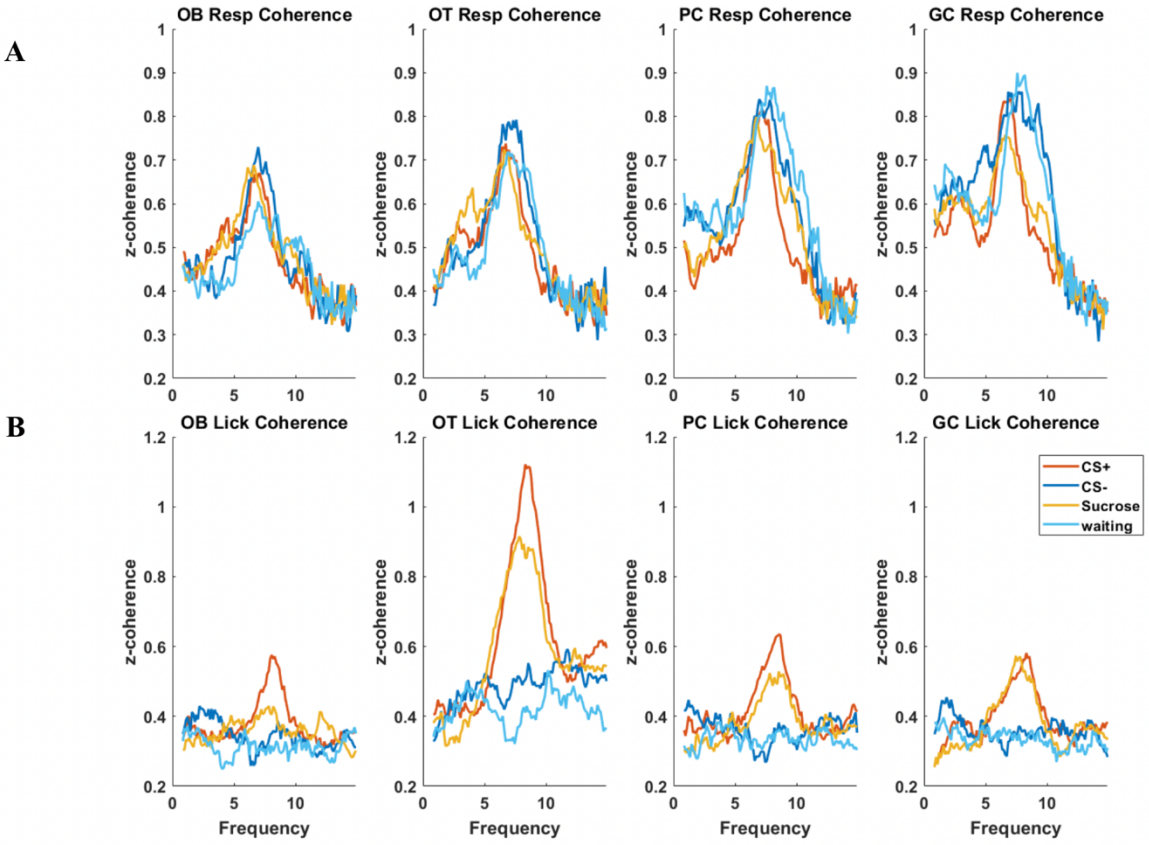

Figure 5.12. Respiratory and licking signals are coherent with LFPs. (A) The respiratory signal is coherent with LFPs recorded during CS+ and CS- trials and the corresponding response periods

at the respiratory frequency between 5-10Hz. (B) The licking signal is coherent with LFPs recorded during CS+ trials and the following sucrose licking period.

Discussion

In this chapter, I investigated the temporal dynamics of LFPs in the olfactory system with a focus on the change in gamma and beta band power. The olfactory network during retronasal odor discrimination is characterized during three different time points, pre-, early- and late-retronasal odor sampling periods. The two odor cues, CS+ and CS-, are associated with different behavioral responses and oscillatory patterns in the olfactory system during retronasal odor sampling. CS+ elicits constant licking and suppression of gamma and beta power in the OB but increases beta power in the PC, OT, and GC. Withdrawal from the odor-port in response to CS- increases gamma and beta oscillation power in the OB during the late odor period. The higher cortical areas display similar patterns with elevated beta power for both CS+ and CS-. Coherence in the beta and gamma range increases over odor sampling, with no odor-cue effect. The effects of the learning phase and volatility were also examined but showed no differences between levels, suggesting that the dynamics are stereotypic in retronasal odor discrimination.

Change in oscillatory power reflects retronasal odor sampling characteristics

Gamma in OB

Previous studies (Beshel et al., 2007; Frederick et al., 2016) focusing on the functional role of gamma oscillations in orthonasal olfaction paradigms demonstrate an increase of gamma power in the OB when animals discriminate extremely similar odorants, like heptanol and hexanol, two alcohols one carbon away in a difficult task (Beshel et al., 2007) or the same odor with different trace contaminants in an easier task (Frederick et al., 2016). One of my original

hypotheses was that retronasal delivery routes are associated with weaker perceptual intensity and higher detection threshold (Hummel & Heilmann, 2008; Furudono et al., 2013; Gautam & Verhagen, 2012), which would result in an increase in task demand and gamma power. However, retronasal tasks for the odor pairs selected are not difficult; rats acquire the task and perform above chance on the first day of training, and a gamma power increase might not be expected due to the low task demand.

OB gamma is suppressed during retronasal odor sampling. The suppression of OB gamma is also reported in research using Go/No-Go orthonasal odor tasks in rodents (Ravel et al., 2003; Martin et al., 2004; Martin et al., 2007; Liu et al., 2020), and gamma power returns to baseline after the odor sampling period. This pattern is observed in CS- trials in which gamma power decreases at the beginning of odor sampling and then recovers, but not CS+, which stays low compared to the baseline. This is the time period where rats are actively licking and breathing slower, and it suggests that gamma is suppressed not only when animals engage in easy odor-cued discrimination tasks but can also be affected by behavioral states like licking.

The OB excitatory-inhibitory network can be modulated as the input pattern changes. Craft et al. (2021) recorded the spiking activity of OB mitral cells in anesthetized rats with retro and orthonasal stimuli and found that retronasal stimuli elicited a higher firing rate but with low covariance in spiking across neurons. They were able to replicate mitral cell activities for retro- and orthonasal olfaction by modeling OSN inputs as slowly increasing to peak amplitude with a long decay time for retronasal inputs and faster increase, fast decay of input for orthonasal olfaction. Although urethane anesthesia can decrease gamma and beta oscillations OB (Li et al.,

2012), the simulation of OSN inputs may resemble how retronasal odorants bind to OSNs in freely behaving animals, leading to less synchronous firing and decreased gamma.

Gamma in PC, OT & GC

During retronasal sampling, gamma power decreases in PC and OT but remains stable in GC. The oscillatory patterns may shed light on coordination within the olfactory-gustatory network. Suppression of PC gamma during licking confirms earlier observations by Freeman (1960).

A recent study in mice by Gonzalez et al. (2022) shows that PC gamma is driven by respiration, and optogenetic activation OB mitral cell projections trigger feedback inhibition-based gamma oscillations. Their findings replicate the phase-locking results of pyramidal cell activity and gamma (Litaudon et al., 2008) and showed odor decoding accuracy using principal component analysis correlates with the amplitude of gamma in PC, suggesting that PC gamma plays a significant role in odor processing.

Potential mechanisms for PC suppression may involve a reduction or desynchronized mitral cell firing. OT receives inputs from both mitral and tufted cells in the OB, and the modification in odor inputs may also exert a similar effect of reducing gamma power in the local network in OB.

Beta

I hypothesized that beta power and coherence may change in the retronasal olfactory discrimination task because of the role of beta power and coherence in orthonasal learning (Martin et al., 2004, 2007; Kay & Beshel, 2010; Frederick et al., 2016).

OB beta power is significantly affected by the odor cues and the types of response elicited. CS+ associated with continued licking decreases beta, while CS- associated with withdrawing from the port is usually accompanied by increased beta power in the later odor sampling period. This increase in beta may be similar to the beta oscillation power increases observed in orthonasal olfaction that occurs later in the orthonasal discrimination tasks, coincident with preparing to leave the odor port and produce a trained response (Frederick et al., 2016).

Interestingly, beta band coherence between OB and higher cortical regions PC, OT, and GC increases through the odor sampling period, regardless of which odor cue is present or the beta power in the OB. The results show strong beta coherence across the olfactory-gustatory system, which supports the argument that beta oscillations are more global than gamma and facilitate information processing.

Beta oscillations in the motor cortex are related to movement preparation (Leventhal et al., 2012; Khanna & Carmena, 2015). One limitation with Go/No-Go tasks is that sometimes it is difficult to distinguish whether a phenomenon is elicited by the perceptual experience or by the response type. Unfortunately, the time point when a rat withdraws from an odor port was not recorded. Therefore, I was unable to align LFPs to transitional behaviors other than the respiration and licking cycle in this experiment.

CHAPTER 6: Sleep Analysis for Retronasal Olfactory Learning

The olfactory network is modulated by learning, and plasticity in cortical activities has been reported by many (Barnes et al., 2014; Manabe et al., 2011; Narikiyo et al., 2014; Wilson & Yan, 2010). The OB LFP shows state-dependent oscillations and can be leveraged to identify sleep stages (Wake/REM/NREM). Retronasal olfaction may induce similar changes in the olfactory system post-training.

In this chapter, I first replicate a sleep scoring algorithm proposed by Bagur et al. (2018) that leverages OB gamma and hippocampal LFP for sleep stage classification. To explore how learning modifies the olfactory network and sleep behaviors, sleep stages are classified over several days when rats were transferred to new odor sets. I summarize my findings about sleep behaviors and related physiological patterns observed in olfactory LFP recordings collected from pre- and post-retronasal olfactory task training.

Methods

Sessions were recorded on the day when rats were transferred to a new learning context (i.e., when CS- was first introduced, from T to R1, and from R1 to R2). 4 of the rats (2M) from the original 8 rats in Experiment 3 were used for this analysis. 12 pre-training and 12 post-training sleep periods were recorded (3 from each rat). A repeated measure ANOVA was used to examine the effect of learning on sleep behavior and SPW-R probability.

Sleep stage identification

OB and HPC LFPs were used to classify sleep stages using the sleep scoring algorithm (Bagur et al., 2018). For sleep/wake states, OB LFPs are first band-passed through a gamma (45-100Hz) frequency filter and then Hilbert transformed for instantaneous gamma power. The instantaneous gamma is binned by 5-second windows, and its distribution can be fitted by the sum of two Gaussian functions (Figure 6.1). The Gaussian distributions correspond to sleep (low gamma power) and awake (high gamma power) states. The threshold for dividing the two states is determined by the intersection of the two Gaussian functions. A time window with OB gamma power below the threshold is identified as sleep, and above the threshold is identified as waking.

REM and NREM sleep are classified by the HPC theta (5-10 Hz) to delta (1-4Hz) ratio. Theta and delta power are calculated using the multitaper method for power spectral density and then summing the power within the frequency bands. A time window of 5 seconds is used for good temporal resolution of microarousal states (Soltani et al., 2019). The distribution of HPC theta and delta ratio is fitted by a Gaussian distribution, and the threshold is determined to be 2 standard deviations above the center of the distribution.

Videos recorded during sleep sessions before and after training were manually coded to identify motion and sleep states by 4 coders for validity check. A long (>15 seconds) and immobile period is identified as sleep, and visible micro-arousals are reported in manual coding. The rat's home cage, in which sleep recordings were made, has a small hole (diameter ~1cm), and rats sometimes poke their nose into the hole. This behavior looks very similar to that of odor sampling, usually accompanied by fast sniffing and low LFP amplitudes (observations during the experiment and also seen in Rojas-Líbano et al., 2014). Therefore, this nose-in-hole (NIH)

behavior is also coded for data exploration. The video coders coded the same 5 videos together to check for consistency and coded the rest of the videos separately.

Identification of Sharp Wave Ripples

Hippocampal LFP recorded during home cage activity pre- and post-training is first filtered for high frequency 150-250 Hz and Hilbert-transformed to obtain the envelope for the high-passed signal. A gaussian window of 32 msec was used to smooth the signal and 3 standard deviations above the mean were the threshold. SPW-Rs are identified as >50 msec with elevated fast-frequency activity (Jadhav et al., 2012).

Results

Sleep stage scoring

Figures 6.1 and 6.2 show samples of how the hippocampal theta-to-delta (T/D) ratio and OB gamma can be utilized for sleep stage classification in one sleep session. The thresholds for wake, REM and NREM are extracted from the probability density function of their distributions (Figure 6.1A). Sleep stages for each 5-second period are classified according to the algorithm, as the three main clusters shown in the four quadrants of Figure 6.1B.

Spectrograms of OB and hippocampal LFPs (Figure 6.2A, C) show characteristics corresponding to previous research on OB gamma decreases during sleep (Barnes & Wilson, 2014; Bagur et al., 2018), and hippocampal slow waves dominate NREM (Buzsáki, 2006). Similar distribution patterns were observed in the 4 rats I used for the sleep analysis (Figure 6.3).

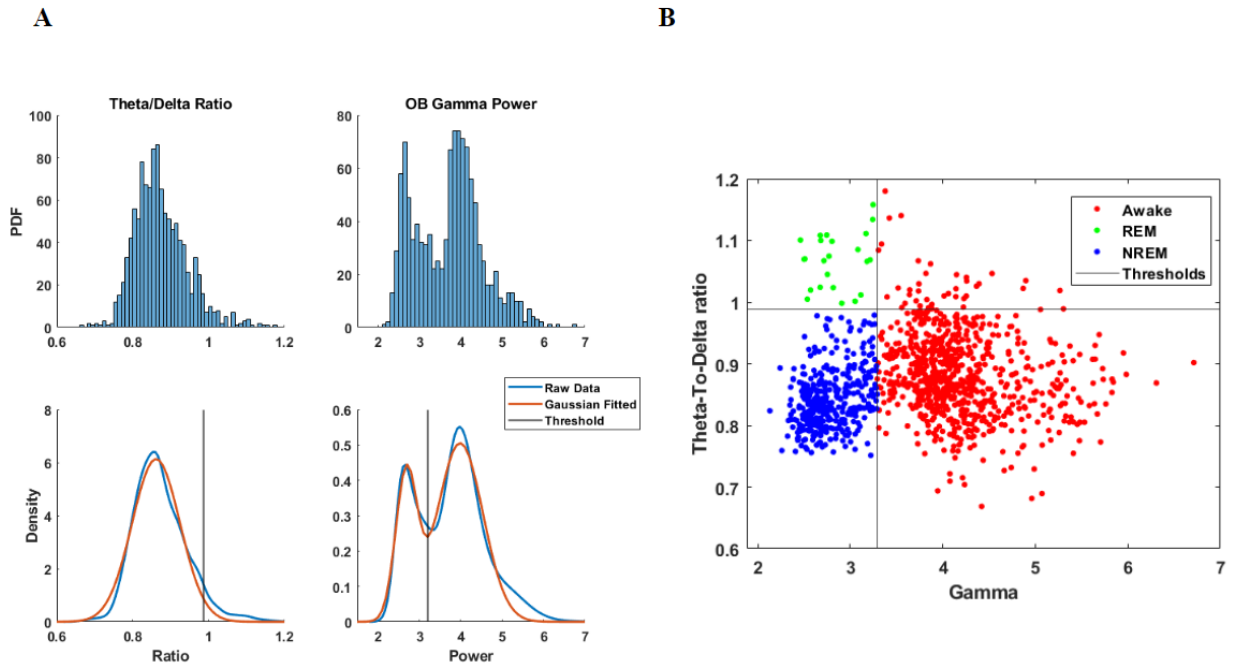

Figure 6.1. Sleep stage classification method. (A) The probability density function (PDF) of HPC theta to delta ratio and OB gamma power are fitted by gaussian distributions. The threshold for NREM and REM is identified as 2 standard deviations above the mean of the theta-to-delta ratio. The threshold for the wake and sleep stage is the intersection between the two gaussian distributions fitted on gamma power. (B) The Sleep States grouped classified by the algorithm include three main clusters: wake (red), REM (green), and NREM (blue)

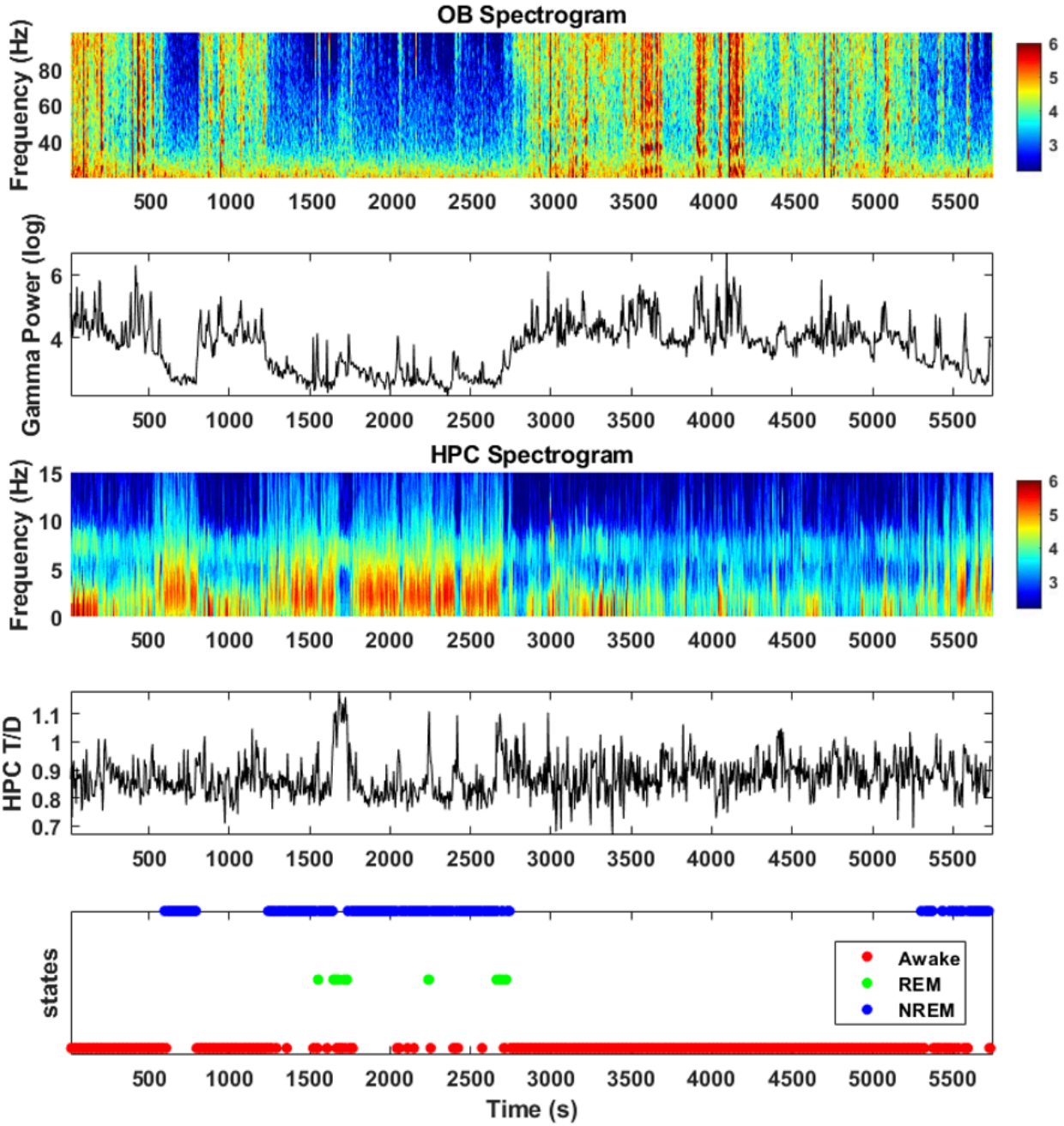

Figure 6.2. Sleep LFPs in OB and HPC and sleep stage identification.

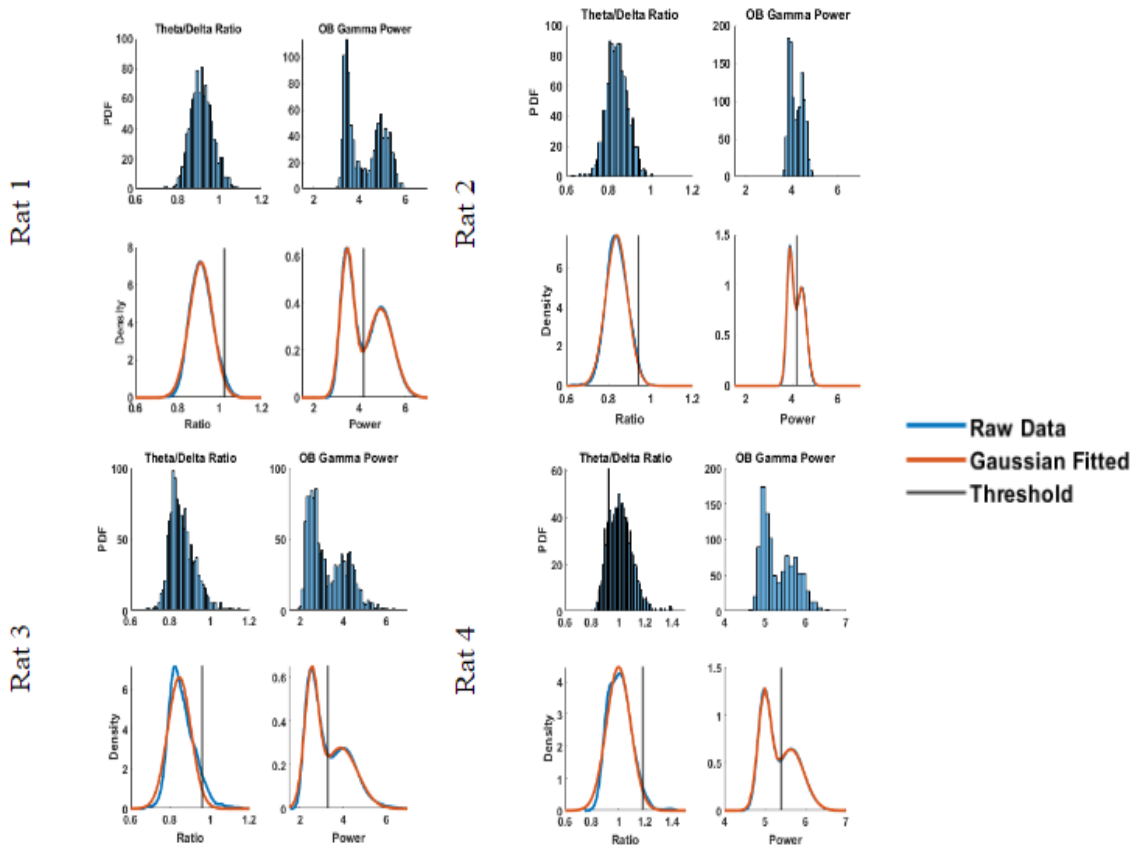

Figure 6.3. Distribution for all 4 rats used in the sleep analysis. Similar probability distribution functions for T/D ratio and OB gamma power are observed.

To check for consistency between the manual scoring (MS) and the algorithm scoring, I compare the sleep/awake states from the algorithm with that identified by the coders manually. Video coding cannot discriminate between REM or NREM but can identify micro-arousals that are noted in the hand coding. The conditional probabilities are calculated with 3000 5-second windows randomly selected from the four rats. Figure 6.4 shows the overlapping sleep stages (i.e., same states by both methods) divided by the number of sleep stages using either method.

The sleep scores overlapped between the two methods are above 80%, and future direction of this project may include improving the accuracy of the sleep coding algorithm using signals from other brain structures.

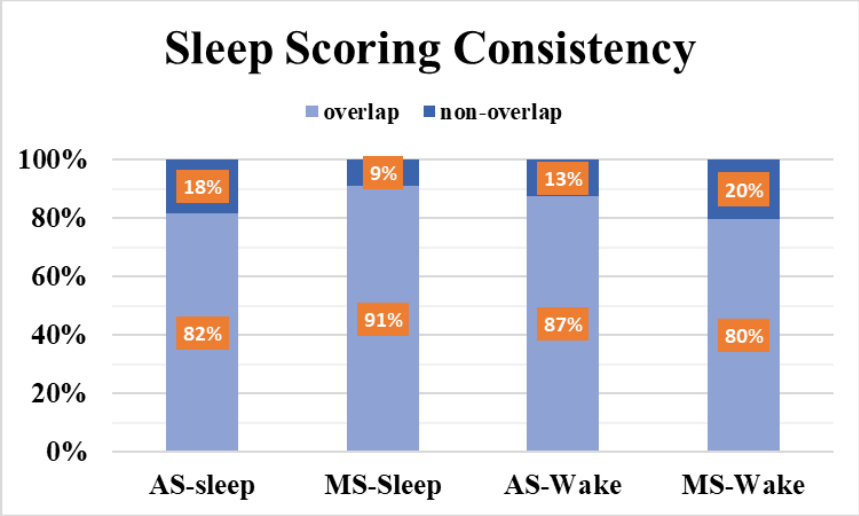

Figure 6.4. Verification of algorithm vs. manual scoring of sleep and wake stages. AS - algorithm scored; MS - manually scored.

Training Effect on sleep LFP

I expected the sleeping time to be longer in the 90-minute recording for olfactory memory consolidation. The percentages of time spent in the Wake, REM, and NREM states in a recording session are plotted in Figure 6.5. Paired-sample t-tests show that rats are awake longer (Pre- M: 33.3%; SD: 14.2%; Post- M: 49.5%; SD: 10.1%; p=0.004; Figure 6.5A) and have less REM sleep (Pre- M: 2.8%; SD:2.2%; Post- M: 1.3%; SD: 0.1%; p=0.048; Figure 6.5B) post-training compared to pre-training. No significant difference was found between the percentages of time spent sleeping pre- and post-training.

The results are the opposite of my prediction. An alternative explanation for the longer wake time may be a circadian effect. Nocturnal rats sleep less later in the day as the time for waking approaches. In addition, it could be that the task is relatively easy, and therefore little consolidation was needed.

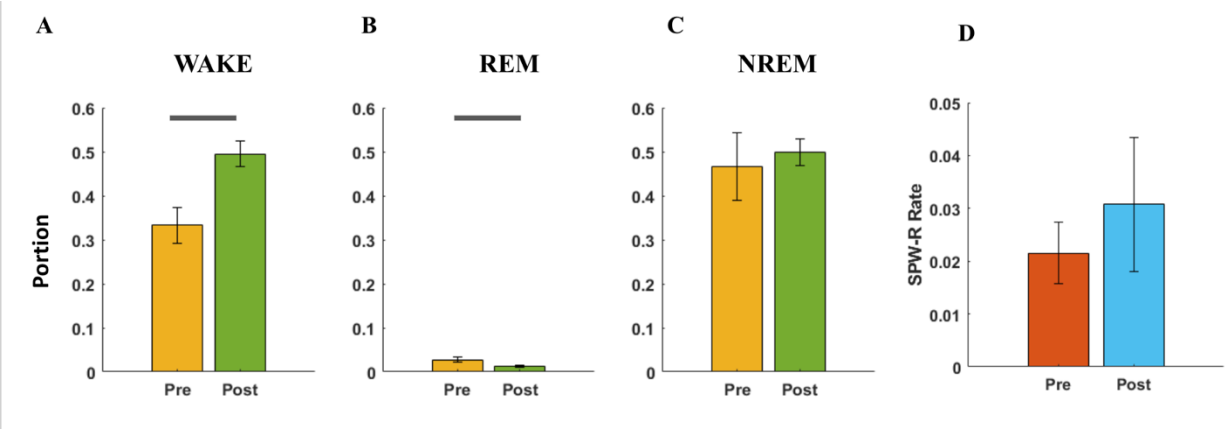

Figure 6.5. Comparison between time spent in sleep stages and sharp wave ripples pre and post-sleep. The black line indicates significant differences ($p<0.05$). For REM and NREM, percentages refer to portions of the total time. SPW-R rate in D is the rate per second during NREM.

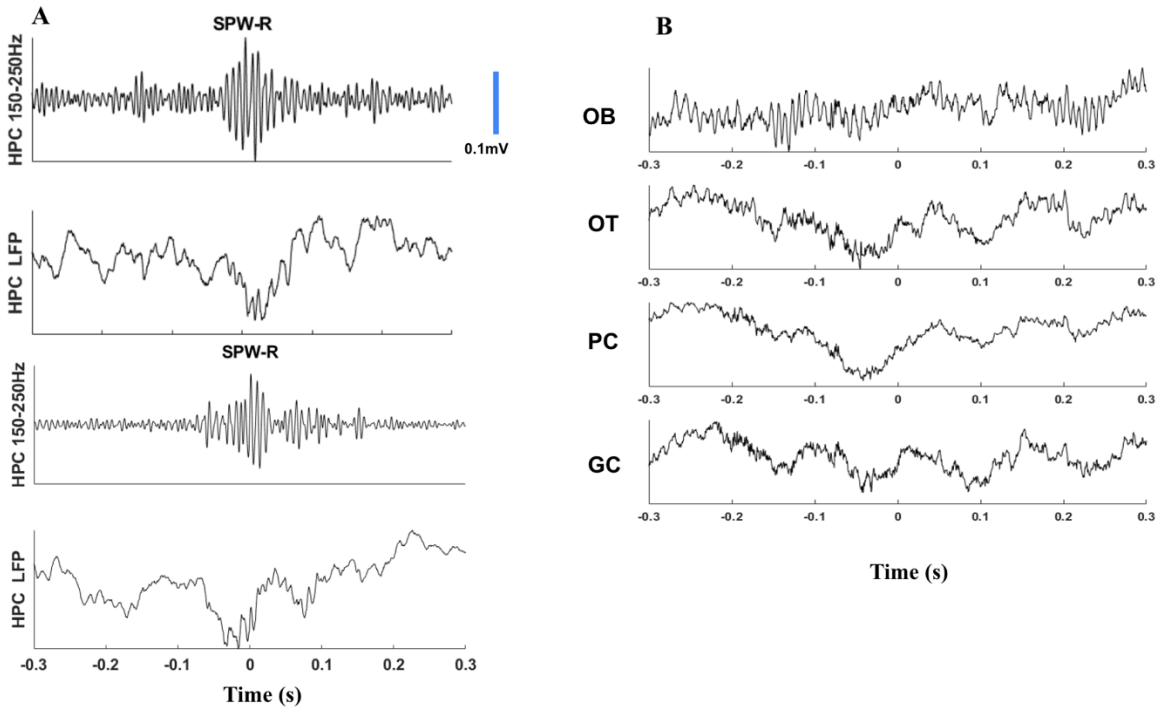

Figure 6.6. Examples of sleep SPW-R. (A) Hippocampal SPW-R shows fast, high amplitude oscillations (B) LFPs in OB, OT, PC, and GC recorded during the top left panel of SPW-R.

One hypothesis about the effect of training is that it induces SPW-R after training to consolidate olfactory memory (Eschenko et al., 2008). I test this hypothesis with the data set and investigate whether retronasal olfactory learning can increase hippocampal SPW-R in the NREM period during post-training. SPW-R occurrence rate (numbers of ripple per second) in NREM showed no significant difference between the pre- (M: .02; STD: 0.02) and post-training (M: 0.03, STD: 0.043; p=0.623).

CHAPTER 7: Conclusions

In this dissertation, I addressed the question: can one odorant generate the same or different percept retronasally and orthonasally.

The answer is mixed. In Chapter 3 I showed that retronasal experience affects orthonasal learning of the same odorants if they are strong (highly volatile), suggesting that there could be a shared percept that potentiates learning in one route when an odorant has been experienced from the other (He et al., 2021).

I used a retronasal olfactory discrimination paradigm to try to understand how the retronasal route engages the olfactory and gustatory network (Chapters 4 and 5). The electrophysiological study does not directly answer the question about the shared percept, but it describes the oscillatory patterns evoked by retronasal olfaction that have not previously been characterized, such as suppression of gamma power in the olfactory system, including OB, PC, and OT, and the coupling between LFPs and sensorimotor inputs during retronasal odor sampling. Retronasal OB beta power increases for CS- similarly to the increase of beta usually observed in orthonasal tasks, but CS+ odors showed the opposite effect - decreases in OB beta. However, beta coherence between OB and higher cortical regions increases over odor sampling. While the same network is engaged in retronasal olfaction, the oscillatory patterns can look very different from orthonasal olfaction, and this different pattern may contribute to the different percepts.

The retro- and orthonasal dual-percept theory (Rozin, 1982) has fascinated me since I first learned about it. It is intriguing that if we think of human or animal brains as information processors, why would the CPU process the same input (i.e., same chemical) to generate two

different outputs (i.e., qualitatively different percepts)? Our own body serves as a mediator of the signal by adjusting the concentration, inhalation, etc. The computer analogy could be that the information is also pre-processed by rubbing against the monitor.

However, I am not sure if the computer would be a good analogy to understand olfaction, because the assumption here is that the chemical structure of an odorant should dominate the quality of olfactory percept, and that was why it was particularly surprising when the effect of olfactory route overshadowed this chemical effect.

Olfaction has many other functions beyond odor identification and discrimination. Odorants usually have a hedonic value (Richard & Zucco, 1989), and people either like or dislike an odor. Khan et al. (2007) argue that olfactory pleasantness can be innate and predicted by the odor structure, and it is also the primary predictor of odor perception. If we consider the retronasal and orthonasal olfactory percepts in the framework of odor pleasantness, not chemical components of odorants, we may expect the two routes to overlap significantly as their functions converge in food consumption. Olfaction also plays a role in spatial navigation (Jacobs, 2012; Poo et al., 2022), which almost exclusively involves orthonasal but not retronasal olfaction. The discussion of retro- and orthonasal olfaction would be incomplete without considering the ethological functions of olfaction.

REFERENCES

Abel, T., Havekes, R., Saletin, J. M., & Walker, M. P. (2013). Sleep, plasticity and memory from molecules to whole-brain networks. *Curr Biol*, *23*(17), R774-788. https://doi.org/10.1016/j.cub.2013.07.025

Bagur, S., Lacroix, M. M., de Lavilleon, G., Lefort, J. M., Geoffroy, H., & Benchenane, K. (2018). Harnessing olfactory bulb oscillations to perform fully brain-based sleep-scoring and real-time monitoring of anaesthesia depth. *PLoS Biol*, *16*(11), e2005458. https://doi.org/10.1371/journal.pbio.2005458

Barnes, D. C., & Wilson, D. A. (2014). Slow-wave sleep-imposed replay modulates both strength and precision of memory. *J Neurosci*, *34*(15), 5134-5142. https://doi.org/10.1523/JNEUROSCI.5274-13.2014

Bekkers, J. M., & Suzuki, N. (2013). Neurons and circuits for odor processing in the piriform cortex. *Trends Neurosci*, *36*(7), 429-438. https://doi.org/10.1016/j.tins.2013.04.005

Beshel, J., Kopell, N., & Kay, L. M. (2007). Olfactory bulb gamma oscillations are enhanced with task demands. *J Neurosci*, *27*(31), 8358-8365. https://doi.org/10.1523/JNEUROSCI.1199-07.2007

Bird, C. M., & Burgess, N. (2008). The hippocampus and memory: insights from spatial processing. *Nat Rev Neurosci*, *9*(3), 182-194. https://doi.org/10.1038/nrn2335

Blankenship, M. L., Grigorova, M., Katz, D. B., & Maier, J. X. (2019). Retronasal Odor Perception Requires Taste Cortex, but Orthonasal Does Not. *Curr Biol*, *29*(1), 62-69 e63. https://doi.org/10.1016/j.cub.2018.11.011

Bodyak, N., & Slotnick, B. (1999). Performance of mice in an automated olfactometer: odor detection, discrimination and odor memory. *Chemical senses*, *24*(6), 637-645.

Bokil, H., Andrews, P., Kulkarni, J. E., Mehta, S., & Mitra, P. P. (2010). Chronux: a platform for analyzing neural signals. *J Neurosci Methods*, *192*(1), 146-151. https://doi.org/10.1016/j.jneumeth.2010.06.020

Bolding, K. A., & Franks, K. M. (2017). Complementary codes for odor identity and intensity in olfactory cortex. *Elife*, *6*. https://doi.org/10.7554/eLife.22630

Bowyer, S. M. (2016). Coherence a measure of the brain networks: past and present. *Neuropsychiatric Electrophysiology*, *2*(1). https://doi.org/10.1186/s40810-015-0015-7

Boyce, R., Williams, S., & Adamantidis, A. (2017). REM sleep and memory. *Curr Opin Neurobiol*, *44*, 167-177. https://doi.org/10.1016/j.conb.2017.05.001

Brunjes, P. C., Illig, K. R., & Meyer, E. A. (2005). A field guide to the anterior olfactory nucleus (cortex). *Brain Res Brain Res Rev*, *50*(2), 305-335. https://doi.org/10.1016/j.brainresrev.2005.08.005

Buzsáki, G. (1986). Hippocampal sharp waves: their origin and significance. *Brain research*, *398*(2), 242-252.

Buzsaki, G. (2005). Theta rhythm of navigation: link between path integration and landmark navigation, episodic and semantic memory. *Hippocampus*, *15*(7), 827-840. https://doi.org/10.1002/hipo.20113

Buzsaki, G. (2015). Hippocampal sharp wave-ripple: A cognitive biomarker for episodic memory and planning. *Hippocampus*, *25*(10), 1073-1188. https://doi.org/10.1002/hipo.22488

Buzsaki, G., & Schomburg, E. W. (2015). What does gamma coherence tell us about inter-regional neural communication? *Nat Neurosci*, *18*(4), 484-489. https://doi.org/10.1038/nn.3952

Carlson, K. S., Dillione, M. R., & Wesson, D. W. (2014). Odor- and state-dependent olfactory tubercle local field potential dynamics in awake rats. *J Neurophysiol*, *111*(10), 2109-2123. https://doi.org/10.1152/jn.00829.2013

Carskadon, M. A., & Dement, W. C. (2005). Normal human sleep: an overview. *Principles and practice of sleep medicine*, *4*(1), 13-23.

Carr, M. F., Jadhav, S. P., & Frank, L. M. (2011). Hippocampal replay in the awake state: a potential substrate for memory consolidation and retrieval. *Nat Neurosci*, *14*(2), 147-153. https://doi.org/10.1038/nn.2732

Carr, M. F., Karlsson, M. P., & Frank, L. M. (2012). Transient slow gamma synchrony underlies hippocampal memory replay. *Neuron*, *75*(4), 700-713. https://doi.org/10.1016/j.neuron.2012.06.014

Chabaud, P., Ravel, N., Wilson, D. A., & Gervais, R. (1999). Functional coupling in rat central olfactory pathways: a coherence analysis. *Neuroscience letters*, *276*(1), 17-20.

Chapuis, J., Messaoudi, B., Ferreira, G., & Ravel, N. (2007). Importance of retronasal and orthonasal olfaction for odor aversion memory in rats. *Behav Neurosci*, *121*(6), 1383-1392. https://doi.org/10.1037/0735-7044.121.6.1383

Cleland, T. A., Chen, S. Y., Hozer, K. W., Ukatu, H. N., Wong, K. J., & Zheng, F. (2011). Sequential mechanisms underlying concentration invariance in biological olfaction. *Front Neuroeng*, *4*, 21. https://doi.org/10.3389/fneng.2011.00021

Cleland, T. A., Morse, A., Yue, E. L., & Linster, C. (2002). Behavioral models of odor similarity. *Behav Neurosci*, *116*(2), 222-231. https://doi.org/10.1037//0735-7044.116.2.222

Colgin, L. L. (2016). Rhythms of the hippocampal network. *Nat Rev Neurosci*, *17*(4), 239-249. https://doi.org/10.1038/nrn.2016.21

Craft, M. F., Barreiro, A. K., Gautam, S. H., Shew, W. L., & Ly, C. (2021). Differences in olfactory bulb mitral cell spiking with ortho- and retronasal stimulation revealed by data-driven models. *PLoS Comput Biol*, *17*(9), e1009169. https://doi.org/10.1371/journal.pcbi.1009169

Darling, F. M., & Slotnick, B. M. (1994). Odor-cued taste avoidance: a simple and efficient method for assessing olfactory detection, discrimination and memory in the rat. *Physiology & behavior*, *55*(5), 817-822.

Eeckman, F. H., & Freeman, W. J. (1991). Asymmetric sigmoid non-linearity in the rat olfactory system. *Brain Research*, *557*(1–2), 13–21. https://doi.org/10.1016/0006-8993(91)90110-H

Engel, A. K., & Fries, P. (2010). Beta-band oscillations--signalling the status quo? *Curr Opin Neurobiol*, *20*(2), 156-165. https://doi.org/10.1016/j.conb.2010.02.015

Eschenko, O., Ramadan, W., Molle, M., Born, J., & Sara, S. J. (2008). Sustained increase in hippocampal sharp-wave ripple activity during slow-wave sleep after learning. *Learn Mem*, *15*(4), 222-228. https://doi.org/10.1101/lm.726008

Fendt, M., & Endres, T. (2008). 2,3,5-Trimethyl-3-thiazoline (TMT), a component of fox odor - just repugnant or really fear-inducing? *Neurosci Biobehav Rev*, *32*(7), 1259-1266. https://doi.org/10.1016/j.neubiorev.2008.05.010

Fernández-Ruiz, A., Oliva, A., Fermino de Oliveira, E., Rocha-Almeida, F., Tingley, D., & Buzsáki, G. (2019). Long-duration hippocampal sharp wave ripples improve memory. *Science*, *364*(6445), 1082-1086.

Fitzgerald, B. J., Richardson, K., & Wesson, D. W. (2014). Olfactory tubercle stimulation alters odor preference behavior and recruits forebrain reward and motivational centers. *Front Behav Neurosci*, *8*, 81. https://doi.org/10.3389/fnbeh.2014.00081

Fortes-Marco, L., Lanuza, E., Martinez-Garcia, F., & Agustin-Pavon, C. (2015). Avoidance and contextual learning induced by a kairomone, a pheromone and a common odorant in female CD1 mice. *Front Neurosci*, *9*, 336. https://doi.org/10.3389/fnins.2015.00336

Fourcaud-Trocme, N., Courtiol, E., & Buonviso, N. (2014). Two distinct olfactory bulb sublaminar networks involved in gamma and beta oscillation generation: a CSD study in the anesthetized rat. *Front Neural Circuits*, *8*, 88. https://doi.org/10.3389/fncir.2014.00088

Freeman, W. J., & Schneider, W. (1982). Changes in spatial patterns of rabbit olfactory EEG with conditioning to odors. *Psychophysiology*, *19*(1), 44-56.

Frederick, D. E., Brown, A., Brim, E., Mehta, N., Vujovic, M., & Kay, L. M. (2016). Gamma and Beta Oscillations Define a Sequence of Neurocognitive Modes Present in Odor Processing. *J Neurosci*, *36*(29), 7750-7767. https://doi.org/10.1523/JNEUROSCI.0569-16.2016

Frederick, D. E., Brown, A., Tacopina, S., Mehta, N., Vujovic, M., Brim, E., Amina, T., Fixsen, B., & Kay, L. M. (2017). Task-Dependent Behavioral Dynamics Make the Case for Temporal Integration in Multiple Strategies during Odor Processing. *J Neurosci*, *37*(16), 4416-4426. https://doi.org/10.1523/JNEUROSCI.1797-16.2017

Fries, P. (2015). Rhythms for Cognition: Communication through Coherence. *Neuron*, *88*(1), 220-235. https://doi.org/10.1016/j.neuron.2015.09.034

Furudono, Y., Cruz, G., & Lowe, G. (2013). Glomerular input patterns in the mouse olfactory bulb evoked by retronasal odor stimuli. *BMC neuroscience*, *14*(1), 1-14.

Gadziola, M. A., Tylicki, K. A., Christian, D. L., & Wesson, D. W. (2015). The olfactory tubercle encodes odor valence in behaving mice. *J Neurosci*, *35*(11), 4515-4527. https://doi.org/10.1523/JNEUROSCI.4750-14.2015

Gautam, S. H., & Verhagen, J. V. (2012). Retronasal odor representations in the dorsal olfactory bulb of rats. *J Neurosci*, *32*(23), 7949-7959. https://doi.org/10.1523/JNEUROSCI.1413-12.2012

Giessel, A. J., & Datta, S. R. (2014). Olfactory maps, circuits and computations. *Curr Opin Neurobiol*, *24*(1), 120-132. https://doi.org/10.1016/j.conb.2013.09.010

Girardeau, G., Benchenane, K., Wiener, S. I., Buzsaki, G., & Zugaro, M. B. (2009). Selective suppression of hippocampal ripples impairs spatial memory. *Nat Neurosci*, *12*(10), 1222-1223. https://doi.org/10.1038/nn.2384

González, J., Torterolo, P., & Tort, A. B. (2022). Mechanisms and functions of respiration-driven gamma oscillations in the piriform cortex. *bioRxiv*.

Gross-Isseroff, R., & Lancet, D. (1988). Concentration-dependent changes of perceived odor quality. *Chemical senses*, *13*(2), 191-204.

Gutierrez, R., Simon, S. A., & Nicolelis, M. A. (2010). Licking-induced synchrony in the taste-reward circuit improves cue discrimination during learning. *J Neurosci*, *30*(1), 287-303. https://doi.org/10.1523/JNEUROSCI.0855-09.2010

Haberly, L. B. (1985). Neuronal circuitry in olfactory cortex: anatomy and functional implications. *Chemical senses*.

Hacklander, R. P. M., Janssen, S. M. J., & Bermeitinger, C. (2019). An in-depth review of the methods, findings, and theories associated with odor-evoked autobiographical memory. *Psychon Bull Rev*, *26*(2), 401-429. https://doi.org/10.3758/s13423-018-1545-3

Hannum, M., Stegman, M. A., Fryer, J. A., & Simons, C. T. (2018). Different Olfactory Percepts Evoked by Orthonasal and Retronasal Odorant Delivery. *Chem Senses*, *43*(7), 515-521. https://doi.org/10.1093/chemse/bjy043

He, R., Dukes, T. C., & Kay, L. M. (2021). Transfer of Odor Perception From the Retronasal to the Orthonasal Pathway. *Chem Senses*, *46*. https://doi.org/10.1093/chemse/bjaa074

Hebb, D. O. (1949). The first stage of perception: growth of the assembly. *The Organization of Behavior*, (4), 60–78. https://doi.org/10.1016/0301-0082(84)90021-2

Herz, R. S., Eliassen, J., Beland, S., & Souza, T. (2004). Neuroimaging evidence for the emotional potency of odor-evoked memory. *Neuropsychologia*, *42*(3), 371-378. https://doi.org/10.1016/j.neuropsychologia.2003.08.009

Hummel, T., & Heilmann, S. (2008). Olfactory event-related potentials in response to ortho- and retronasal stimulation with odors related or unrelated to foods. *International Dairy Journal*, *18*(8), 874-878. https://doi.org/10.1016/j.idairyj.2007.10.010

Hummel, T., Heilmann, S., Landis, B. N., Reden, J., Frasnelli, J., Small, D. M., & Gerber, J. (2006). Perceptual differences between chemical stimuli presented through the ortho- or retronasal route. *Flavour and Fragrance Journal*, *21*(1), 42-47. https://doi.org/10.1002/ffj.1700

Hummel, T., & Livermore, A. (2002). Intranasal chemosensory function of the trigeminal nerve and aspects of its relation to olfaction. *Int Arch Occup Environ Health*, *75*(5), 305-313. https://doi.org/10.1007/s00420-002-0315-7

Igarashi, K. M., Ieki, N., An, M., Yamaguchi, Y., Nagayama, S., Kobayakawa, K., Kobayakawa, R., Tanifuji, M., Sakano, H., Chen, W. R., & Mori, K. (2012). Parallel mitral and tufted cell pathways route distinct odor information to different targets in the olfactory cortex. *J Neurosci*, *32*(23), 7970-7985. https://doi.org/10.1523/JNEUROSCI.0154-12.2012

Imamura, F., Ito, A., & LaFever, B. J. (2020). Subpopulations of Projection Neurons in the Olfactory Bulb. *Front Neural Circuits*, *14*, 561822. https://doi.org/10.3389/fncir.2020.561822

Jacobs, L. F. (2012). From chemotaxis to the cognitive map: the function of olfaction. *Proc Natl Acad Sci U S A*, *109 Suppl 1*, 10693-10700. https://doi.org/10.1073/pnas.1201880109

Jadhav, S. P., Kemere, C., German, P. W., & Frank, L. M. (2012). Awake hippocampal sharp-wave ripples support spatial memory. *Science*, *336*(6087), 1454-1458.

Jessberger, J., Zhong, W., Brankack, J., & Draguhn, A. (2016). Olfactory Bulb Field Potentials and Respiration in Sleep-Wake States of Mice. *Neural Plast*, *2016*, 4570831. https://doi.org/10.1155/2016/4570831

Kay, L. M. (2005). Theta oscillations and sensorimotor performance. *Proc Natl Acad Sci U S A*, *102*(10), 3863-3868. https://doi.org/10.1073/pnas.0407920102

Kay, L. M., & Beshel, J. (2010). A beta oscillation network in the rat olfactory system during a 2-alternative choice odor discrimination task. *J Neurophysiol*, *104*(2), 829-839. https://doi.org/10.1152/jn.00166.2010

Kay, L. M., & Freeman, W. J. (1998). Bidirectional processing in the olfactory-limbic axis during olfactory behavior. *Behavioral neuroscience*, *112*(3), 541.

Kay, L. M., & Laurent, G. (1999). Odor- and context-dependent modulation of mitral cell activity in behaving rats. *Nature Neuroscience*, *2*(11), 1003–1009. https://doi.org/10.1038/14801

Kepecs, A., Uchida, N., & Mainen, Z. F. (2007). Rapid and precise control of sniffing during olfactory discrimination in rats. *J Neurophysiol*, *98*(1), 205-213. https://doi.org/10.1152/jn.00071.2007

Kermen, F., Mandairon, N., & Chalencon, L. (2021). Odor hedonics coding in the vertebrate olfactory bulb. *Cell Tissue Res*, *383*(1), 485-493. https://doi.org/10.1007/s00441-020-03372-w

Khan, R. M., Luk, C. H., Flinker, A., Aggarwal, A., Lapid, H., Haddad, R., & Sobel, N. (2007). Predicting odor pleasantness from odorant structure: pleasantness as a reflection of the physical world. *J Neurosci*, *27*(37), 10015-10023. https://doi.org/10.1523/JNEUROSCI.1158-07.2007

Lagier, S., Panzanelli, P., Russo, R. E., Nissant, A., Bathellier, B., Sassoe-Pognetto, M., Fritschy, J. M., & Lledo, P. M. (2007). GABAergic inhibition at dendrodendritic synapses tunes gamma oscillations in the olfactory bulb. *Proc Natl Acad Sci U S A*, *104*(17), 7259-7264. https://doi.org/10.1073/pnas.0701846104

LeDoux, J. (2007). The amygdala. *Curr Biol*, *17*(20), R868-874. https://doi.org/10.1016/j.cub.2007.08.005

Li, A., Zhang, L., Liu, M., Gong, L., Liu, Q., & Xu, F. (2012). Effects of different anesthetics on oscillations in the rat olfactory bulb. *Journal of the American Association for Laboratory Animal Science*, *51*(4), 458-463.

Liljenstrom, H. A. N. S., & Hasselmo, M. E. (1995). Cholinergic modulation of cortical oscillatory dynamics. *Journal of Neurophysiology*, *74*(1), 288-297.

Linster, C., Johnson, B. A., Yue, E., Morse, A., Xu, Z., Hingco, E. E., ... & Leon, M. (2001). Perceptual correlates of neural representations evoked by odorant enantiomers. *Journal of Neuroscience*, *21*(24), 9837-9843.

Litaudon, P., Garcia, S., & Buonviso, N. (2008). Strong coupling between pyramidal cell activity and network oscillations in the olfactory cortex. *Neuroscience*, *156*(3), 781-787. https://doi.org/10.1016/j.neuroscience.2008.07.077

Liu, P., Cao, T., Xu, J., Mao, X., Wang, D., & Li, A. (2020). Plasticity of Sniffing Pattern and Neural Activity in the Olfactory Bulb of Behaving Mice During Odor Sampling, Anticipation, and Reward. *Neurosci Bull*, *36*(6), 598-610. https://doi.org/10.1007/s12264-019-00463-9

Liu, Z., Wang, Y., Cai, L., Li, Y., Chen, B., Dong, Y., & Huang, Y. H. (2016). Prefrontal Cortex to Accumbens Projections in Sleep Regulation of Reward. *J Neurosci*, *36*(30), 7897-7910. https://doi.org/10.1523/JNEUROSCI.0347-16.2016

Lowry, C. A., & Kay, L. M. (2007). Chemical factors determine olfactory system beta oscillations in waking rats. *J Neurophysiol*, *98*(1), 394-404. https://doi.org/10.1152/jn.00124.2007

Luna, V. M., & Schoppa, N. E. (2008). GABAergic circuits control input-spike coupling in the piriform cortex. *J Neurosci*, *28*(35), 8851-8859. https://doi.org/10.1523/JNEUROSCI.2385-08.2008

Maier, J. X. (2017). Single-neuron responses to intraoral delivery of odor solutions in primary olfactory and gustatory cortex. *J Neurophysiol*, *117*(3), 1293-1304. https://doi.org/10.1152/jn.00802.2016 s

Maier, J. X., Blankenship, M. L., Li, J. X., & Katz, D. B. (2015). A Multisensory Network for Olfactory Processing. *Curr Biol*, *25*(20), 2642-2650. https://doi.org/10.1016/j.cub.2015.08.060

Maier, J. X., Wachowiak, M., & Katz, D. B. (2012). Chemosensory convergence on primary olfactory cortex. *J Neurosci*, *32*(48), 17037-17047. https://doi.org/10.1523/JNEUROSCI.3540-12.2012

Manabe, H., Kusumoto-Yoshida, I., Ota, M., & Mori, K. (2011). Olfactory cortex generates synchronized top-down inputs to the olfactory bulb during slow-wave sleep. *J Neurosci*, *31*(22), 8123-8133. https://doi.org/10.1523/JNEUROSCI.6578-10.2011

Manabe, I. (2011). Chronic inflammation links cardiovascular, metabolic and renal diseases. *Circ J*, *75*(12), 2739-2748. https://doi.org/10.1253/circj.cj-11-1184

Mandairon, N., Stack, C., Kiselycznyk, C., & Linster, C. (2006). Broad activation of the olfactory bulb produces long-lasting changes in odor perception. *Proc Natl Acad Sci U S A*, *103*(36), 13543-13548. https://doi.org/10.1073/pnas.0602750103

Martin, C., Beshel, J., & Kay, L. M. (2007). An olfacto-hippocampal network is dynamically involved in odor-discrimination learning. *J Neurophysiol*, *98*(4), 2196-2205. https://doi.org/10.1152/jn.00524.2007

Martin, C., Gervais, R., Hugues, E., Messaoudi, B., & Ravel, N. (2004). Learning modulation of odor-induced oscillatory responses in the rat olfactory bulb: a correlate of odor recognition? *J Neurosci*, *24*(2), 389-397. https://doi.org/10.1523/JNEUROSCI.3433-03.2004

Mathisen, G. H., Yazdani, M., Rakkestad, K. E., Aden, P. K., Bodin, J., Samuelsen, M., Nygaard, U. C., Goverud, I. L., Gaarder, M., Loberg, E. M., Bolling, A. K., Becher, R., & Paulsen, R. E. (2013). Prenatal exposure to bisphenol A interferes with the development of cerebellar granule neurons in mice and chicken. *Int J Dev Neurosci*, *31*(8), 762-769. https://doi.org/10.1016/j.ijdevneu.2013.09.009

Mori, K., & Sakano, H. (2011). How is the olfactory map formed and interpreted in the mammalian brain? *Annu Rev Neurosci*, *34*, 467-499. https://doi.org/10.1146/annurev-neuro-112210-112917

Moriceau, S., & Sullivan, R. M. (2004). Unique neural circuitry for neonatal olfactory learning. *J Neurosci*, *24*(5), 1182-1189. https://doi.org/10.1523/JNEUROSCI.4578-03.2004

Muzur, A., Pace-Schott, E. F., & Hobson, J. A. (2002). The prefrontal cortex in sleep. *Trends in Cognitive Sciences*, *6*(11), 475-481. https://doi.org/10.1016/s1364-6613(02)01992-7

Nagayama, S., Enerva, A., Fletcher, M. L., Masurkar, A. V., Igarashi, K. M., Mori, K., & Chen, W. R. (2010). Differential axonal projection of mitral and tufted cells in the mouse main olfactory system. *Front Neural Circuits*, *4*. https://doi.org/10.3389/fncir.2010.00120

Narikiyo, K., Manabe, H., & Mori, K. (2014). Sharp wave-associated synchronized inputs from the piriform cortex activate olfactory tubercle neurons during slow-wave sleep. *J Neurophysiol*, *111*(1), 72-81. https://doi.org/10.1152/jn.00535.2013

Nusser, Z., Kay, L. M., Laurent, G., Homanics, G. E., & Mody, I. (2001). Disruption of GABAA receptors on GABAergic interneurons leads to increased oscillatory power in the olfactory bulb network. *Journal of neurophysiology*, *86*(6), 2823-2833.

Osinski, B. L., & Kay, L. M. (2016). Granule cell excitability regulates gamma and beta oscillations in a model of the olfactory bulb dendrodendritic microcircuit. *J Neurophysiol*, *116*(2), 522-539. https://doi.org/10.1152/jn.00988.2015

Osinski, B. L., Kim, A., Xiao, W., Mehta, N. M., & Kay, L. M. (2018). Pharmacological manipulation of the olfactory bulb modulates beta oscillations: testing model predictions. *J Neurophysiol*, *120*(3), 1090-1106. https://doi.org/10.1152/jn.00090.2018

Parker, P. R. L., Brown, M. A., Smear, M. C., & Niell, C. M. (2020). Movement-Related Signals in Sensory Areas: Roles in Natural Behavior. *Trends Neurosci*, *43*(8), 581-595. https://doi.org/10.1016/j.tins.2020.05.005

Pashkovski, S. L., Iurilli, G., Brann, D., Chicharro, D., Drummey, K., Franks, K. M., Panzeri, S., & Datta, S. R. (2020). Structure and flexibility in cortical representations of odour space. *Nature*, *583*(7815), 253-258. https://doi.org/10.1038/s41586-020-2451-1

Peever, J., & Fuller, P. M. (2017). The Biology of REM Sleep. *Curr Biol*, *27*(22), R1237-R1248. https://doi.org/10.1016/j.cub.2017.10.026

Pierce, J., & Halpern, B. P. (1996). Orthonasal and retronasal odorant identification based upon vapor phase input from common substances. *Chemical Senses*, *21*(5), 529–543. https://doi.org/10.1093/chemse/21.5.529

Poo, C., Agarwal, G., Bonacchi, N., & Mainen, Z. F. (2022). Spatial maps in piriform cortex during olfactory navigation. *Nature*, *601*(7894), 595-599. https://doi.org/10.1038/s41586-021-04242-3

Portero-Tresserra, M., Marti-Nicolovius, M., Guillazo-Blanch, G., Boadas-Vaello, P., & Vale-Martinez, A. (2013). D-cycloserine in the basolateral amygdala prevents extinction and enhances reconsolidation of odor-reward associative learning in rats. *Neurobiol Learn Mem*, *100*, 1-11. https://doi.org/10.1016/j.nlm.2012.11.003

Ramadan, W., Eschenko, O., & Sara, S. J. (2009). Hippocampal sharp wave/ripples during sleep for consolidation of associative memory. *PLoS One*, *4*(8), e6697. https://doi.org/10.1371/journal.pone.0006697

Ravel, N., Chabaud, P., Martin, C., Gaveau, V., Hugues, E., Tallon-Baudry, C., Bertrand, O., & Gervais, R. (2003). Olfactory learning modifies the expression of odour-induced oscillatory responses in the gamma (60-90 Hz) and beta (15-40 Hz) bands in the rat olfactory bulb. *Eur J Neurosci*, *17*(2), 350-358. https://doi.org/10.1046/j.1460-9568.2003.02445.x

Rebello, M. R., Kandukuru, P., & Verhagen, J. V. (2015). Direct behavioral and neurophysiological evidence for retronasal olfaction in mice. *PLoS One*, *10*(2), e0117218. https://doi.org/10.1371/journal.pone.0117218

Rojas-Libano, D., Frederick, D. E., Egana, J. I., & Kay, L. M. (2014). The olfactory bulb theta rhythm follows all frequencies of diaphragmatic respiration in the freely behaving rat. *Front Behav Neurosci*, *8*, 214. https://doi.org/10.3389/fnbeh.2014.00214

Rojas-Libano, D., & Kay, L. M. (2008). Olfactory system gamma oscillations: the physiological dissection of a cognitive neural system. *Cogn Neurodyn*, *2*(3), 179-194. https://doi.org/10.1007/s11571-008-9053-1

Rojas-Libano, D., & Kay, L. M. (2012). Interplay between sniffing and odorant sorptive properties in the rat. *J Neurosci*, *32*(44), 15577-15589. https://doi.org/10.1523/JNEUROSCI.1464-12.2012

Roumis, D. K., & Frank, L. M. (2015). Hippocampal sharp-wave ripples in waking and sleeping states. *Curr Opin Neurobiol*, *35*, 6-12. https://doi.org/10.1016/j.conb.2015.05.001

Rozin, P. (1982). "Taste-smell confusions" and the duality of the olfactory sense. *Perception & Psychophysics*, *31*(4), 397–401. https://doi.org/10.3758/BF03202667

Schaffer, E. S., Stettler, D. D., Kato, D., Choi, G. B., Axel, R., & Abbott, L. F. (2018). Odor Perception on the Two Sides of the Brain: Consistency Despite Randomness. *Neuron*, *98*(4), 736-742 e733. https://doi.org/10.1016/j.neuron.2018.04.004

Schoppa, N. E. (2006). Synchronization of olfactory bulb mitral cells by precisely timed inhibitory inputs. *Neuron*, *49*(2), 271-283. https://doi.org/10.1016/j.neuron.2005.11.038

Scott, J. W., Sherrill, L., Jiang, J., & Zhao, K. (2014). Tuning to odor solubility and sorption pattern in olfactory epithelial responses. *J Neurosci*, *34*(6), 2025-2036. https://doi.org/10.1523/JNEUROSCI.3736-13.2014

Sheriff, A., Pandolfi, G., Nguyen, V. S., & Kay, L. M. (2021). Long-Range Respiratory and Theta Oscillation Networks Depend on Spatial Sensory Context. *J Neurosci*, *41*(48), 9957-9970. https://doi.org/10.1523/JNEUROSCI.0719-21.2021

Siapas, A. G., & Wilson, M. A. (1998). Coordinated interactions between hippocampal ripples and cortical spindles during slow-wave sleep. *Neuron*, *21*(5), 1123-1128.

Sirota, A., Csicsvari, J., Buhl, D., & Buzsaki, G. (2003). Communication between neocortex and hippocampus during sleep in rodents. *Proc Natl Acad Sci U S A*, *100*(4), 2065-2069. https://doi.org/10.1073/pnas.0437938100

Slotnick, B. (2007). Odor-sampling time of mice under different conditions. *Chem Senses*, *32*(5), 445-454. https://doi.org/10.1093/chemse/bjm013

Small, D. M., Gerber, J. C., Mak, Y. E., & Hummel, T. (2005). Differential neural responses evoked by orthonasal versus retronasal odorant perception in humans. *Neuron*, *47*(4), 593-605. https://doi.org/10.1016/j.neuron.2005.07.022

Soltani, S., Chauvette, S., Bukhtiyarova, O., Lina, J. M., Dube, J., Seigneur, J., Carrier, J., & Timofeev, I. (2019). Sleep-Wake Cycle in Young and Older Mice. *Front Syst Neurosci*, *13*, 51. https://doi.org/10.3389/fnsys.2019.00051

Soucy, E. R., Albeanu, D. F., Fantana, A. L., Murthy, V. N., & Meister, M. (2009). Precision and diversity in an odor map on the olfactory bulb. *Nature neuroscience*, *12*(2), 210-220.

Stettler, D. D., & Axel, R. (2009). Representations of odor in the piriform cortex. *Neuron*, *63*(6), 854-864. https://doi.org/10.1016/j.neuron.2009.09.005

Stevenson, R. J., Boakes, R. A., & Wilson, J. P. (2000). Resistance to extinction of conditioned odor perceptions: evaluative conditioning is not unique. *J Exp Psychol Learn Mem Cogn*, *26*(2), 423-440. https://doi.org/10.1037//0278-7393.26.2.423

Stopfer, M., Jayaraman, V., & Laurent, G. (2003). Intensity versus identity coding in an olfactory system. *Neuron*, *39*(6), 991-1004. https://doi.org/10.1016/j.neuron.2003.08.011

Storace, D. A., & Cohen, L. B. (2017). Measuring the olfactory bulb input-output transformation reveals a contribution to the perception of odorant concentration invariance. *Nat Commun*, *8*(1), 81. https://doi.org/10.1038/s41467-017-00036-2

Tsuno, Y., Kashiwadani, H., & Mori, K. (2008). Behavioral state regulation of dendrodendritic synaptic inhibition in the olfactory bulb. *J Neurosci*, *28*(37), 9227-9238. https://doi.org/10.1523/JNEUROSCI.1576-08.2008

Uchida, N., & Mainen, Z. F. (2003). Speed and accuracy of olfactory discrimination in the rat. *Nat Neurosci*, *6*(11), 1224-1229. https://doi.org/10.1038/nn1142

Voss, J. L., Bridge, D. J., Cohen, N. J., & Walker, J. A. (2017). A Closer Look at the Hippocampus and Memory. *Trends Cogn Sci*, *21*(8), 577-588. https://doi.org/10.1016/j.tics.2017.05.008

Wachowiak, M., & Cohen, L. B. (2001). Representation of odorants by receptor neuron input to the mouse olfactory bulb. *Neuron*, *32*(4), 723-735.

Walker, M. P., & Stickgold, R. (2006). Sleep, memory, and plasticity. *Annu Rev Psychol*, *57*, 139-166. https://doi.org/10.1146/annurev.psych.56.091103.070307

Weiss, M. S., & Di Lorenzo, P. M. (2012). Not so fast: taste stimulus coding time in the rat revisited. *Front Integr Neurosci*, *6*, 27. https://doi.org/10.3389/fnint.2012.00027

Wesson, D. W. (2020). The Tubular Striatum. *J Neurosci*, *40*(39), 7379-7386. https://doi.org/10.1523/JNEUROSCI.1109-20.2020

Wesson, D. W., Verhagen, J. V., & Wachowiak, M. (2009). Why sniff fast? The relationship between sniff frequency, odor discrimination, and receptor neuron activation in the rat. *J Neurophysiol*, *101*(2), 1089-1102. https://doi.org/10.1152/jn.90981.2008

Wesson, D. W., & Wilson, D. A. (2011). Sniffing out the contributions of the olfactory tubercle to the sense of smell: hedonics, sensory integration, and more? *Neurosci Biobehav Rev*, *35*(3), 655-668. https://doi.org/10.1016/j.neubiorev.2010.08.004

Wilson, D. A., & Sullivan, R. M. (2011). Cortical processing of odor objects. *Neuron*, *72*(4), 506-519. https://doi.org/10.1016/j.neuron.2011.10.027

Wilson, D. A., & Yan, X. (2010). Sleep-like states modulate functional connectivity in the rat olfactory system. *J Neurophysiol*, *104*(6), 3231-3239. https://doi.org/10.1152/jn.00711.2010

Xia, C. Z., Adjei, S., & Wesson, D. W. (2015). Coding of odor stimulus features among secondary olfactory structures. *J Neurophysiol*, *114*(1), 736-745. https://doi.org/10.1152/jn.00902.2014